bioRxiv preprint doi: https://doi.org/10.1101/2022.07.05.498815; this version posted July 5, 2022. The copyright holder for this preprint (which was not certified by peer review) is the author/funder, who has granted bioRxiv a license to display the preprint in perpetuity. It is made available under aCC-BY-NC-ND 4.0 International license.

Full paper

A Physcomitrella PIN protein acts in spermatogenesis and sporophyte abortion

Volker M. Lüth[1], Christine Rempfer[1,2], Oliver Herzog[1], Melanie Roecker[1,*], Marion Braun[1], Eva L. Decker[1] and Ralf Reski[1,2,3,4]

[1]Plant Biotechnology, Faculty of Biology, University of Freiburg, Freiburg, Germany

[2]Speman Graduate School of Biology and Medicine (SGBM), University of Freiburg, Freiburg, Germany

[3]CIBSS – Centre for Integrative Biological Signalling Studies, University of Freiburg, Freiburg, Germany

[4]Cluster of Excellence *liv*MatS @ FIT – Freiburg Center for Interactive Materials and Bioinspired Technologies, University of Freiburg, Freiburg, Germany

Current address:

* Leibniz Institute of Vegetable and Ornamental Crops (IGZ), Großbeeren, Germany

Author for correspondence: *Ralf Reski, Email: ralf.reski@biologie.uni-freiburg.de*

Key words: auxin, bryophyte, flagellum, moss, plant development, sperm, spermatozoid

Summary

- The auxin efflux PIN-FORMED (PIN) proteins are conserved in all land plants and important players in plant development. In the moss Physcomitrella (*Physcomitrium patens*) three canonical PINs (PpPINA-C) are expressed in the gametophore. PpPINA and PpPINB show functional activity in vegetative growth and sporophyte development. Here, we examined the role of PpPINC in the life cycle of Physcomitrella.
- We established reporter and knockout lines for PpPINC and analysed vegetative and reproductive tissues using microscopy and transcriptomic sequencing of moss gametangia.
- PpPINC is expressed in immature leaves, mature gametangia and during sporophyte development. The sperm cells (spermatozoids) of knockout mutants exhibit increased motility compared to the wild type and show an altered flagella phenotype. Further, the knockout mutants have a significantly increased fertility, and an increased abortion rate of premeiotic sporophytes.
- Here, we show that PpPINC is an important regulator for spermatogenesis and sporophyte development. We propose an evolutionary conserved way of polar growth during early moss embryo development and sporophyte attachment, while suggesting the mechanical function in sporophyte securement of a ring structure, the Lorch ring.

bioRxiv preprint doi: https://doi.org/10.1101/2022.07.05.498815; this version posted July 5, 2022. The copyright holder for this preprint (which was not certified by peer review) is the author/funder, who has granted bioRxiv a license to display the preprint in perpetuity. It is made available under aCC-BY-NC-ND 4.0 International license.

Introduction

The auxin signal transduction pathway is conserved in all land plants (Paponov *et al.*, 2009; Flores-Sandoval *et al.*, 2015; Thelander *et al.*, 2018; Cancé *et al.*, 2022). In the model moss Physcomitrella (*Physcomitrium patens*), the main auxin biosynthesis pathway is, as in Arabidopsis, the conversion of tryptophan by TAR enzymes to indole-3-pyruvate (IPyA) from where it is converted by YUC enzymes into active auxin (indole-3-acetic acid, IAA) (Landberg *et al.*, 2020). Auxin homeostasis plays an important role during the life cycle of Physcomitrella, maintaining growth and organogenesis (Ludwig-Müller *et al*., 2009; Thelander *et al.*, 2018). However, there is no indication for a polar auxin transport in the moss shoot (Fujita *et al.*, 2008), although the protein family responsible for polar auxin transport, Pin-formed (PIN), is conserved in all land plants, including bryophytes (Bennett *et al.*, 2014a; Zhang *et al.*, 2020).

Canonical PIN proteins share four highly conserved motifs in the hydrophilic loop and a strong conservation in the N'- and C' terminal transmembrane regions, while noncanonical PINs are defined by a higher variability (Bennett *et al.*, 2014a). Structures and mechanism of auxin transport have recently been elucidated in great detail for the *Arabidopsis thaliana* PIN8 protein (Ung *et al*., 2022). The Physcomitrella genome encodes four PIN genes, the three canonical *PpPINA*, *PpPINB* and *PpPINC*, and the noncanonical *PpPIND*, with *PpPINA* and *PpPINB* being the most similar to each other (Bennett *et al.*, 2014b). The Physcomitrella PIN proteins form an outgroup with other bryophytes to vascular plants and lycophytes, where the canonical PpPINs cluster with PIN proteins from other mosses, while the noncanonical PpPIND is separated together with several PIN proteins of the liverwort *Marchantia polymorpha* (Bennett *et al.*, 2014a).

In the gametophore, apical stem cells show the highest expression of *PpTAR* genes, indicating biosynthesis of IPyA (Landberg *et al.*, 2020), with auxin accumulating beneath the stem apex and at the stem base (Bierfreund *et al.*, 2003; Fujita *et al.*, 2008). The growth of developing leaves (phylloids) in Physcomitrella is marked by high auxin activity (Thelander *et al.*, 2019) with all three canonical *PpPIN* genes being active (Viaene *et al.*, 2014). While *PpPINA* is the highest expressed *PIN* gene in Physcomitrella tissues, *PpPINC* has the lowest expression level of all canonical PINs (Bennett *et al.*, 2014b). Single knockouts of *PpPIN* genes have no severe effect on gametophore growth (Viaene *et al.*, 2014), while the double knockout of *PpPINA* and *PpPINB* leads to elongated leaves, a phenotype similar to Physcomitrella gametophores treated with excess auxin or auxin transport inhibitors (Decker *et al.*, 2006; Bennett *et al.*, 2014b).

When introduced to short day conditions with low temperatures, the monoecious moss Physcomitrella initiates the formation of sexual organs on the gametophore apex (Hohe *et al.*, 2002) with specialized stem cells for female archegonia and male antheridia development (Kofuji & Hasebe, 2014). Growth of antheridia and archegonia is highly synchronized, beginning with the formation of the antheridia while

bioRxiv preprint doi: https://doi.org/10.1101/2022.07.05.498815; this version posted July 5, 2022. The copyright holder for this preprint (which was not certified by peer review) is the author/funder, who has granted bioRxiv a license to display the preprint in perpetuity. It is made available under aCC-BY-NC-ND 4.0 International license.

archegonia develop later but mature faster, so that self-fertilization is possible (Cove, 2005; Landberg *et al.*, 2013). The development and growth of gametangia is controlled by the auxin-biosynthesis regulators *SHORT INTERNODE/STYLISH* (*SHI/STY*) and TAR enzymes, influencing the neck length of archegonia and growth of antheridia. During the growth of antheridia, the expression of *PpSHI* and *PpTAR* genes overlap with the expression of *PpPINA* and the accumulation of auxin in apical cells, before spermatogenesis begins. This activity slowly declines and reaches its lowest point during spermatogenesis, indicating a process where auxin plays a minor role (Landberg *et al.*, 2013; Landberg *et al.*, 2020). Spermatogenesis in Physcomitrella is tightly regulated, producing motile, biflagellate sperm cells, relying on the availability of water to swim to the egg cell (Reski, 1998; Cove, 2005; Ortiz-Ramírez *et al.*, 2017; Koshimizu *et al.*, 2018; Gu *et al.*, 2022). Like in antheridia, the activity of auxin biosynthesis, signalling and accumulation are the highest in archegonia during early growth phases. The precursor egg cell and apical neck cells show the highest activity, while there is a minimum of expression during egg maturation (Landberg *et al.*, 2013; Landberg *et al.*, 2020). After fertilization of the egg cell, a diploid embryo grows from the zygote and develops into the moss sporophyte (Horst *et al.*, 2016). The sporophyte in Physcomitrella is reduced compared to other mosses (Kirbis *et al.*, 2020), even within its own family (Ostendorf *et al.*, 2021), and consists of the sporophyte foot, a short seta and the spore capsule, which rips open after maturation to release the spores (Cove, 2005). Auxin is distributed dynamically in a polar manner during sporophyte growth, with an auxin maximum in the apex of the early embryo which later localizes to the foot of the young sporophyte where it slowly recedes during maturation (Fujita *et al.*, 2008). The sporophyte foot is secured in a maternal cavity (vaginula) and covered at its base with haustorial cells, important for the uptake of nutrients provided by the gametophore (Regmi *et al.*, 2017). Formation of sporophytes is a complex process and regulated by a number of genetic elements (Mosquna *et al.*, 2009; Horst *et al.*, 2016; Ortiz-Ramírez *et al.*, 2016; Lopez-Obando *et al.*, 2016; Hashida *et al.*, 2020; Kirbis *et al.*, 2020; Sakakibara *et al.*, 2008; Takechi *et al.*, 2021, Landberg *et al.* 2022). However, auxin remains a crucial player in sporophyte growth (Fujita *et al.*, 2008), with the two Physcomitrella *PIN* genes *PpPINA* and *PpPINB* showing functional activity in the development of sporophytes (Bennett *et al.*, 2014b), whereas the role of the canonical *PpPINC* remains unclear.

Here, we elucidate the role of PpPINC in the Physcomitrella life cycle. We found that PpPINC influences spermatogenesis-related gene expression, controls motility and phenotype of moss sperm cells, and is important in preventing early abortion of premeiotic sporophytes, while it has no obvious role in vegetative growth.

Material and Methods

Plant material and culture conditions

bioRxiv preprint doi: https://doi.org/10.1101/2022.07.05.498815; this version posted July 5, 2022. The copyright holder for this preprint (which was not certified by peer review) is the author/funder, who has granted bioRxiv a license to display the preprint in perpetuity. It is made available under aCC-BY-NC-ND 4.0 International license.

The *Physcomitrella patens* (Hedw.) Bruch & Schimp. ecotype Gransden covers several laboratory strains which are descendants of the first original cultivated single clone (Haas *et al.*, 2020) and was recently renamed to *Physcomitrium patens* (Hedw.) Mitt.. We used as wild type (WT) a fertile Gransden line, which underwent sexual reproduction regularly as a basis for all transgenic lines. Plants were cultivated using Knop medium (pH 5.8) according to Reski & Abel (1985) containing microelements according to Egener *et al.* (2002). For solid medium, 12 g/l agar (OXOID, Thermo Scientific) were added. Standard growth conditions were long day 16 hours light with 70±5 µmol m^{-2} s^{-2} and 22°C. Sporophyte induction was modified after Hohe *et al.* (2002). Plants were grown in long day conditions, before being transferred to sporophyte inducing conditions (Hohe *et al.*, 2002). At day 18 of sporophyte induction, plants were watered (H_2O dest., 10 ml for 9 cm petri dish), which was removed from the plate at day 25. All moss lines used are stored in the International Moss Stock Center (IMSC; https://www.moss-stock-center.org) with the following accession numbers: *PinCPromCit* = 40917, *pin*C#10 = 40918, *pin*C#29 = 40919, *pin*C#69 = 40420, WT = 40095.

Generation of transgenic lines

Transgenic lines were created via highly efficient homologous recombination (Reinhard *et al.*, 2004) in transformed protoplasts (Hohe & Reski, 2002). For the generation of targeted *pinC* mutants the region upstream from the beginning of the first exon to the untranslated region after exon six was amplified (2915 bp) from genomic DNA using the following primers: P3-KO Fw + P3-KO Rv (Supp. Tab. 1). The amplified fragment was sub-cloned into the vector *pJET1.2*. Using *SacI* and *NcoI* a piece of the *PpPINC* gene (1696 bp) was replaced with a sulfadiazine selection cassette (Parsons *et al.*, 2012). For the generation of the reporter line, 2.1 kb upstream of the start codon of the *PpPINC* gene were fused to the citrine cds and nos terminator via Gibson cloning (Gibson *et al.*, 2009), upper case letters are for *PpPINC* promoter amplification: 5PinCprom_f+CA5 + 3PinCprom_r+Citrin (Supp. Tab. 1). The expression cassette was cloned between homologous regions of the carbonic anhydrase locus (Wiedemann *et al.*, 2018), erasing the citrine expression of the parental plant when correctly integrated into the genome.

Molecular analysis of transgenic lines

Initial screening of lines was done with leaflet PCR, according to Schween *et al.* (2002), to test for the presence of the construct. For RT-PCR total RNA was extracted from 6 weeks old gametophores, 21 days after the sporophyte induction started using the innuPREP Plant RNA Kit (Analytik Jena AG, Jena, Germany) and reversely transcribed using oligo-d(T)16 primers with Superscript III reverse transcriptase (Life Technologies, Thermo Fisher Scientific). Analysis for the absence of *PpPINC* RNA was performed with the gene-specific primers Pin3f_ex1-2 + Pin3r_ex2 (Supp. Tab. 1). Presence of cDNA was tested with C45_fwd and C45_rev (Supp. Tab. 1) amplifying the constitutively expressed gene L21. Transgene copy numbers were tested via quantitative Real-Time PCR according to Noy-Malka *et al.* (2014). Genomic DNA was isolated from protonema, one week after the last tissue disruption using the innuPREP Plant DNA Kit (Analytic Jena AG). Transgene copy numbers were

bioRxiv preprint doi: https://doi.org/10.1101/2022.07.05.498815; this version posted July 5, 2022. The copyright holder for this preprint (which was not certified by peer review) is the author/funder, who has granted bioRxiv a license to display the preprint in perpetuity. It is made available under aCC-BY-NC-ND 4.0 International license.

determined comparing relative values of the transgene 35S promoter (35SPqPCR_f + 35SPqPCR_r; Supplemental Table 1) with the single copy transgene carbonic anhydrase line used in Wiedemann *et al.* (2018), for normalization, the single copy gene CLF was used (Noy-Malka *et al.*, 2014).

Tissue isolation for gene expression analysis using SMARTseq

Triplicates of tissue samples were collected 18 days after gametophores were exposed to sporophyte-inducing conditions. Mature archegonia and antheridia were collected manually using a stereoscope (Olympus SZX7) and stored directly in TRIzol® (Fisher Scientific GmbH, Schwerte, Germany). All lines used were grown together on the same plate. For each sample eight archegonia or antheridia were collected. Tissues were homogenized using small pistils and mixed with chloroform. The aqueous phase was then further processed using the Direct-zol RNA Microprep Kit (Zymo Research Europe GmbH, Freiburg, Germany). The resulting RNA was treated with RiboLock RNase Inhibitor (Fisher Scientific GmbH, Schwerte, Germany). The cDNA library was created at the Genomics Unit in the Instituto Gulbenkian de Ciencia, Portugal according to Picelli *et al.* (2014). Libraries were sequenced using the Illumina RNASeq platform from Novogene (Novogene Company Limited, Cambridge, UK).

Transcriptomic data processing

Raw data was trimmed using Trim Galore (Version 0.6.6; adapter stringency = 1 bp; minimum required sequence length for retaining a read pair = 20 bp; 3'clipping = 1 bp). All further steps were done using the Galaxy platform (Afgan *et al.*, 2018). The 150 bp paired-end reads were then mapped to the Physcomitrella genome version 3.3 (downloaded from Phytozome (Goodstein *et al.*, 2012) using HISAT2 (Galaxy Version 2.1.0; spliced alignment activated). Mapped reads were counted with feature counts (Galaxy Version 2.0.1; excluding chimeric fragments; only fragments with both reads aligned, GFF feature type filter = CDS; GFF gene identifier = gene_id). Differential gene expression was analyzed using DESeq2 (Galaxy Version 2.11.40.6+galaxy1) and filtered for enriched gene ontology terms with GOEnrichment (Galaxy Version 2.0.1). Quality of mapping and read counts were controlled with MultiQC (Galaxy Version 1.11+galaxy0) and FastQC (Galaxy Version 0.73+galaxy0).

Calcium measurement in sperm cells

Sperm packets of single antheridia where extracted directly after being released from the antheridium and spotted on polylysine-covered glass slides according to Horst & Reski (2017). Sperm cells where incubated in a Fluo-4 solution according to Ortiz-Ramírez *et al.* (2017) for 20 minutes, photographed (see microscopy) and pictures were then analyzed using ImageJ (Schneider *et al.*, 2012).

Sporophyte count

For all lines we analyzed all gametophores on the respective plate. After removal of the leaves, sporophytes, embryos, empty vaginulae and aborted sporophytes were counted.

bioRxiv preprint doi: https://doi.org/10.1101/2022.07.05.498815; this version posted July 5, 2022. The copyright holder for this preprint (which was not certified by peer review) is the author/funder, who has granted bioRxiv a license to display the preprint in perpetuity. It is made available under aCC-BY-NC-ND 4.0 International license.

Statistical analysis

Stem length, leaf length and leaf width were tested with Student's t-Test with $p < 0.05$. Significance of motility was assessed with one-sided ANOVA and Tukey-Kramer test, flagellar phenotype with one-sided ANOVA. All tests were performed with Microsoft Excel and the XLMiner Analysis ToolPak.

Protein alignments and motif analysis

Needleman-Wunsch (Needleman & Wunsch, 1970) and multiple sequence alignments (Larkin *et al.*, 2007) with Clustal Omega (1.2.4) were performed using the European Bioinformatics Institute (EMBL-EBI) web tools (https://www.ebi.ac.uk/services) (Madeira *et al.*, 2019). Needleman-Wunsch alignments were performed with BLOSUM62, a gap penalty of 10 and extend penalty of 0.5. Multiple sequence alignments were performed with default settings. Transmembrane protein motifs were assessed using TMHMM 2.0 (Krogh *et al.*, 2001; Sonnhammer *et al.*, 1998).

Flow cytometry

Flow cytometry analysis was performed according to Heck *et al.* (2021).

Microscopy

For preparation of samples, we used an Olympus SZX7 stereoscope and for extraction of sperm packages a Zeiss Axiovert microscope. Fluorescence and bright-field microscopy pictures were taken with a Zeiss Axioplan 100 with a Zeiss MRc5 camera and Zeiss AxioVision software (Version 3.8.2).

Results

Physcomitrella PIN family

The Physcomitrella genome (Lang *et al.*, 2018) encodes three canonical PIN proteins, PpPINA (Pp3c23_10200), PpPINB (Pp3c24_2970) and PpPINC (Pp3c10_24880). These genes are similar in structure and length (Supplemental Fig. S1 a), consisting like all canonical PIN proteins in land plants of two transmembrane regions (five helices each), separated by a hydrophilic loop (Supplemental Fig. S1 b). The transmembrane regions have the same length in all three proteins, whereas the hydrophilic loop of PpPINC is 15 amino acids (AA) shorter than those of PpPINA and PpPINB (Table 1, Supplemental Fig. S1 b). While PpPINA and PpPINB are very similar in their AA sequences, PpPINC differs more, especially in the hydrophilic loop (Supplemental Fig. S2 a, c). While PpPINA and PpPINB share a sequence identity above 86 %, for PpPINC it is below 65% compared to the others (Table 1, Supplemental Fig. S2b). We hypothesise that PpPINA and PpPINB are the result of a gene duplication event in the recent genomic history of Physcomitrella (Lang *et al.*, 2018), after the event that led to PpPINC.

bioRxiv preprint doi: https://doi.org/10.1101/2022.07.05.498815; this version posted July 5, 2022. The copyright holder for this preprint (which was not certified by peer review) is the author/funder, who has granted bioRxiv a license to display the preprint in perpetuity. It is made available under aCC-BY-NC-ND 4.0 International license.

Compared to the canonical PIN proteins of Arabidopsis (AtPIN1,2,3,4,7), the hydrophilic loop of Physcomitrella PINs are between 51 and 97 AA longer, while there is strong conservation in the transmembrane regions (Supplemental Fig. S2b), as there is among all land plants (Bennett *et al.*, 2014a; Zhang *et al.*, 2020).

Table 1: Identity, similarity and length of Physcomitrella PpPIN protein motifs

	A vs B	A vs C	B vs C	PpPINA	PpPINB	PpPINC
	Identity; Similarity of AA in %			Length AA		
TM N’	96.1;98.7	87.7;93.5	88.4;93.5	155	155	155
HL	86.3;91.4	64.7;76.9	64.4;76.8	409	409	394
TM C’	95.3;98.7	80.0;88.0	77.3;86.7	150	150	150

A = PpPINA, B = PpPINB, C= PpPINC, TM N’ = N-teminal transmembrane region, HL = Hydrophilic loop, TM C’=C-terminal transmembrane region.

Stage-specific expression of *PpPINC*

We compared *PpPIN* expression in publicly available expression data (PEATmoss database; Fernandez-Pozo *et al.*, 2020) for the two Physcomitrella ecotypes Gransden and Reute in two or three datasets, respectively (Hiss *et al.*, 2014; Ortiz-Ramírez *et al.*, 2016; Perroud *et al.*, 2018). As reported in Bennett *et al.* (2014b), *PpPINA* is the highest expressed gene of the three, followed by *PpPINB* with lower, but similar expression rates. Consistent across the three data sets, *PpPINC* is the lowest expressed of the three. While there are some differences in the expression in single tissues in the different data sets, the overall expression of *PIN* genes in both Physcomitrella ecotypes is very similar. In protonema, the expression of all three *PIN*s is the lowest, while the highest expression of *PpPINA* and *PpPINB* can be found in gametophores and developing sporophytes. For *PpPINC*, the expression in vegetative tissues is very low, while there is a dynamic expression during sporophyte development in both ecotypes, which is nonetheless lower compared to the other two PINs in the same sporophytic tissues (Supplemental Fig. S3).

For a closer look at the activity of PpPINC, we created a moss line expressing citrine (*pinCPromCit*) under the influence of the native *PpPINC* promoter region (2.1 kb upstream CDS start). This construct was targeted to the carbonic anhydrase-citrine tagged locus used in Wiedemann *et al.* (2018), because of the high expression of the carbonic anhydrase gene. We screened for altered citrine signals in transformed plants compared to the ever-present citrine expression of the parental line and thus recovered a line with targeted integration of the *pinCPromCit* construct (Supplemental Fig. S4a, b). Under standard growth conditions we did not observe any *PINC*-driven citrine fluorescence, neither in

bioRxiv preprint doi: https://doi.org/10.1101/2022.07.05.498815; this version posted July 5, 2022. The copyright holder for this preprint (which was not certified by peer review) is the author/funder, who has granted bioRxiv a license to display the preprint in perpetuity. It is made available under aCC-BY-NC-ND 4.0 International license.

protonemal cells, rhizoids, stems, nor in adult leaves (Fig. 1a). In contrast, citrine fluorescence was clearly visible in the apices of young leaves. From here, fluorescence proceeds towards the base until maturation of the leaf. Intriguingly, *PpPINC* expression was highest in parts of the mid-rip and in leaf margins (Fig. 1b, c).

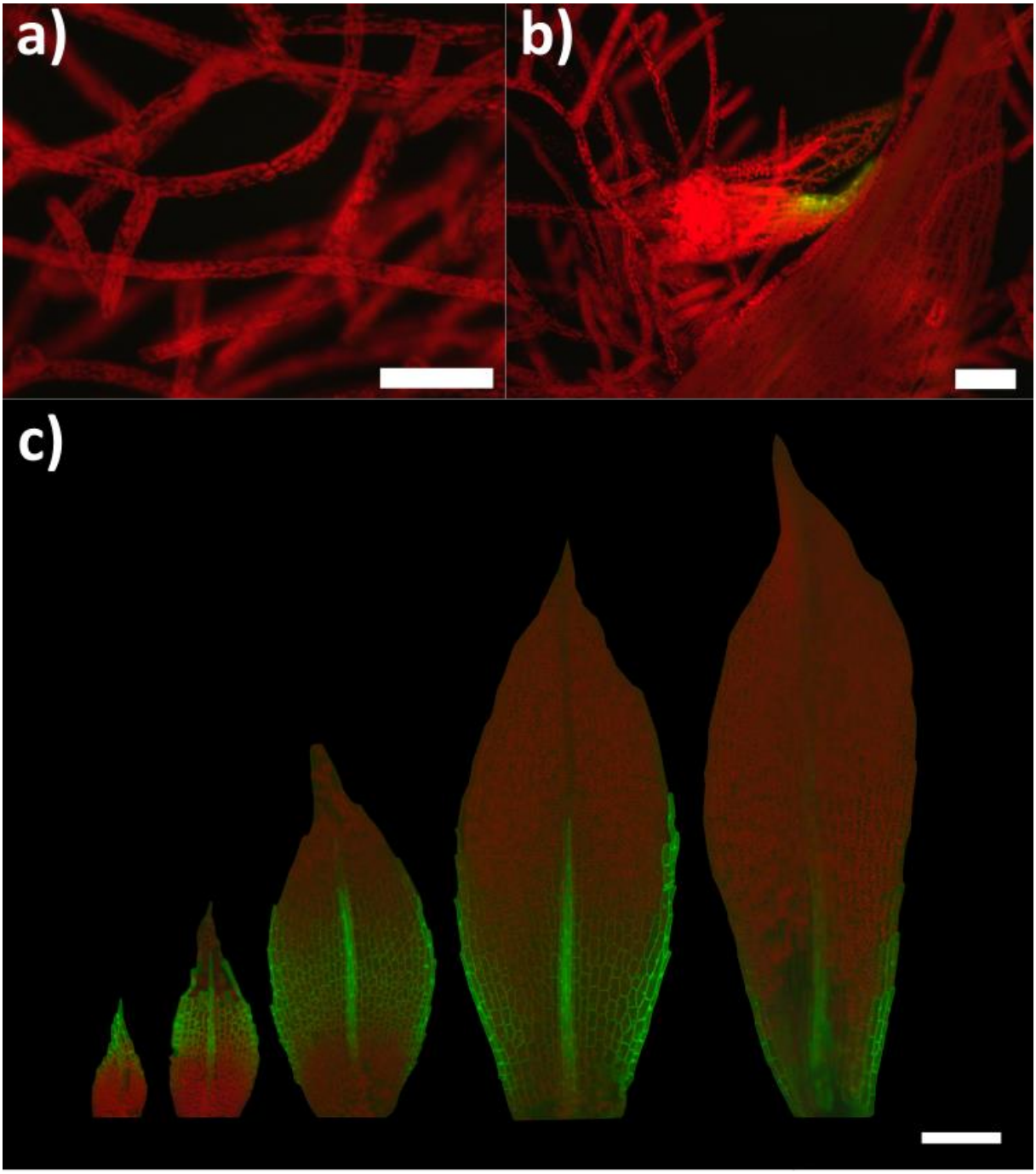

Figure 1: *Pp*PINC is expressed in developing leaves of Physcomitrella. Fluorescence microscopy to visualize citrine expression in a *PpPINC* promoter line (green). Red marks autofluorescence of chlorophyll: a) protonema (bar = 100 µm) b) budding gametophore (bar = 100 µm) c) the youngest leaves of a moss gametophore (bar = 200 µm).

bioRxiv preprint doi: https://doi.org/10.1101/2022.07.05.498815; this version posted July 5, 2022. The copyright holder for this preprint (which was not certified by peer review) is the author/funder, who has granted bioRxiv a license to display the preprint in perpetuity. It is made available under aCC-BY-NC-ND 4.0 International license.

In addition, citrine expression was detectable in developing gametangia. In mature antheridia close to releasing their sperm cells (antheridium stage 9 in Landberg *et al.* (2013)), the signal was found in the foot cells separating the antheridial body from the gametophore apex (Fig. 2a). In archegonia, a citrine signal was visible only after the neck canal had opened, surrounding the transition zone between canal and archegonial body above the egg cell (Fig. 2b).

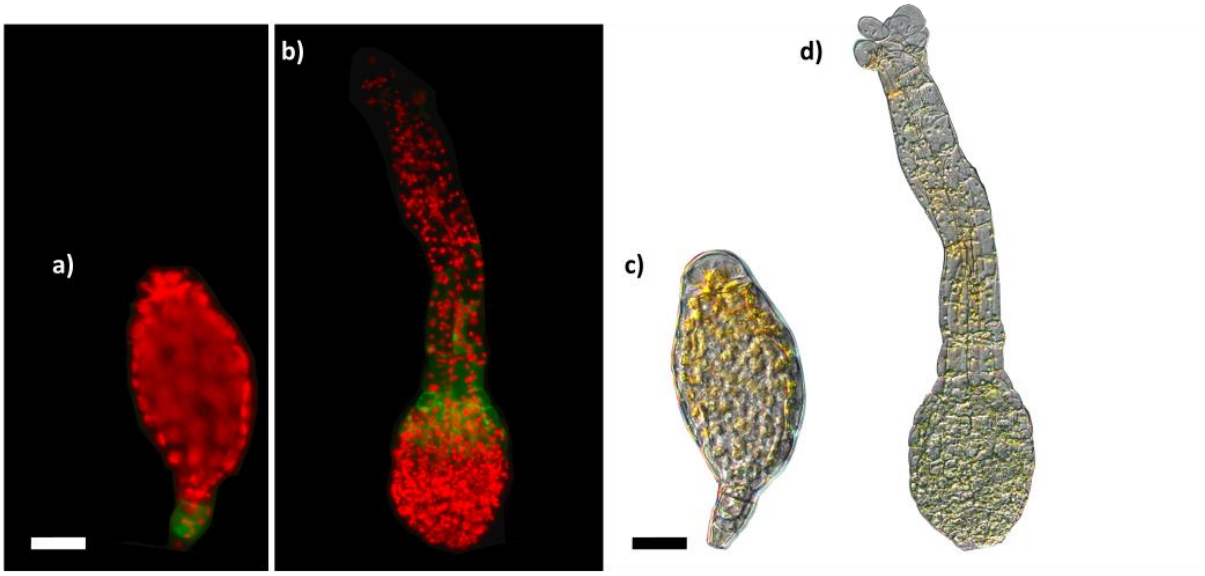

Figure 2: In Physcomitrella, *PpPINC* is dynamically expressed in reproductive organs. With fluorescence-microscopy we visualized citrine expression in a *PpPINC* promoter line (green). Red marks autofluorescence of chlorophyll: a) and c) mature antheridium shortly before sperm cells are released (scale bar = 25 µm). Sperm cells can be seen inside the antheridium in c). b) and d) mature and opened archegonium (scale bar = 50 µm).

Vegetative growth is unaltered in *pin*C mutant

To understand the role of *PpPINC* in the Physcomitrella life cycle, we created targeted knockout mutants via homologous recombination in the background of a fertile Physcomitrella WT. Out of 12 targeted mutant lines devoid of *PpPINC* expression, three independent, haploid mutant lines (*pin*C#10, *pin*C#29, *pin*C#69) with single integration of the knockout construct in the genome were chosen for further analysis (Supplemental Fig. S5). On solid medium we could not detect obvious phenotypic differences to WT regarding stem length, leaf length and leaf width as well as overall growth (Supplemental Fig. S6).

Altered sperm motility and phenotype in *pin*C mutants

When WT and *pinC* mutants were grown in gametangia-inducing conditions, i.e. 15° C and short day (Hohe *et al*., 2002), male and female gametangia developed without any observable differences.

bioRxiv preprint doi: https://doi.org/10.1101/2022.07.05.498815; this version posted July 5, 2022. The copyright holder for this preprint (which was not certified by peer review) is the author/funder, who has granted bioRxiv a license to display the preprint in perpetuity. It is made available under aCC-BY-NC-ND 4.0 International license.

However, we detected an increased motility of *pinC* mutant sperm cells (spermatozoids). In WT, 38.9 ± 1 % of spermatozoids are motile 5 minutes after release from the opened antheridium. All three *pin*C mutant lines showed a significantly increased motility ($p < 0.00001$) of more than 60 % compared to WT (*pin*C#10 = 64.8 ± 2.75 %, *pin*C#29 = 63.8 ± 1.51 %, *pin*C#69 = 62.3 ± 2.32 %) (Fig. 3a, b, c). For a deeper analysis we focused on the line *pin*C#29. When looking closer at the phenotype of the spermatozoids we observed that a majority of WT spermatozoids have coiled flagella (59.8 ± 11.96 % coiled) (Fig. 3d, g, h), while in the mutant *pin*C#29 the vast majority of spermatozoids have non-coiled flagella (94.48 ± 5.22 %) (Fig. 3e, f). It was shown by Ortiz-Ramírez *et al.* (2017) that calcium concentration in Physcomitrella sperm cells can alter their motility. However, staining with the calcium-sensitive dye Fluo-4 did not reveal differences in calcium concentrations inside the sperms of WT and mutant *pin*C#29 (Supplemental Fig. S7).

bioRxiv preprint doi: https://doi.org/10.1101/2022.07.05.498815; this version posted July 5, 2022. The copyright holder for this preprint (which was not certified by peer review) is the author/funder, who has granted bioRxiv a license to display the preprint in perpetuity. It is made available under aCC-BY-NC-ND 4.0 International license.

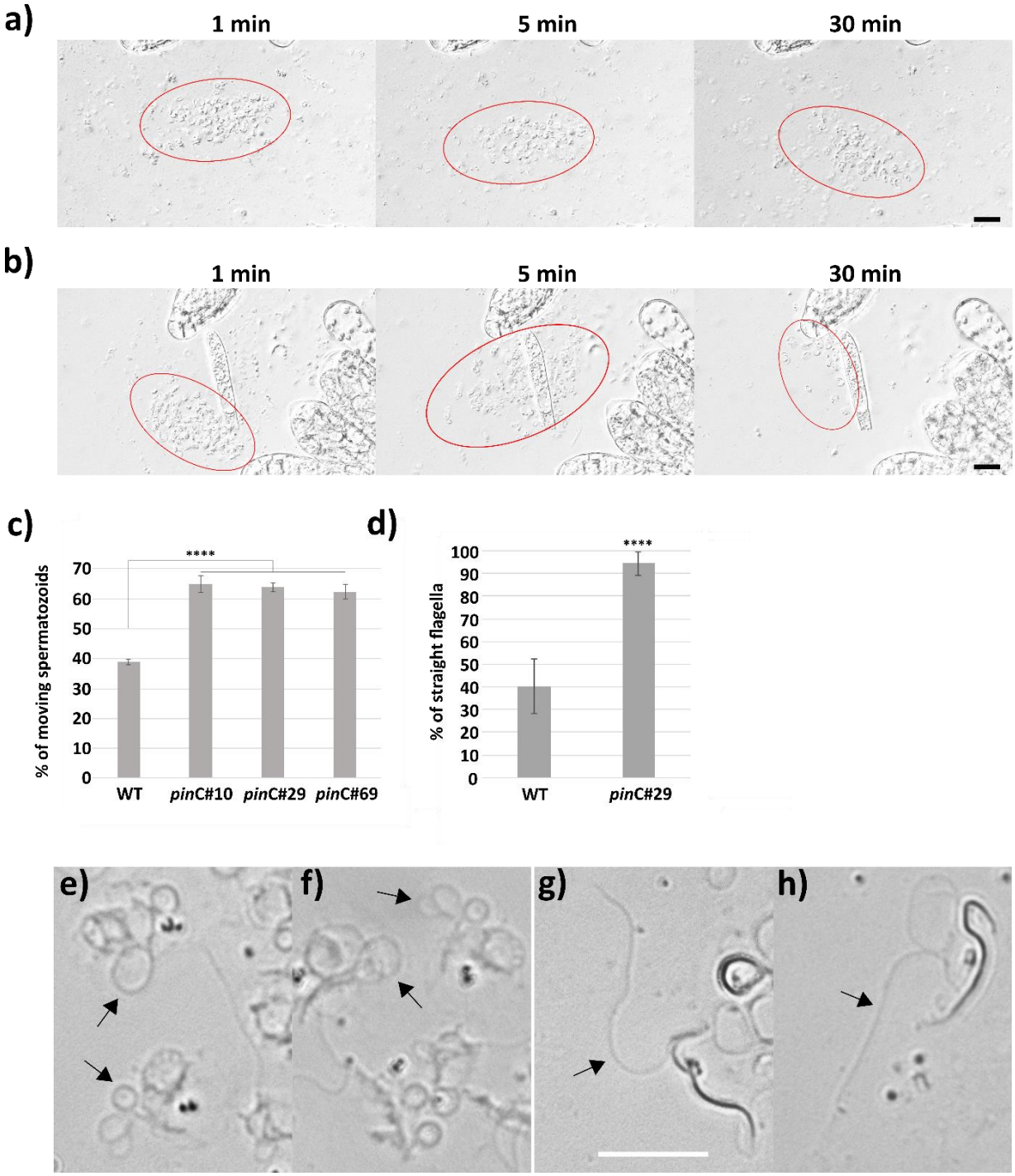

Figure 3: Sperm morphology and motility in Physcomitrella WT and *pin*C mutants. Mutant sperm cells are more motile and have less coiled flagella compared to WT sperm cells. a) WT and b) *pin*C#29 spermatozoids one, five and 30 minutes after being released from a single antheridium, respectively (bar = 20 µm). Areas circled in red highlight spermatozoids after release. c) Percentage of moving spermatozoids after being released from the antheridium (n = 10). d) Percentage of non-coiled flagella compared to coiled flagella (WT: n = 7 antheridia, *pin*C#29: n = 9 antheridia). Asterisks in c) and d) = $p \leq 0.0001$. e) and f) WT spermatozoids with coiled flagella marked by arrows. g) and h) *pin*C#29

bioRxiv preprint doi: https://doi.org/10.1101/2022.07.05.498815; this version posted July 5, 2022. The copyright holder for this preprint (which was not certified by peer review) is the author/funder, who has granted bioRxiv a license to display the preprint in perpetuity. It is made available under aCC-BY-NC-ND 4.0 International license.

spermatozoids with non-coiled flagella marked by arrows. e) – h) bar = 10 µm. For better resolution of sperm cells pictures in a, b, e-h are stacked pictures.

Organ-specific differential gene expression

To identify genes underlying the differences in sperm flagella phenotype, we performed RNAseq analysis on WT and mutant gametangia. For this we collected mature archegonia and antheridia from WT and the *pinC*#29 mutant, cultivated on the same plate, 20 days after start of sporophyte induction. For each line and organ, we pooled eight gametangia per sample which were collected on three different occasions (three samples per organ and line). Mapping of sequenced samples resulted in alignment rates of 71.8 – 93.8 % with the version 3.3 of the Physcomitrella genome (Lang *et al.*, 2018). With 150 bp paired-end Illumina platform-based sequencing, we reached read counts between 19 and 39.8 million for the feature coding sequence (CDS) (Supplemental Fig. S8). No reads could be mapped to the deleted area of *PpPINC* in the mutant line *pin*C#29, which confirms the efficient gene knockout (Supplemental Fig. S9). Between all mutant and all WT samples, we could not find significant differences in gene expression. In contrast, we found a clear separation between male and female gametangia, while the difference between WT and *pin*C mutant was not strong (Fig. 4a). When comparing the samples to each other, we found that for the male samples (WT antheridia WM vs mutant antheridia PM) there were two upregulated (*Pp3c26_6020, Pp3c26_3990*) and nine downregulated genes (*Pp3c9_8920, Pp3c14_8940, Pp3c20_22670, Pp3c1_22810, Pp3c19_15670, Pp3c3_4950, Pp3c3_11110, Pp3c21_8410, Pp3c12_11710*) ($p \leq 0.05$, Fold change (FC) > ± 2, Table 2) (Supplemental Table 2a). Three of the downregulated genes are not annotated so far, while the other genes show counts only in a local part of the gene or exhibit obscure gene structures consisting of only one exon or 22 micro exons. Comparing the female samples, we found one upregulated (*Pp3c11_4360*) and two downregulated (*Pp3c7_8820, Pp3c6_26100)* genes (Supplemental Table 2b), while these genes also show expression only in one part of the gene or show unusual gene structures. When comparing samples derived from antheridia against archegonia, we observed a strong upregulation of genes in male gametangia of both lines. The ratio of upregulated to downregulated genes is higher than 4. The highest number of upregulated genes was found in the comparison between all male and all female samples with 1920 genes upregulated and 397 downregulated genes (Table 2). The results of all DEG experiments are compiled in Supplemental Table 3.

Table 2: Up- and downregulated genes in male (M) and female (F) tissue samples from Physcomitrella WT (W) and *pin*C#29 (P).

	Upregulated genes	**Downregulated genes**
PM vs WM	2	9
PF vs WF	1	2

bioRxiv preprint doi: https://doi.org/10.1101/2022.07.05.498815; this version posted July 5, 2022. The copyright holder for this preprint (which was not certified by peer review) is the author/funder, who has granted bioRxiv a license to display the preprint in perpetuity. It is made available under aCC-BY-NC-ND 4.0 International license.

***pinC*#29 vs WT**	0	0
PM vs PF	1361	245
WM vs WF	1323	298
Male vs Female	1920	397

We analysed the gene ontology (GO) terms of the differentially expressed genes (DEGs) to look for accumulation of specific terms for all experiments (p-value cut off 0.01) but could find enriched terms only in the comparisons between sexes (Fig. 4b), we also found GO enrichment in the upregulated genes only. For the comparison of WT antheridia against WT archegonia (WM vs WF) we found a weak enrichment of the GO term axonemal dynein complex (0.08 %). In the experiment PM vs PF (mutant antheridia vs mutant archegonia) we found that five GO terms were most prominent in the upregulated genes, three of them can be associated with spermatogenesis and one each with energy consumption and DNA synthesis (Cellular Components: cilium = 0.36 %, microtubule organizing center = 0.23 %; Biological Process: carbohydrate catabolic process = 7.2 %, cilium assembly = 1.3 %, purine ribonucleotide metabolic process = 7%). The same is true for the comparison of all antheridia samples with all archegonia samples, where four GO terms associated with spermatogenesis were overrepresented (Cellular Components: cilium = 3.9 %, dynein complex = 2.2 %, intraciliary transport particle B = 0.84 %; Biological Process: cell projection organization = 1.3 %) (Supplemental Table 1). Most of the upregulated DEGs found in the comparison of the sexes were shared between WT and mutant (Fig. 4c). The number of DEGs found exclusively in the mutant was similar between upregulated and downregulated genes (119 / 117). The WT shared the least downregulated genes with the mutant, while contributing more downregulated DEGs to the comparison between male and female (Fig. 4d). We identified some single DEGs, which had been reported to play roles in flagella formation or auxin homeostasis. The coiled coil-like protein *Ppccdc39* (Meyberg *et al.*, 2020) was upregulated almost 3-fold (FC) in male samples compared to female ones (FC = 2.98). While it is also significantly upregulated in the comparison of WT male against female gametangia (FC = 2.4, p = 0.0005), the fold change was even larger in the mutant samples, but due to high variation in the male samples not statistically significant. The arl13b homologue *Pp3c1_40600*, which is involved in flagella stability, was significantly upregulated in the comparison of male against female gametangia (FC = 3.44, p = 0.025), which is also upregulated in the Reute ecotype compared to Gransden (Meyberg *et al.*, 2020). In all comparisons of male against female tissues the arabinogalactan 31 homologue *Pp3c5_9210*, found to be active during spermatogenesis (Meyberg *et al.*, 2020), was upregulated with a higher fold change in PM vs PF (FC = 7.24, p = 2.06E-10) than in WM vs WF (FC = 4.62, p = 1.20E-07) (male vs female FC = 5.34, p = 1.61E-08). We could also find that *PpBELL2* (Horst *et al.*, 2016) was significantly downregulated in all male samples compared to female samples (PM vs PF: FC = -7.53, p = 8.17E-09; WM vs WF: FC = -3.07, p = 0.013, male vs female: FC = -3.85, p = 0.0029). The two PHD clade IIa genes PpMS1A and PpMS1B, are significantly higher expressed in male tissues compared to female

bioRxiv preprint doi: https://doi.org/10.1101/2022.07.05.498815; this version posted July 5, 2022. The copyright holder for this preprint (which was not certified by peer review) is the author/funder, who has granted bioRxiv a license to display the preprint in perpetuity. It is made available under aCC-BY-NC-ND 4.0 International license.

(PpMS1A: Male vs Female FC = 2.35, p = 0.029, *PpMS1B*: Male vs Female FC = 2.81, p = 0.036, WM vs WF FC = 2.04, p = 0.035), as it was also reported in Landberg *et al*. (2022). While not being differentially expressed, we observed expression of all six *PpTAR* genes in both gametangia, with *PpTARB* being the highest expressed, followed by *PpTARA* and *PpTARC*, while *PpTARE* and *PpTARF* being lower expressed and *PpTARD* the lowest of all six genes. We could also find higher expression levels of the two *PpYUCB* and *PpYUCF* in both gametangia, while *PpYUCD* showed a very low, but significantly upregulated expression in archegonia. This indicates active auxin synthesis in mature gametangia. While our transcriptomic data reveal trends in general gene expression, we could not identify any single DEG which could be responsible for the difference in sperm flagella phenotype in the comparison of WT and the mutant.

bioRxiv preprint doi: https://doi.org/10.1101/2022.07.05.498815; this version posted July 5, 2022. The copyright holder for this preprint (which was not certified by peer review) is the author/funder, who has granted bioRxiv a license to display the preprint in perpetuity. It is made available under aCC-BY-NC-ND 4.0 International license.

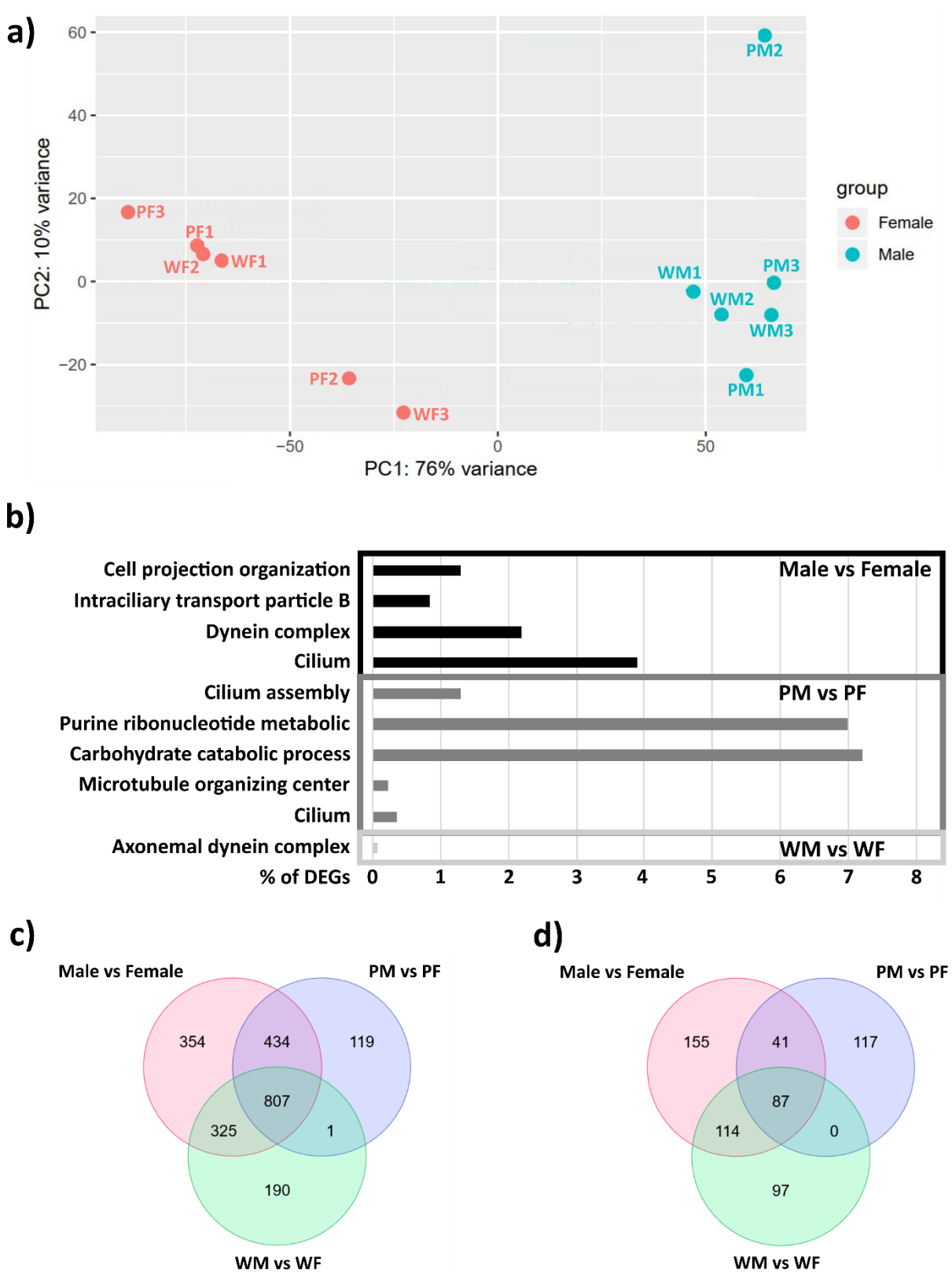

Figure 4: Transcriptomic analysis of Physcomitrella WT and mutant gametangia. a) Variance of all samples. Samples group together into male and female, but there is no clear separation between WT and mutant samples. M = male (antheridia), F = female (archegonia), W = wild type, P = *pin*C#29. b)

bioRxiv preprint doi: https://doi.org/10.1101/2022.07.05.498815; this version posted July 5, 2022. The copyright holder for this preprint (which was not certified by peer review) is the author/funder, who has granted bioRxiv a license to display the preprint in perpetuity. It is made available under aCC-BY-NC-ND 4.0 International license.

All enriched gene ontology terms in upregulated DEGs in the comparison of all male against all female samples (Male vs Female), all wild type male against wild type female (WM vs WF) and mutant male against mutant female samples (PM vs PF). c) Venn diagram of all up- and d) downregulated genes in the comparisons of male and female samples.

No *PpPINC* differences between Gransden and Reute

After we compared expression data of *PpPINC* in the Gransden and Reute ecotype and could not find any differences, we checked for differences in genomic sequences using published data (Lang *et al.*, 2018). We compared the whole genomic *PpPINC* sequence from the 5'UTR to the 3'UTR and could confirm the *PpPINC* gene to be identical between both ecotypes.

Altered fertility and abortion rate

We did not observe any differences in the morphology of mature spore capsules or germination rates of spores between WT and mutant (Supplemental Fig. S10). In contrast, the increased motility of spermatozoids of the *pinC* mutant led to a significantly higher fertility rate in all three lines (Supplemental Fig. S11). Low fertility rates of WT Gransden have been reported (Perroud *et al.*, 2011; Hiss *et al.*, 2017; Meyberg *et al.*, 2020), and in our experiments 5.5 ± 0.4 % of all WT gametophores of a colony produced a sporophyte. In contrast, all *pinC* mutants developed significantly more spore capsules, ranging from 14.5 ± 0.6 % for *pinC*#69, 39.8 ± 1.6 % for *pinC*#10 and 63.2 ± 4.5 % for *pinC*#29. In addition to increased fertility, we detected an increased abortion rate of sporophytes in the mutants (gametophores with aborted sporophytes: WT = 0.1 ± 0.03 %, *pinC*#10 = 8.7 ± 1.3 %, *pinC*#29 = 35.4 ± 1.7 %, *pinC*#69 = 6.5 ± 0.2 %). The aborted sporophytes were no longer attached to the maternal tissue (vaginula). Abortion happened around two weeks after fertilization of the egg cell (for reference of sporophyte development see Ortiz-Ramírez *et al.* (2016) and Lopez-Obando *et al.* (2022)).

In the early embryo, *PpPINC* was active in the lower half, excluding the basal tip cells, as well as in the walls of the maternal tissue that surrounds the young embryo (epigonium) (Fig. 5a). Development of the sporophyte foot and the maternal tissue are highly synchronized. When the embryo has doubled in size and the foot is secured in the now fully developed vaginula (Fig. 5b), the seta forms and rips apart the surrounding tissue of the epigonium, while the later developing spore capsule also starts to separate (Fig. 5c), splitting the epigonium into the calyptra at the apex and the vaginula at the basis of the premeiotic sporophyte. The expression of *PpPINC* slowly declines in the foot of the embryo (Fig. 5a-c), while it increases in the maternal tissue during sporophyte foot growth, forming a distinct ring structure at the border of maternal and sporophytic tissue (Fig. 5b). After the growth spurt, *PpPINC* expression can be found only in the apophysis (region between seta and premeiotic tissue), while excluding the stomata cells (Fig. 5d). We found that Physcomitrella develops a true-type vaginula, where the foot of the sporophyte does not penetrate the gametophore tissue under the vaginula (Fig. 5e, f). Sporophyte

bioRxiv preprint doi: https://doi.org/10.1101/2022.07.05.498815; this version posted July 5, 2022. The copyright holder for this preprint (which was not certified by peer review) is the author/funder, who has granted bioRxiv a license to display the preprint in perpetuity. It is made available under aCC-BY-NC-ND 4.0 International license.

development is polar in Physcomitrella, where the foot of the sporophyte develops faster than the seta or premeiotic spore capsule. The basis of the foot was not in direct contact with the maternal cells, which is in line with an earlier report (Regmi *et al.*, 2017), while the vaginula tightened at its apical border to the sporophyte, which is visible as a reddish-brown coloured ring after the emergence of the premeiotic sporophyte (Fig. 5g, i). In the mature sporophyte, no *PpPINC* expression was detectable.

Aborted sporophytes in WT and mutants were in the premeiotic phase after the separation of the epigonium (comparable to stage shown in Fig. 5g), and no longer attached to the vaginula. No visible defects could be detected, apart from the separation of the gametophore. On one occasion we could observe a sporophyte slipping out of the cavity of the vaginula, not losing contact as the basis of the foot was stuck in the tighter apical end (Fig. 5h). Empty vaginulae clearly showed the coloured ring formation at the apical opening (Fig. 5i). The aborted sporophytes had fully developed foot structures, with haustorium cells at the basis, seta, stomata cells and a depression between seta and haustorium cells, which we believe results from the securement of the sporophyte by the coloured ring formation (Fig. 5j). We could find no morphological differences in the aborted sporophytes between mutants and WT, except for an increase in the number of abortions in the mutants. The calyptra could be removed without resistance, some aborted sporophytes had already lost them (Fig. 5k, l).

bioRxiv preprint doi: https://doi.org/10.1101/2022.07.05.498815; this version posted July 5, 2022. The copyright holder for this preprint (which was not certified by peer review) is the author/funder, who has granted bioRxiv a license to display the preprint in perpetuity. It is made available under aCC-BY-NC-ND 4.0 International license.

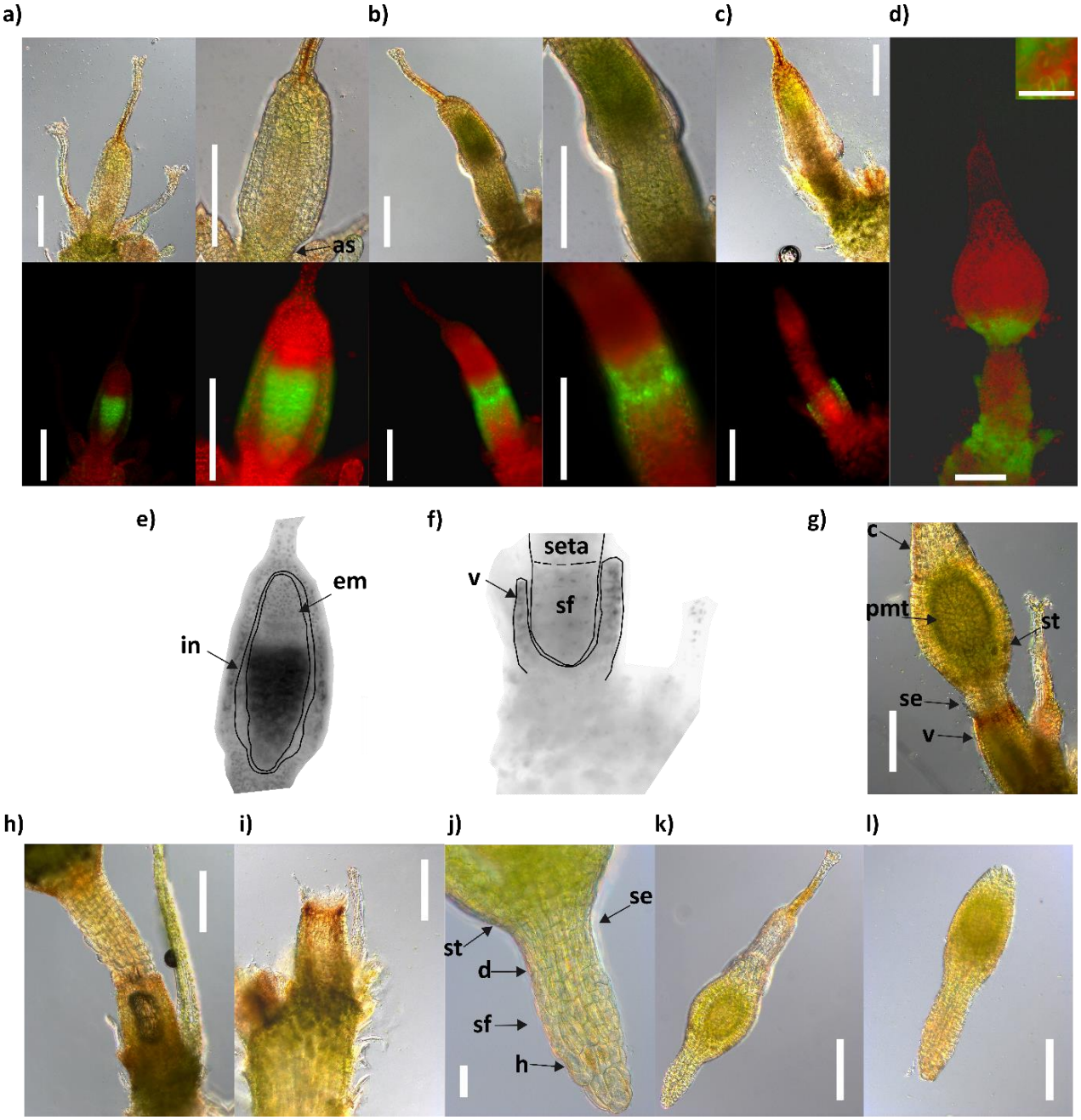

Figure 5: Sporophyte development in Physcomitrella. a)-d) Bright-field and fluorescent microscopy pictures of Physcomitrella PpPINC reporter line. a) Embryo (probably 128 cell stadium) inside the epigonium, as = archegonial stalk. b) Embryo has doubled in size, vaginula and sporophyte foot are fully developed. c) Growth phase of seta, epigonium is about to rupture. d) Premeiotic sporophyte around 14 days post fertilization. The fluorescent signal is concentrated in the apophysis excluding stomata cells (smaller picture, bar = 25 µm). e) and f) = Negative grayscale cut out of a) = e) and c) = f), e) em = embryo, and in = inner wall epigonium are outlined in black. f) Fully developed vaginula (v) with sporophyte foot (sf) and growing seta are indicated by black lines. g) Premeiotic sporophyte, after the epigonium has split into the calyptra (c) and vaginula (v), pmt = premeiotic tissue, se = seta, st = stomata. h) Premeiotic sporophyte slips out of vaginula. f) Empty vaginula after abortion. j) Lower half of an aborted premeiotic sporophyte, d = depression, h = haustorium cells, se = seta, sf = sporophyte foot, st

bioRxiv preprint doi: https://doi.org/10.1101/2022.07.05.498815; this version posted July 5, 2022. The copyright holder for this preprint (which was not certified by peer review) is the author/funder, who has granted bioRxiv a license to display the preprint in perpetuity. It is made available under aCC-BY-NC-ND 4.0 International license.

= stomata). k) Aborted premeiotic sporophyte covered by calyptra. h) – k) = *pinC*#29 mutant. l) Aborted premeiotic sporophyte from WT, not attached to calyptra. Bars in a), c), d), g), h), i), k), and l) = 200 µm. Bar in j) = 50 µm.

Discussion

Auxin plays crucial roles in plant development (Santner & Estelle, 2009; Weijers & Wagner, 2016), including Physcomitrella development (Decker *et al.*, 2006; Menand *et al.*, 2007; Fujita *et al.*, 2008; Coudert *et al.*, 2017; Nemec-Venza *et al.*, 2022) and biotechnology (Ruiz-Molina *et al.*, 2022). Although PIN proteins are central in auxin transport and action (Adamowski & Friml, 2015; Sauer & Kleine-Vehn, 2019; Ung *et al.*, 2022), only two of the three canonical Physcomitrella PIN proteins have been fully characterized; the similar and relatively highly expressed PpPINA and PpPINB. In contrast, little was known about the function of the more divergent and less expressed PpPINC. Here, we strived to close this knowledge gap.

Our data on the expression of *PpPIN*C in young Physcomitrella leaves is in line with an earlier report (Viaene *et al.*, 2014). It was known that the single knockout of *PpPINA* or *PpPINB* has no visible effect on the morphology of the gametophore (Bennett *et al.*, 2014b), and this is also true for *PpPINC*, as we have shown here. However, a double knockout of *PpPINA* and *PpPINB* lead to elongated leaves and stems, similar to treatments with exogenous auxin or auxin transport inhibitors (Bennett *et al.*, 2014b). This means that, while *PpPINA* or *PpPINB* together with *PpPINC* can rescue the knockout of either *A* or *B*, *PpPINC* alone cannot replace the function of both proteins in a double knockout line. The publicly available expression data for canonical PIN proteins in the two Physcomitrella ecotypes Gransden and Reute is not always comparable, as they are different experimental data sets describing specific tissue stages. However, all three canonical PINs have a similar expression pattern regarding tissue and ecotype. All three PINs are expressed in gametophores and sporophytes, with PpPINA and PpPINB being more highly expressed than PpPINC. The expression of all three PINs in vegetative tissue has been reported (Viaene *et al.*, 2014), as well as the important role of PpPINA and PpPINB in sporophyte formation (Bennett *et al.*, 2014b). We could not find any differences between the expression of *PpPINC* in the Gransden and Reute data sets. Further, we did not observe any vegetative phenotype alteration in *pinC* knockout mutants. In contrast, we could identify PpPINC as an important regulator of spermatogenesis and sporophyte development. We therefore conclude that PpPINC is functionally active only in gametangia and sporophytic tissues, contrary to the other two canonical Physcomitrella PIN proteins.

It has been reported that the low fertility of the Physcomitrella ecotype Gransden is based on reduced male fertility (Perroud *et al.*, 2011). This is partially caused by coiled up flagella of spermatozoids in the Gransden ecotype, which results in low sperm motility (Meyberg *et al.*, 2020). We confirm this spermatozoid phenotype for the Gransden ecotype, with a high percentage of coiled flagella and a

bioRxiv preprint doi: https://doi.org/10.1101/2022.07.05.498815; this version posted July 5, 2022. The copyright holder for this preprint (which was not certified by peer review) is the author/funder, who has granted bioRxiv a license to display the preprint in perpetuity. It is made available under aCC-BY-NC-ND 4.0 International license.

motility of under 50 %, resulting in a very low sporophyte production rate. In contrast, the *pin*C mutants, which we generated in the Gransden background, resemble in their sperm morphology and fertility rate the Reute ecotype, which has no coiled flagella, a high sperm motility and a high sporophyte rate (Hiss *et al.*, 2017; Meyberg *et al.*, 2020). The Gransden ecotype was introduced by Engel (1968) as a laboratory strain from one single spore from the UK, and has been propagated mostly vegetatively in laboratories around the world since, while the Reute ecotype was introduced relatively recently as a collection from Germany (Hiss *et al.*, 2017). Compared to Reute, Gransden accumulated somatic, epigenetic mutations, probably leading to the faults in spermatogenesis (Haas *et al.*, 2020).

Here, we found that mature antheridia of a *PpPINC* knockout mutant have a higher expression of spermatogenesis-related genes compared to WT. Activity of a *TAR* gene and *PpPINA* in the apical cells of the mature antheridium has been reported (Landberg *et al.*, 2013; Landberg *et al.*, 2020), while there are no reports of deviating gametangia in *PpPINA* mutants. Here, we also found evidence for expression of auxin synthesis-genes in mature gametangia. With *PpPINC* being expressed in the foot of the mature antheridium, contrary to *PpPINA* in the apical tip cell, it seems to be more important for spermatogenesis controlling auxin homeostasis at the bottom of the antheridium than at the tip. Wether this mode of action is part of a polar auxin homeostasis in a moss organ controlled by PIN proteins needs further clarification.

Gaining the ability to move the flagellum is one of the final steps of spermatogenesis before spermatozoids are released and activated. In mammals, this ability is gained in the epididymis, and is controlled by different external and internal factors (Pereira *et al.*, 2017; O'Flaherty, 2019; Björkgren & Sipilä, 2019). Due to the complexity of the process and a large number of influences, sperm populations are not homogenous, but vary regarding phenotype, motility or activity (Gómez Montoto *et al.*, 2011; Genau *et al*., 2021; Martins-Bessa *et al.*, 2021). A key role in metazoan and Physcomitrella spermatogenesis is played by the evolutionary conserved DNA Topoisomerase 1α, which facilitates chromatin condensation towards the compact sperm head (Gu *et al*., 2022). Activation of the flagella of released spermatozoids depends on changes in pH, calcium concentration, or presence of a chemoattractant released by the egg cell (Nakajima, 2005; Suarez, 2008; Morita *et al.*, 2009). While mammalian spermatozoids are transported through the epididymis during maturation, spermatogenesis in the moss antheridium is stationary. This increases pressure on the exact spatiotemporal expression of spermatogenesis-related genes. As in mammals, Physcomitrella releases heterogeneous sperm populations from one antheridium. This was true for WT where motility (~40 %) and non-coiled flagella (~40 %) seem to fit nicely, whereas in the *pinC*#29 mutant over 90 % of all spermatozoids were straight, with an overall motility of 60 %. While the phenotype of the spermatozoids changed drastically in the mutant, motility did not increase at the same rate. As we have shown, *PpPINC* is expressed only shortly before sperm cells are released, reducing the time it can influence spermatogenesis to a short window. Therefore, alterations in duration and strength of expression, which are likely to occur after somatic

bioRxiv preprint doi: https://doi.org/10.1101/2022.07.05.498815; this version posted July 5, 2022. The copyright holder for this preprint (which was not certified by peer review) is the author/funder, who has granted bioRxiv a license to display the preprint in perpetuity. It is made available under aCC-BY-NC-ND 4.0 International license.

mutations, could explain the differences in sperm morphology between the two ecotypes Gransden and Reute (Meyberg *et al.*, 2020). The *PpPINC* gDNA sequence between the Gransden ecotype (v3.3 Phytozome genome ID:318) and Reute (SRX1528135; Hiss *et al.*, 2017) is identical. Given that the mutant antheridia exhibit an increase in spermatogenesis-related gene expression together with an overall increased motility and fertility, one could argue that PpPINC acts as a repressor for spermatogenesis. The repression of spermatogenesis at the end of the whole process could be a molecular signal for sperm release or activation of flagella. The difference in expression between both ecotypes would be an earlier repression in Gransden, halting spermatogenesis when most of the flagella are coiled and not yet ready for release, while the signal in Reute comes later, when spermatogenesis has progressed to a majority of non-coiled sperm flagella. The unknown activating signal of *PpPINC* expression could therefore be the culprit responsible for reduced male fertility in the Gransden ecotype.

Male sexuality is reduced in many bryophytes, with a female-biased sex ratio (Cameron & Wyatt, 1990; Stark *et al.*, 2010; Pépin *et al.*, 2013; Bisang *et al.*, 2015; de Jong *et al.*, 2018), or size of the plants, with the occurrence of dwarf males (nannandry), which are unique in bryophytes among land plants (Pedersen *et al.*, 2006; Rosengren & Cronberg, 2014; Rosengren *et al.*, 2016; Lang *et al.*, 2021). Dwarf males grow on the leaves of female plants (Pichonet & Gradstein, 2012; Rosengren & Cronberg, 2014; Rosengren *et al.*, 2016; Lang *et al.*, 2021) and increase fertilization success (Hedenäs & Bisang 2012; Rosengren & Cronberg, 2014), in the absence of a female, male spores develop normally. In *Macromitrium japonicum*, dwarf males grew in culture on medium containing auxin, but developed normally on auxin-free medium (Une, 1985). Dioecious mosses grow mostly vegetatively and sporophyte production can be rare due to absence of a sexual partner, while monoecious mosses produce sporophytes more frequently, as the chances for fertilization are higher (Haig, 2016). However, self-fertilization leads to homozygous spores, while self-produced sperm are rarely outcompeted by non-self sperm (Taylor *et al.*, 2007; Rosengren *et al.*, 2016). Reducing male fertility in a monoecious moss increases the chance for outcrossing and could therefore be an internal mechanism, controlling the need to refresh genetic material (McDaniel *et al*., 2010; Haig, 2016; Szovenyi *et al*., 2017). In a monoecious moss like Physcomitrella with a very short life cycle (3-6 months) (Cove, 2005), pressure on mutations regarding the sexual life cycle is strong, as changes in fertility would be lethal (Haig, 2016). Cultivation in vegetative culture in laboratories around the world (Haas *et al.*, 2020) could reduce this pressure on fertility, increasing the risk for severe mutations in the sexual signalling cascade (Meyberg *et al.*, 2020; Haas *et al.*, 2020). As male gametes need more energy and are more complex to build than female gametes (Rydgren & Økland, 2003; Stark *et al.*, 2000, 2009; Horsley *et al.*, 2011; Santos *et al.*, 2022), risk for mutations is higher. This cost calculation would also favour intentionally reducing male rather than female fertility, as more energy is required to constantly produce sperm cells, rather than egg cells, which are waiting for fertilization, ending the gamete production cycle and starting the growth of propagules.

bioRxiv preprint doi: https://doi.org/10.1101/2022.07.05.498815; this version posted July 5, 2022. The copyright holder for this preprint (which was not certified by peer review) is the author/funder, who has granted bioRxiv a license to display the preprint in perpetuity. It is made available under aCC-BY-NC-ND 4.0 International license.

In Arabidopsis, the expression of PIN proteins plays an important role during pollen development, together with anther-specific expression of YUCCA genes (Cecchetti *et al.*, 2008; Dal Bosco *et al.*, 2012). PIN8 locates to the ER and regulates auxin homeostasis with a rate-limiting activity during pollen grain development and pollen tube growth. It is functionally active only during male gametophyte development and a knockout of PIN8 leads to misshaped and aborted pollen (Ding *et al.*, 2012; Bosco *et al.*, 2012). The activity of PIN proteins in male gametophytic tissues is also reported in algae, in *Chara vulgaris* a PIN2-like protein is expressed during spermatogenesis (Żabka *et al.*, 2016). Together with our findings it seems plausible that PIN proteins can play important roles during male gametophytic development in all plants. However, the exclusive function of PIN1 in Arabidopsis in the formation of floral organs, could not be rescued by the Physcomitrella PpPINA protein expressed under the PIN1 promoter, while it complements the vegetative phenotype of the knockout (Zhang *et al.*, 2020).

The abortion of embryos is a natural process. Unfavourable environmental conditions, genetic mutations, injury of the embryo or of maternal tissue can trigger abortion. In mosses, the normal abortion rate differs among species (Stark & Stephenson, 1983; Stark *et al.*, 2009; Rosengren *et al.*, 2016; Hedenäs & Bisang, 2019) and seems to be resource-limited (Stark *et al.*, 2000). Mosses have to allocate their energy between clonal regeneration and sexual reproduction (Stark *et al.*, 2009), and sporophyte survival positively correlates with vegetative growth prior to fertilization (Stark & Stephenson, 1983). In these cases, aborted sporophytes were no longer supported with nutrients and stopped growing inside the vaginula, contrary to the active abortion we observed here.

The haustorium cells of the sporophyte foot are not pressed against the vaginula tissue but surrounded by a placenta-like space, while both tissues are separated by a diffusion barrier (Uzawa & Higuchi, 2010; Regmi *et al.*, 2017). The foot of the sporophyte is wider than the seta with a small depression between seta and foot, while vital sporophytes are tightly attached to the gametophore. We observed a clear polarity during early embryo development favouring growth of the foot, while the upper part of the embryo starts to increase only after the foot is secured in the vaginula. *PpPINC* is active in the maternal tissues which will form the vaginula and the sclerotized ring structure after the sporophyte ruptures the epigonium. Premeiotic sporophytes were aborted after the epigonium had ruptured and the sporophyte foot had to be secured in the vaginula. The increased abortion rate in our mutants, combined with the activity of *PpPINC* at the vaginula-seta junction, point to a regulation of sporophyte securement controlled at least partially by *PpPINC*. Based on our observations, we suggest that the sclerotized, brown ring structure at the vaginula-seta junction has the mechanical function of securing the sporophyte foot.

The polarity of early embryo development we observed here in Physcomitrella as well as the functional significance of the sclerotized ring structure is in line with the findings of Lorch (1909) in the moss family Polytrichaceae. He reported that the sporophyte foot develops first, before the seta subsequently elongates, and as the lumen in the vaginula is not completely filled by the foot, the sclerotized ring

bioRxiv preprint doi: https://doi.org/10.1101/2022.07.05.498815; this version posted July 5, 2022. The copyright holder for this preprint (which was not certified by peer review) is the author/funder, who has granted bioRxiv a license to display the preprint in perpetuity. It is made available under aCC-BY-NC-ND 4.0 International license.

structure must secure the sporophyte (Lorch, 1909). As we could not find a name for this ring structure in the literature, we propose to name the reddish-brown ring structure, formed at the junction of vaginula and seta, the Lorch ring.

Taken together, the canonical Physcomitrella PINC protein is functional in reproductive tissues only, an important regulator of late spermatogenesis and of active abortion of premeiotic sporophytes. Thus, it may integrate environmental signals with developmental programs to regulate sexual reproduction, at least in moss gametangia and early stages of embryo development.

Acknowledgements: We gratefully acknowledge Nico van Gessel for consultation on transcriptomic sequence analysis, Richard Haas for expert technical advice and assistance extracting RNA from gametangia, and Anne Katrin Prowse for proof-reading of the manuscript.

Author contributions: VML, CR, ELD and RR planned and designed the research. VML did most of the experimental work. Data analysis of transcriptomic sequences was done by VML, guided by CR. MB created the knockout constructs and first knockout plants. OH took pictures of spermatozoids and aborted sporophytes. MR did measurements of stems and leaves, while data analysis for this was done by VML. ELD and RR supervised research. VML wrote the manuscript with help by ELD and RR. We gratefully acknowledge funding by the Deutsche Forschungsgemeinschaft (DFG, German Research Foundation) under Germany's Excellence Strategy EXC-2189 (CIBSS to RR) and EXC-2193/1 – 390951807 (*liv*MatS to RR). All authors read and approved the final version of the manuscript.

Declaration: All authors declare to have no competing interests.

ORCID IDs

VLM: 0000-0002-2923-4236; CR: 0000-0002-0672-3897; OH: 0000-0003-3958-5061;

MR: 0000-0002-2659-3372; MB: 0000-0002-3601-5250; ELD: 0000-0002-9151-1361;

RR: 0000-0002-5496-6711

Data availability

All RNA-seq samples as well as the DEG experiments created in this study are available via the NCBI GEO project **GSE205257**. All moss lines used are available via the International Moss Stock Center (IMSC; https://www.moss-stock-center.org) with the following accession numbers: WT = 40095, *PinCPromCit* = 40917, *pin*C#10 = 40918, *pin*C#29 = 40919, *pin*C#69 = 40420.

bioRxiv preprint doi: https://doi.org/10.1101/2022.07.05.498815; this version posted July 5, 2022. The copyright holder for this preprint (which was not certified by peer review) is the author/funder, who has granted bioRxiv a license to display the preprint in perpetuity. It is made available under aCC-BY-NC-ND 4.0 International license.

References

Adamowski M, Friml J. 2015. PIN-dependent auxin transport: Action, regulation, and development. *Plant Cell* **27**: 20–32.

Bennett T, Brockington SF, Rothfels C, Graham SW, Stevenson D, Kutchan T, Rolf M, Thomas P, Wong GK-S, Leyser O, *et al.* 2014a. Paralogous radiations of PIN proteins with multiple origins of noncanonical PIN structure. *Molecular Biology and Evolution* **31**: 2042–2060.

Bennett TA, Liu MM, Aoyama T, Bierfreund NM, Braun M, Coudert Y, Dennis RJ, O'Connor D, Wang XY, White CD, *et al.* 2014b. Plasma membrane-targeted PIN proteins drive shoot development in a moss. *Current Biology* **24**: 2776–2785.

Bierfreund NM, Reski R, Decker EL. 2003. Use of an inducible reporter gene system for the analysis of auxin distribution in the moss *Physcomitrella patens*. *Plant Cell Reports* **21**: 1143–1152.

Bisang I, Ehrlén J, Korpelainen H, Hedenäs L. 2015. No evidence of sexual niche partitioning in a dioecious moss with rare sexual reproduction. *Annals of Botany* **116**: 771–779.

Björkgren I, Sipilä P. 2019. The impact of epididymal proteins on sperm function. *Reproduction* **158**: R155–R167.

Bosco CD, Dovzhenko A, Liu X, Woerner N, Rensch T, Eismann M, Eimer S, Hegermann J, Paponov IA, Ruperti B, *et al.* 2012. The endoplasmic reticulum localized PIN8 is a pollen-specific auxin carrier involved in intracellular auxin homeostasis: Endoplasmic reticulum localized PIN8. *Plant Journal* **71**: 860–870.

Cameron RG, Wyatt R. 1990. Spatial patterns and sex ratios in dioecious and monoecious mosses of the genus Splachnum. *The Bryologist* **93**: 161-166.

Cancé C, Martin-Arevalillo R, Boubekeur K, Dumas R. 2022. ARFs are keys to the many auxin doors. *New Phytologist*: doi: 10.1111/NPH.18159.

Cecchetti V, Altamura MM, Falasca G, Costantino P, Cardarelli M. 2008. Auxin regulates *Arabidopsis* anther dehiscence, pollen maturation, and filament elongation. *Plant Cell* **20**: 1760–1774.

Coudert Y, Bell NE, Edelin C, Harrison CJ. 2017. Multiple innovations underpinned branching form diversification in mosses. *New Phytologist* **215**: 840-850.

Cove D. 2005. The moss *Physcomitrella patens*. *Annual Review of Genetics* **39**: 339-358.

Dal Bosco C, Dovzhenko A, Palme K. 2012. Intracellular auxin transport in pollen: PIN8, PIN5 and PILS5. *Plant Signaling & Behavior* **7**: 1504–1505.

Decker EL, Frank W, Sarnighausen E, Reski R. 2006. Moss systems biology *en route*: Phytohormones in Physcomitrella development. *Plant Biology* **8**: 397–406.

Ding Z, Wang B, Moreno I, Dupláková N, Simon S, Carraro N, Reemmer J, Pěnčík A, Chen X, Tejos R, *et al.* 2012. ER-localized auxin transporter PIN8 regulates auxin homeostasis and male gametophyte development in Arabidopsis. *Nature Communications* **3**: 941.

Egener T, Granado J, Guitton M-C, Hohe A, Holtorf H, Lucht JM, Rensing SA, Schlink K, Schulte J, Schween G, *et al.* 2002. High frequency of phenotypic deviations in *Physcomitrella patens* plants transformed with a gene-disruption library. *BMC Plant Biology* **2**: 6.

Fernandez-Pozo N, Haas FB, Meyberg R, Ullrich KK, Hiss M, Perroud P, Hanke S, Kratz V, Powell AF, Vesty EF, *et al.* 2020. PEATmoss (*Physcomitrella* Expression Atlas Tool): a unified gene expression atlas for the model plant *Physcomitrella patens*. *Plant Journal* **102**: 165–177.

bioRxiv preprint doi: https://doi.org/10.1101/2022.07.05.498815; this version posted July 5, 2022. The copyright holder for this preprint (which was not certified by peer review) is the author/funder, who has granted bioRxiv a license to display the preprint in perpetuity. It is made available under aCC-BY-NC-ND 4.0 International license.

Flores-Sandoval E, Eklund DM, Bowman JL. **2015**. A simple auxin transcriptional response system regulates multiple morphogenetic processes in the liverwort *Marchantia polymorpha*. *PLOS Genetics* **11**: e1005207.

Fujita T, Sakaguchi H, Hiwatashi Y, Wagstaff SJ, Ito M, Deguchi H, Sato T, Hasebe M. **2008**. Convergent evolution of shoots in land plants: lack of auxin polar transport in moss shoots: Convergent evolution of shoots in land plants. *Evolution & Development* **10**: 176–186.

Genau AC, Li Z, Renzaglia KS, Pozo NF, Nogué F, Haas FB, Wilhelmson PKI, Ullrich KK, Schreiber M, Meyberg R, et al. **2021**. HAG1 and SWI3A/B control of male germ line development in *P. patens* suggests conservation of epigenetic reproductive control across land plants. *Plant Reproduction* **34**: 149–173.

Gómez Montoto L, Magaña C, Tourmente M, Martín-Coello J, Crespo C, Luque-Larena JJ, Gomendio M, Roldan ERS. **2011**. Sperm competition, sperm numbers and sperm quality in muroid rodents. *PLOS ONE* **6**: e18173.

Gu N, Chen C, Kabeya Y, Hasebe M, Tamada Y. **2022**. Topoisomerase 1α is required for synchronous spermatogenesis in *Physcomitrium patens*. *New Phytologist* **234**: 137–148.

Haig D. **2016**. Living together and living apart: the sexual lives of bryophytes. *Philosophical Transactions of the Royal Society B: Biological Sciences* **371**: 20150535.

Hashida Y, Takechi K, Abiru T, Yabe N, Nagase H, Hattori K, Takio S, Sato Y, Hasebe M, Tsukaya H, *et al.* 2020. Two *ANGUSTIFOLIA* genes regulate gametophore and sporophyte development in *Physcomitrella patens*. *Plant Journal* **101**: 1318–1330.

Heck MA, Lüth VM, van Gessel N, Krebs M, Kohl M, Prager A, Joosten H, Decker EL, Reski R. 2021. Axenic *in vitro* cultivation of 19 peat moss (*Sphagnum* L.) species as a resource for basic biology, biotechnology and paludiculture. *New Phytologist* **229**: 861-876.

Hedenäs L, Bisang I. **2012**. Sex expression and sex ratios in dwarf male-producing pleurocarpous mosses – have we missed something? *Plant Ecology & Diversity* **5**, 387 – 393.

Hedenäs L, Bisang I. **2019**. Episodic but ample sporophyte production in the moss *Drepanocladus turgescens* (Bryophyta: Amblystegiaceae) in SE Sweden. *Acta Musei Silesiae, Scientiae Naturales* **68**: 83–93.

Hiss M, Laule O, Meskauskiene RM, Arif MA, Decker EL, Erxleben A, Frank W, Hanke ST, Lang D, Martin A, *et al.* 2014. Large-scale gene expression profiling data for the model moss *Physcomitrella patens* aid understanding of developmental progression, culture and stress conditions. *Plant Journal* **79**: 530–539.

Hiss M, Meyberg R, Westermann J, Haas FB, Schneider L, Schallenberg-Rüdinger M, Ullrich KK, Rensing SA. **2017**. Sexual reproduction, sporophyte development and molecular variation in the model moss *Physcomitrella patens*: introducing the ecotype Reute. *Plant Journal* **90**: 606–620.

Hohe A, Reski R. **2002**. Optimisation of a bioreactor culture of the moss Physcomitrella patens for mass production of protoplasts. *Plant Science* **163**: 69–74.

Hohe A, Rensing SA, Mildner M, Lang D, Reski R. **2002**. Day length and temperature strongly influence sexual reproduction and expression of a novel MADS-box gene in the moss *Physcomitrella patens*. *Plant Biology* **4**: 595–602.

Horst NA, Reski R. **2017**. Microscopy of *Physcomitrella patens* sperm cells. *Plant Methods* **13**: 33.

Horst NA, Katz A, Pereman I, Decker EL, Ohad N, Reski R. **2016**. A single homeobox gene triggers phase transition, embryogenesis and asexual reproduction. *Nature Plants* **2**: 15209.

bioRxiv preprint doi: https://doi.org/10.1101/2022.07.05.498815; this version posted July 5, 2022. The copyright holder for this preprint (which was not certified by peer review) is the author/funder, who has granted bioRxiv a license to display the preprint in perpetuity. It is made available under aCC-BY-NC-ND 4.0 International license.

de Jong TJ, During HJ, Shmida A. **2018**. Differences and similarities of sex ratios between dioecious angiosperms and dioicous bryophytes. *Evolutionary Ecology Research* **19**: 365–386.

Karlin EF, Hotchkiss SC, Boles SB, Stenøien HK, Hassel K, Flatberg KI, Shaw AJ. **2012**. High genetic diversity in a remote island population system: *sans* sex. *New Phytologist* **193**: 1088–1097.

Kirbis A, Waller M, Ricca M, Bont Z, Neubauer A, Goffinet B, Szövényi P. **2020**. Transcriptional landscapes of divergent sporophyte development in two mosses, *Physcomitrium* (Physcomitrella) *patens* and *Funaria hygrometrica*. *Frontiers in Plant Science* **11**: 747.

Kofuji R, Hasebe M. **2014**. Eight types of stem cells in the life cycle of the moss *Physcomitrella patens*. *Current Opinion in Plant Biology* **17**: 13–21.

Koshimizu S, Kofuji R, Sasaki-Sekimoto Y, Kikkawa M, Shimojima M, Ohta H, Shigenobu S, Kabeya Y, Hiwatashi Y, Tamada Y, *et al.* 2018. Physcomitrella MADS-box genes regulate water supply and sperm movement for fertilization. *Nature Plants* **4**: 36–45.

Krogh A, Larsson B, von Heijne G, Sonnhammer ELL. **2001**. Predicting transmembrane protein topology with a hidden Markov model: application to complete genomes. *Journal of Molecular Biology* **305**: 567–580.

Landberg K, Pederson ERA, Viaene T, Bozorg B, Friml J, Jonsson H, Thelander M, Sundberg E. **2013**. The moss *Physcomitrella patens* reproductive organ development is highly organized, affected by the two SHI/STY genes and by the level of active auxin in the SHI/STY expression domain. *Plant Physiology* **162**: 1406–1419.

Landberg K, Šimura J, Ljung K, Sundberg E, Thelander M. **2020**. Studies of moss reproductive development indicate that auxin biosynthesis in apical stem cells may constitute an ancestral function for focal growth control. *New Phytologist* **229**: 845-860.

Landberg K, Lopez-Obando M, Sanchez Vera V, Sundberg E, Thelander M. 2022. *MS1/MMD1* homologs in the moss *Physcomitrium patens* are required for male and female gametogenesis. *New Phytologist* doi:10.1111/nph.18352

Lang D, Ullrich KK, Murat F, Fuchs J, Jenkins J, Haas FB, Piednoel M, Gundlach H, Van Bel M, Meyberg R, *et al.* 2018. The *Physcomitrella patens* chromosome-scale assembly reveals moss genome structure and evolution. *Plant Journal* **93**: 515–533.

Lang AS, Gehrmann T, Cronberg N. **2021**. Genetic diversity and population structure in bryophyte with facultative nannandry. *Frontiers in Plant Science* **12**: 517547.

Larkin MA, Blackshields G, Brown NP, Chenna R, McGettigan PA, McWilliam H, Valentin F, Wallace IM, Wilm A, Lopez R, *et al.* 2007. Clustal W and Clustal X version 2.0. *Bioinformatics* **23**: 2947–2948.

Ludwig-Müller J, Sülke S, Bierfreund NM, Decker EL, Reski R. **2009**. Moss (*Physcomitrella patens*) GH3 proteins act in auxin homeostasis. *New Phytologist* **181**: 323–338.

Lopez-Obando M, Hoffmann B, Géry C, Guyon-Debast A, Téoulé E, Rameau C, Bonhomme S, Nogué F. **2016**. Simple and efficient targeting of multiple genes through CRISPR-Cas9 in *Physcomitrella patens*. *G3 (Bethesda, Md.)* **6**: 3647–3653.

Lopez-Obando M, Landberg K, Sundberg E, Thelander M. **2022**. Dependence on clade II bHLH transcription factors for nursing of haploid products by tapetal-like cells is conserved between moss sporangia and angiosperm anthers. *New Phytologist*: nph.17972.

Lorch W. **1909**. Die Polytrichaceen. Eine biologische Monographie. *Abhandlungen der Bayerischen Akademie der Wissenschaften - Mathematisch-naturwissenschaftliche Klasse*: 445–546.

bioRxiv preprint doi: https://doi.org/10.1101/2022.07.05.498815; this version posted July 5, 2022. The copyright holder for this preprint (which was not certified by peer review) is the author/funder, who has granted bioRxiv a license to display the preprint in perpetuity. It is made available under aCC-BY-NC-ND 4.0 International license.

Maciel-Silva A, Cavalcanti Pôrto K. **2014**. Reproduction in Bryophytes. In: Gopal Ramawat K, Merillon JM, Shivanna KR, eds. Reproductive Biology of Plants. CRC Press, 57–84.

Madeira F, Park Y mi, Lee J, Buso N, Gur T, Madhusoodanan N, Basutkar P, Tivey ARN, Potter SC, Finn RD, *et al.* 2019. The EMBL-EBI search and sequence analysis tools APIs in 2019. *Nucleic Acids Research* **47**: W636–W641.

Martins-Bessa A, Quaresma M, Leiva B, Calado A, Navas González FJ. **2021**. Bayesian linear regression modelling for sperm quality parameters using age, body weight, testicular morphometry, and combined biometric indices in donkeys. *Animals* **11**: 176.

McDaniel SF, von Stackelberg M, Richardt S, Quatrano RS, Reski R, Rensing SA. **2010**. The speciation history of the Physcomitrium-Physcomitrella species complex. *Evolution* **64**: 217-231.

Menand B, Yi KK, Jouannic S, Hoffmann L, Ryan E, Linstead P, Schaefer DG, Dolan L. **2020**. An ancient mechanism controls the development of cells with a rooting function in land plants. *Science* **316**: 1477-1480.

Meyberg R, Perroud P, Haas FB, Schneider L, Heimerl T, Renzaglia KS, Rensing SA. **2020**. Characterization of evolutionarily conserved key players affecting eukaryotic flagellar motility and fertility using a moss model. *New Phytologist* **227**: 440-454.

Morita M, Kitamura M, Nakajima A, Sri Susilo E, Takemura A, Okuno M. **2009**. Regulation of sperm flagellar motility activation and chemotaxis caused by egg-derived substance(s) in sea cucumber. *Cell Motility and the Cytoskeleton* **66**: 202–214.

Mosquna A, Katz A, Decker EL, Rensing SA, Reski R, Ohad N. **2009**. Regulation of stem cell maintenance by the Polycomb protein FIE has been conserved during land plant evolution. *Development* **136**: 2433–2444.

Nakajima A. **2005**. Increase in intracellular pH induces phosphorylation of axonemal proteins for activation of flagellar motility in starfish sperm. *Journal of Experimental Biology* **208**: 4411–4418.

Needleman SB, Wunsch CD. **1970**. A general method applicable to the search for similarities in the amino acid sequence of two proteins. *Journal of Molecular Biology* **48**: 443–453.

Nemec-Venza Z, Madden C, Stewart A, Liu W, Novak O, Pencik A, Cuming AC, Kamisugi Y, Harrison CJ. **2022**. CLAVATA modulates auxin homeostasis and transport to regulate stem cell identity and plant shape in a moss. *New Phytologist* **234**: 149–163.

Noy-Malka C, Yaari R, Itzhaki R, Mosquna A, Auerbach Gershovitz N, Katz A, Ohad N. **2014**. A single CMT methyltransferase homolog is involved in CHG DNA methylation and development of *Physcomitrella patens*. *Plant Molecular Biology* **84**: 719–735.

O'Flaherty C. **2019**. Orchestrating the antioxidant defenses in the epididymis. *Andrology* **7**: 662-668.

Ortiz-Ramírez C, Hernandez-Coronado M, Thamm A, Catarino B, Wang M, Dolan L, Feijó JA, Becker JD. **2016**. A transcriptome atlas of *Physcomitrella patens* provides insights into the evolution and development of land plants. *Molecular Plant* **9**: 205–220.

Ortiz-Ramírez C, Michard E, Simon AA, Damineli DSC, Hernández-Coronado M, Becker JD, Feijó JA. **2017**. GLUTAMATE RECEPTOR-LIKE channels are essential for chemotaxis and reproduction in mosses. *Nature* **549**: 91–95.

Ostendorf AK, Van Gessel N, Malkowsky Y, Sabovljevic MS, Rensing SA, Roth-Nebelsick A, Reski R. **2021**. Polyploidization within the Funariaceae—a key principle behind speciation, sporophyte reduction and the high variance of spore diameters? *Bryophyte Diversity and Evolution* **43**: 164-179.

bioRxiv preprint doi: https://doi.org/10.1101/2022.07.05.498815; this version posted July 5, 2022. The copyright holder for this preprint (which was not certified by peer review) is the author/funder, who has granted bioRxiv a license to display the preprint in perpetuity. It is made available under aCC-BY-NC-ND 4.0 International license.

Paponov IA, Teale W, Lang D, Paponov M, Reski R, Rensing SA, Palme K. **2009**. The evolution of nuclear auxin signalling. *BMC Evolutionary Biology* **9**: 126.

Parsons J, Altmann F, Arrenberg CK, Koprivova A, Beike AK, Stemmer C, Gorr G, Reski R, Decker EL. **2012**. Moss-based production of asialo-erythropoietin devoid of Lewis A and other plant-typical carbohydrate determinants: Lewis A-free recombinant EPO from moss. *Plant Biotechnology Journal* **10**: 851–861.

Pedersen N, Russell SJ, Newton AE, Ansell SW. **2006**. A novel molecular protocol for the rapid extraction of DNA from bryophytes and the utility of direct amplification of DNA from a single dwarf male. *The Bryologist* **109**: 257–264.

Pépin F, Hugonnot V, Celle J. **2013**. Sex ratio patterns and fertility of *Hamatocaulis vernicosus* (Mitt.) Hedenäs at different spatial scales. *Journal of Bryology* **35**: 20–26.

Pereira R, Sá R, Barros A, Sousa M. **2017**. Major regulatory mechanisms involved in sperm motility. *Asian Journal of Andrology* **19**: 5-14.

Perroud P-F, Cove DJ, Quatrano RS, McDaniel SF. **2011**. An experimental method to facilitate the identification of hybrid sporophytes in the moss *Physcomitrella patens* using fluorescent tagged lines. *New Phytologist* **191**: 301–306.

Perroud P-F, Haas FB, Hiss M, Ullrich KK, Alboresi A, Amirebrahimi M, Barry K, Bassi R, Bonhomme S, Chen H, *et al.* 2018. The *Physcomitrella patens* gene atlas project: large-scale RNA-seq based expression data. *Plant Journal* **95**: 168–182.

Picelli S, Faridani OR, Björklund ÅK, Winberg G, Sagasser S, Sandberg R. **2014**. Full-length RNA-seq from single cells using Smart-seq2. *Nature Protocols* **9**: 171–181.

Regmi KC, Li L, Gaxiola RA. **2017**. Alternate modes of photosynthate transport in the alternating generations of *Physcomitrella patens*. *Frontiers in Plant Science* **8**: 1956.

Reinhard C, Schween G, Reski R, Hohe A, Egener T, Lucht JM, Holtorf H. **2004**. An improved and highly standardised transformation procedure allows efficient production of single and multiple targeted gene-knockouts in a moss, *Physcomitrella patens*. *Current Genetics* **44**: 339–347.

Reski R. **1998**. Development, genetics and molecular biology of mosses. *Botanica Acta* **111**: 1–15.

Reski R, Abel WO. **1985**. Induction of budding on chloronemata and caulonemata of the moss, *Physcomitrella patens*, using isopentenyladenine. *Planta* **165**: 354–358.

Rosengren F, Cronberg N. **2014**. The adaptive background of nannandry: dwarf male distribution and fertilization in the moss *Homalothecium lutescens*. *Biological Journal of the Linnean Society* **113**: 74–84.

Rosengren F, Cronberg N, Hansson B. **2016**. Balance between inbreeding and outcrossing in a nannandrous species, the moss *Homalothecium lutescens*. *Heredity* **116**: 107–113.

Ruiz-Molina N, Parsons J, Schroeder S, Posten C, Reski R, Decker EL. **2022**. Process engineering of biopharmaceutical production in moss bioreactors *via* model-based description and evaluation of phytohormone impact. *Frontiers in Bioengineering and Biotechnology* **10**: 837965.

Santner A, Estelle M. **2009**. Recent advances and emerging trends in plant hormone signalling. *Nature* **459**: 1071–1078.

Santos WL, Pôrto KC, Pinheiro F 2022. Sex-specific differences in reproductive life-history traits of the moss *Weissia jamaicensis*. *American Journal of Botany* **109**: 645-654.

bioRxiv preprint doi: https://doi.org/10.1101/2022.07.05.498815; this version posted July 5, 2022. The copyright holder for this preprint (which was not certified by peer review) is the author/funder, who has granted bioRxiv a license to display the preprint in perpetuity. It is made available under aCC-BY-NC-ND 4.0 International license.

Sauer M, Kleine-Vehn J. **2019**. PIN-FORMED and PIN-LIKES auxin transport facilitators. *Development* **146**: dev168088.

Schaefer DG, Zrÿd J-P. **2001**. The moss *Physcomitrella patens*, now and then. *Plant Physiology* **127**: 1430–1438.

Schween G, Fleig S, Reski R. **2002**. High-throughput-PCR screen of 15,000 transgenic Physcomitrella plants. *Plant Molecular Biology Reporter* **20**: 43–47.

Sonnhammer EL, von Heijne G, Krogh A. 1998. A hidden Markov model for predicting transmembrane helices in protein sequences. *Proc Int Conf Intell Syst Mol Biol* **6**: 175-182.

Stark LR, Stephenson AG. **1983**. Reproductive biology of *Entodon cladorrhizans* (Bryopsida, Entodontaceae). II. Resource-limited reproduction and sporophyte abortion. *Systematic Botany* **8**: 389-394.

Stark LR, Mishler BD, McLetchie DN. **2000**. The cost of realized sexual reproduction: assessing patterns of reproductive allocation and sporophyte abortion in a desert moss. *American Journal of Botany* **87**: 1599–1608.

Stark LR, Brinda JC, McLetchie DN. **2009**. An experimental demonstration of the cost of sex and a potential resource limitation on reproduction in the moss *Pterygoneurum* (Pottiaceae). *American Journal of Botany* **96**: 1712–1721.

Stark LR, McLetchie DN, Eppley SM. **2010**. Sex ratios and the shy male hypothesis in the moss *Bryum argenteum* (Bryaceae). *The Bryologist* **113**: 788–797.

Suarez SS. **2008**. Control of hyperactivation in sperm. *Human Reproduction Update* **14**: 647–657.

Szovenyi P, Ullrich KK, Rensing SA, Lang D, van Gessel N, Stenoien HK, Conti E, Reski R. **2017**. Selfing in haploid plants and efficacy of selection: Codon usage bias in the model moss *Physcomitrella patens*. *Genome Biology and Evolution* **9**: 1528–1546.

Takechi K, Nagase H, Furuya T, Hattori K, Sato Y, Miyajima K, Higuchi T, Matsuda R, Takio S, Tsukaya H, *et al.* 2021. Two atypical ANGUSTIFOLIA without a plant-specific C-terminus regulate gametophore and sporophyte shapes in the moss *Physcomitrium* (*Physcomitrella*) *patens*. *Plant Journal* **105**: 1390–1399.

Thelander M, Landberg K, Sundberg E. **2018**. Auxin-mediated developmental control in the moss *Physcomitrella patens*. *Journal of Experimental Botany* **69**: 277–290.

Thelander M, Landberg K, Sundberg E. **2019**. Minimal auxin sensing levels in vegetative moss stem cells revealed by a ratiometric reporter. *New Phytologist* **224**: 775-788.

Ung KL, Winkler M, Schulz L, Kolb M, Janacek DP, Dedic E, Stokes DL, Hammes UZ, Pedersen BP. 2022. Structures and mechanism of the plant PIN-FORMED auxin transporter. *Nature*, https://doi.org/10.1038/s41586-022-04883-y

Uzawa M, Higuchi M. **2010**. Comparative development of the sporophyte–gametophyte junction in six moss species. *Journal of Plant Research* **123**: 777–787.

Viaene T, Landberg K, Thelander M, Medvecka E, Pederson E, Feraru E, Cooper ED, Karimi M, Delwiche CF, Ljung K, *et al.* 2014. Directional auxin transport mechanisms in early diverging land plants. *Current Biology* **24**: 2786–2791.

Weijers D, Wagner D. **2016**. Transcriptional responses to the auxin hormone. *Annual Review of Plant Biology* **67**: 539–574.

bioRxiv preprint doi: https://doi.org/10.1101/2022.07.05.498815; this version posted July 5, 2022. The copyright holder for this preprint (which was not certified by peer review) is the author/funder, who has granted bioRxiv a license to display the preprint in perpetuity. It is made available under aCC-BY-NC-ND 4.0 International license.

Wiedemann G, van Gessel N, Köchl F, Hunn L, Schulze K, Maloukh L, Nogué F, Decker EL, Hartung F, Reski R. **2018**. RecQ helicases function in development, DNA repair, and gene targeting in *Physcomitrella patens*. *Plant Cell* **30**: 717–736.

Żabka A, Polit JT, Winnicki K, Paciorek P, Juszczak J, Nowak M, Maszewski J. **2016**. PIN2-like proteins may contribute to the regulation of morphogenetic processes during spermatogenesis in *Chara vulgaris*. *Plant Cell Reports* **35**: 1655–1669.

Zhang Y, Rodriguez L, Li L, Zhang X, Friml J. **2020**. Functional innovations of PIN auxin transporters mark crucial evolutionary transitions during rise of flowering plants. *Science Advances* **6**: eabc8895.

bioRxiv preprint doi: https://doi.org/10.1101/2022.07.05.498815; this version posted July 5, 2022. The copyright holder for this preprint (which was not certified by peer review) is the author/funder, who has granted bioRxiv a license to display the preprint in perpetuity. It is made available under aCC-BY-NC-ND 4.0 International license.

Supporting Information

Supplemental Figure S1: Genetic structure and protein motifs of Physcomitrella PIN proteins

Supplemental Figure S2: Alignments of protein sequences of Physcomitrella and Arabidopsis PIN proteins

Supplemental Figure S3: Expression data of Physcomitrella PIN genes from PEATmoss database

Supplemental Figure S4: Molecular evaluation of *pinCPromCit*

Supplemental Figure S5: Molecular analysis of Physcomitrella *pin*C mutant lines

Supplemental Figure S6: Phenotypical characterization of vegetative tissue for Physcomitrella wild type (WT) and *pin*C mutant lines.

Supplemental Figure S7: Calcium concentration in Physcomitrella spermatozoids

Supplemental Figure S8: Quality control RNAseq

Supplemental Figure S9: Proof of *PpPINC* mutation in *pin*C#29

Supplemental Figure S10: Size of spore capsules and spore germination rate

Supplemental Figure S11: Spore capsule numbers

Supplemental Table 1: Primers used in Physcomitrella WT and mutant lines

Supplemental Table 2: Differentially expressed genes in Physcomitrella WT and mutant

Supplemental Table 3: All DEG experiments, including table of single genes already identified in other publications

bioRxiv preprint doi: https://doi.org/10.1101/2022.07.05.498815; this version posted July 5, 2022. The copyright holder for this preprint (which was not certified by peer review) is the author/funder, who has granted bioRxiv a license to display the preprint in perpetuity. It is made available under aCC-BY-NC-ND 4.0 International license.

a)

Gene	Exon 1	Intron 1	Exon 2	Intron 2	Exon 3	Intron 3	Exon 4	Intron 4	Exon 5	Intron 5	Exon 6
Pp3c_23_10200	1465	263	289	208	86	187	158	141	77	178	67
Pp3c24_2970	1462	258	292	203	86	195	158	139	77	191	67
Pp3C10_24880	1417	110	292	209	86	148	158	171	77	133	67

bioRxiv preprint doi: https://doi.org/10.1101/2022.07.05.498815; this version posted July 5, 2022. The copyright holder for this preprint (which was not certified by peer review) is the author/funder, who has granted bioRxiv a license to display the preprint in perpetuity. It is made available under aCC-BY-NC-ND 4.0 International license.

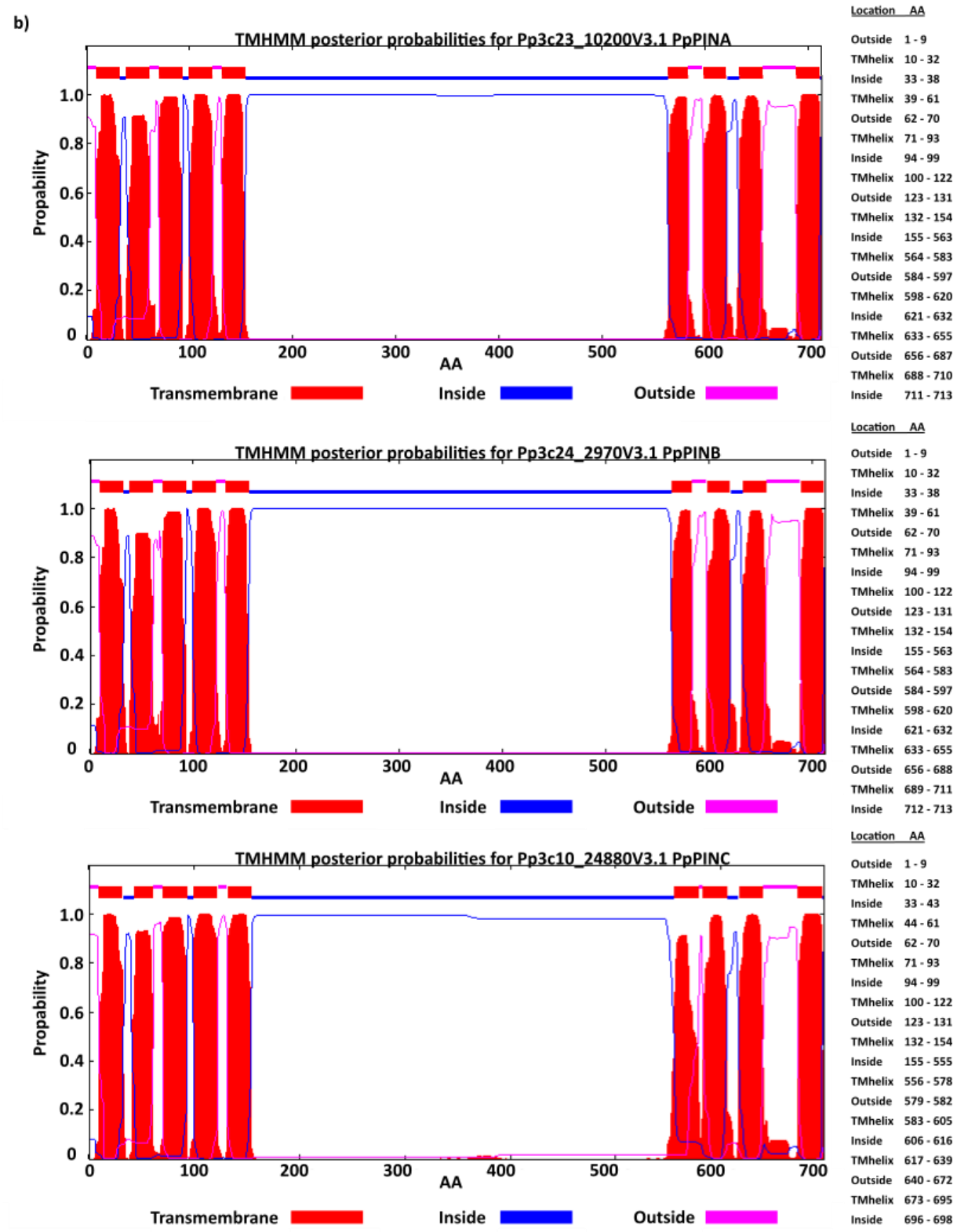

Supplemental Figure S1: Genetic structure and protein motifs of Physcomitrella PIN proteins. a) Genetic structure of canonical Physcomitrella *PIN* genes, length of exons and introns in base pairs (bp) b) Protein motifs of three Physcomitrella PIN proteins assessed with TMHMM2.0 using the DTU Health Tech online tool (Krogh *et al*., 2001).

bioRxiv preprint doi: https://doi.org/10.1101/2022.07.05.498815; this version posted July 5, 2022. The copyright holder for this preprint (which was not certified by peer review) is the author/funder, who has granted bioRxiv a license to display the preprint in perpetuity. It is made available under aCC-BY-NC-ND 4.0 International license.

a)

PpPINA HL and PpPINB HL

```
Length: 409
Identity:     353/409 (86.3%)
Similarity:   374/409 (91.4%)
Gaps:           2/409 (0.5%)
Score: 1819.0

PINALOOP           1 AAKILIMQQFPENAASIVSFKVDSDVMSLDGREPVLTEAEIGDDGKLHVK     50
                     ||||||||||||||.||||||||||||||||||||||||||||||||||||
PINBLOOP           1 AAKILIMQQFPENAGSIVSFKVDSDVMSLDGREPVLTEAEIGDDGKLHVK     50

PINALOOP          51 VRRSVSSRSQGMHSAHHSMPSSKALTPRPSNLTGAEIYSMHSSVNLTPRD    100
                     ||||||||||||||||||||||||||||||||||||||||||||||||||
PINBLOOP          51 VRRSVSSRSQGMHSAHHSMPSSKALTPRPSNLTGAEIYSMHSSVNLTPRD    100

PINALOOP         101 SSFNQGEFHSMMSQRSPHRQSNFDTSDVYSLQSSRGPTPRSSNFNEENSK    150
                     |||||||:.|||:|||||||||||.|||||||||||||||:|||||||||
PINBLOOP         101 SSFNQGEYFSMMAQRSPHRQSNFDISDVYSLQSSRGPTPRTSNFNEENSK    150

PINALOOP         151 DIHTHHRGLNMNSPRFAPPLYRNGMGARMFTPRPGLGGIGVPGTDCTGHG    200
                     |:||||||||:.||||.||||||..|.|||.||.||||:.|.|.|.||||
PINBLOOP         151 DMHTHHRGLNLTSPRFVPPLYRNVAGGRMFMPRTGLGGLPVHGNDPTGHG    200

PINALOOP         201 TLSTLGAPGMGPDGRTIYPGSQTAINILTLGGAANVNATAPSTAVNTQIV    250
                     :|||||.||||||||||||||||||:::|.||..|: ||..|:::|||||
PINBLOOP         201 SLSTLGTPGMGPDGRTIYPGSQTAISLVTPGGTGNI-ATPLSSSLNTQIV    249

PINALOOP         251 NPVYSPQASQIAKKVKDPKASPRADEDAKELHMFVWSANASPVSEAGLHV    300
                     ||||||:||||||||||.:.||::||||||||||||||||||||||||||
PINBLOOP         250 NPVYSPRASQIAKKVKDTRTSPKSDEDAKELHMFVWSANASPVSEAGLHV    299

PINALOOP         301 FGGNDTSANLQQRFDPKEVRMLVHPQLDRGLAAASPRTYDEYTREDFSFG    350
                     ||||||||||.|.||||||||||||||.|.....|:||||||.|.:||||||
PINBLOOP         300 FGGNDTSANLHQSFDPKEVRMLVHPQSDLRHPEANPRTYDNYAQEDFSFG    349

PINALOOP         351 NRNDLKLEDLDKDGPRLD-KFGSTSTAELTPKLAEDEAKKSMPPSAVMIK    399
                     |||||||||||||||||| |||||||||||||:.|||||||||||||||||
PINBLOOP         350 NRNDLKLEDLDKDGPRLDNKFGSTSTAELTPKVPEDEAKKSMPPSAVMIK    399

PINALOOP         400 LIAVMTFRK    408
                     |||||||||
PINBLOOP         400 LIAVMTFRK    408
```

PpPINA HL and PpPINC HL

```
Length: 411
Identity:     266/411 (64.7%)
Similarity:   316/411 (76.9%)
Gaps:          21/411 (5.1%)
Score: 1312.5

PINALOOP           1 AAKILIMQQFPENAASIVSFKVDSDVMSLDGREPVLTEAEIGDDGKLHVK     50
                     ||:||||.:||||||||||||||:||||||||.:|||||||..:||||||:
PINCLOOP           1 AARILIMHRFPENAASIVSFKVESDVMSLDGPDPVLTEAEFRNDGKLHVR     50

PINALOOP          51 VRRSVSSRSQGMHSAHHSMPSSKALTPRPSNLTGAEIYSMHSSVNLTPRD    100
                     |||||||||||:|||:||:|||||||||.|||:.||||||:||||||||.
PINCLOOP          51 VRRSVSSRSQGVHSANHSIPSSKALTPRASNLSNAEIYSMNSSVNLTPRG    100

PINALOOP         101 SSFNQGEFHSMMSQRSPHRQSNFDTSDVYSLQSSRGPTPRSSNFNEENSK    150
                     |||::||..|.|:.|.|:|:|||||||:||||||||||||:|||||||||
PINCLOOP         101 SSFDRGEDCSTMAHRDPNRKSNFDTSDIYSLQSSRGPTPRNSNFNEENSK    150

PINALOOP         151 DIHTHHRGLNMNSPRFAPPLYRNGMGARMFTPRPGLGGIGVPGTDCTGHG    200
                     ::|.|...||:|.||||||||||||.|.|:|..|..|||:|....:...|
PINCLOOP         151 EVHNHRGALNVNIPRFAPPLYRNGSGGRLFMARSDLGGVGALSFEPAAH-    199

PINALOOP         201 TLSTLGAPGMGPDGRTIYPGSQTAINILTLGGAANVNATAPSTAVNTQIV    250
                                 .|||||||||||    |.::|     |..|..|::.|:|.|:
PINCLOOP         200 --------SMGPDGRTIYPG----ITVVT-----NSVAAVPASGVSTHII    232

PINALOOP         251 NPVYSPQASQIAKKVKDPKAS-PRADEDAKELHMFVWSANASPVSEAGLH    299
```

bioRxiv preprint doi: https://doi.org/10.1101/2022.07.05.498815; this version posted July 5, 2022. The copyright holder for this preprint (which was not certified by peer review) is the author/funder, who has granted bioRxiv a license to display the preprint in perpetuity. It is made available under aCC-BY-NC-ND 4.0 International license.

```
                        |||:||..||:||||.||:|| |:.||:||||||||.|||.:.|||..||
PINCLOOP          233 NPVFSPLVSQVAKKVNDPRASIPKTDEEAKELHMFVSSANPTSVSEGELH    282

PINALOOP          300 VFGGNDTSANLQQRFDPKEVRMLVHPQLDRGL-AAASPRTYDEYTREDFS    348
                      ||||:|.|.||||..:|||:.:.||||.:..| .||:.:|.||:.|:.||
PINCLOOP          283 VFGGSDISINLQQSVNPKELHVHVHPQSEHHLPGAANHKTQDEHARQGFS    332

PINALOOP          349 FGNRNDLKLEDLDKDGPRLD-KFGSTSTAELTPKLAEDEAKKSMPPSAVM    397
                      ||||.|||:||:|.:|.:|| ||.|..||||.||...||.|.|||||:||
PINCLOOP          333 FGNRRDLKVEDVDNNGSKLDKKFRSILTAELAPKHPMDEGKTSMPPSSVM    382

PINALOOP          398 IKLIAVMTFRK    408
                      ||||.||||||
PINCLOOP          383 IKLICVMTFRK    393
```

PpPINB HL and PpPINC HL

```
Length: 410
Identity:     264/410 (64.4%)
Similarity:   315/410 (76.8%)
Gaps:          19/410 (4.6%)
Score: 1306.0

PINBLOOP            1 AAKILIMQQFPENAGSIVSFKVDSDVMSLDGREPVLTEAEIGDDGKLHVK     50
                      ||:||||.:|||||.|||||||:||||||||.:|||||||..:||||||:
PINCLOOP            1 AARILIMHRFPENAASIVSFKVESDVMSLDGPDPVLTEAEFRNDGKLHVR     50

PINBLOOP           51 VRRSVSSRSQGMHSAHHSMPSSKALTPRPSNLTGAEIYSMHSSVNLTPRD    100
                      ||||||||||||:|||:||:|||||||||.|||:.||||||:||||||||.
PINCLOOP           51 VRRSVSSRSQGVHSANHSIPSSKALTPRASNLSNAEIYSMNSSVNLTPRG    100

PINBLOOP          101 SSFNQGEYFSMMAQRSPHRQSNFDISDVYSLQSSRGPTPRTSNFNEENSK    150
                      |||::||..|.||.|.|:|:||||.||:||||||||||||.|||||||||
PINCLOOP          101 SSFDRGEDCSTMAHRDPNRKSNFDTSDIYSLQSSRGPTPRNSNFNEENSK    150

PINBLOOP          151 DMHTHHRGLNLTSPRFVPPLYRNVAGGRMFMPRTGLGGLPVHGNDPTGHG    200
                      ::|.|...||:..|||.||||||.:|||:||.|:.|||:.....:|..|
PINCLOOP          151 EVHNHRGALNVNIPRFAPPLYRNGSGGRLFMARSDLGGVGALSFEPAAH-    199

PINBLOOP          201 SLSTLGTPGMGPDGRTIYPGSQTAISLVTPGGTGNIATPLSSSLNTQIVN    250
                              .||||||||||||    |::|    |.::|...:|.::|.|:|
PINCLOOP          200 --------SMGPDGRTIYPG----ITVV----TNSVAAVPASGVSTHIIN    233

PINBLOOP          251 PVYSPRASQIAKKVKDTRTS-PKSDEDAKELHMFVWSANASPVSEAGLHV    299
                      ||:||..||:||||.|.|.| ||:||:||||||||.|||.:.|||..|||
PINCLOOP          234 PVFSPLVSQVAKKVNDPRASIPKTDEEAKELHMFVSSANPTSVSEGELHV    283

PINBLOOP          300 FGGNDTSANLHQSFDPKEVRMLVHPQSDLRHP-EANPRTYDNYAQEDFSF    348
                      |||:|.|.||.||.:|||:.:.|||||:...| .||.:|.|.:|::.|||
PINCLOOP          284 FGGSDISINLQQSVNPKELHVHVHPQSEHHLPGAANHKTQDEHARQGFSF    333

PINBLOOP          349 GNRNDLKLEDLDKDGPRLDNKFGSTSTAELTPKVPEDEAKKSMPPSAVMI    398
                      |||.|||:||:|.:|.:||.||.|..||||.||.|.||.|.|||||:|||
PINCLOOP          334 GNRRDLKVEDVDNNGSKLDKKFRSILTAELAPKHPMDEGKTSMPPSSVMI    383

PINBLOOP          399 KLIAVMTFRK    408
                      |||.||||||
PINCLOOP          384 KLICVMTFRK    393
```

PpPINA TM1 and PpPINB TM1

```
Length: 155
Identity:     149/155 (96.1%)
Similarity:   153/155 (98.7%)
Gaps:           0/155 (0.0%)
Score: 792.0

PINATM1             1 MINGHDIYNVLSAMVPLYVAMMLAYGSVKWWGILTPQQCGGINRFVSIFA     50
                      ||||||||||||||||||||||||||||||||||||||||||||||||||
PINBTM1             1 MINGHDIYNVLSAMVPLYVAMMLAYGSVKWWGILTPQQCGGINRFVSIFA     50

PINATM1            51 VPLLSFQFISGNNPYAMNFKFIAADAVSKVLVLLCLGLWARYAKRGSLEW    100
                      ||||||||||||||||||||:||||||||||.||||||||||||:|||||||
PINBTM1            51 VPLLSFQFISGNNPYAMNFRFIAADAVSKVFVLLCLGLWARYSKRGSLEW    100
```

bioRxiv preprint doi: https://doi.org/10.1101/2022.07.05.498815; this version posted July 5, 2022. The copyright holder for this preprint (which was not certified by peer review) is the author/funder, who has granted bioRxiv a license to display the preprint in perpetuity. It is made available under aCC-BY-NC-ND 4.0 International license.

```
PINATM1          101 MITLFVLITIPNTLVMGTPLLAAMYGAGPGDLTVQAVVLQCIIWYTLLLV    150
                     ||||||||||||||||||||||||||.||||||:||||||||||||||||:
PINBTM1          101 MITLFVLITIPNTLVMGTPLLAAMYGPGPGDLTIQAVVLQCIIWYTLLLL    150

PINATM1          151 MYEYR    155
                     |||||
PINBTM1          151 MYEYR    155
```

PpPINA TM1 and PpPINC TM1

```
Length: 155
Identity:     136/155 (87.7%)
Similarity:   145/155 (93.5%)
Gaps:           0/155 (0.0%)
Score: 726.0

PINATM1            1 MINGHDIYNVLSAMVPLYVAMMLAYGSVKWWGILTPQQCGGINRFVSIFA     50
                     ||.|||:||||||||||||||||||.||||||||||||||.||||||||||
PINCTM1            1 MITGHDMYNVLSAMVPLYVAMMLAYASVKWWGILTPQQCDGINRFVSIFA     50

PINATM1           51 VPLLSFQFISGNNPYAMNFKFIAADAVSKVLVLLCLGLWARYAKRGSLEW    100
                     ||||||||:||||||.|||:||||||||||.||.||||||.|::|||||||
PINCTM1           51 VPLLSFQFVSGNNPYEMNFRFIAADAVSKVFVLSCLGLWVRFSKRGSLEW    100

PINATM1          101 MITLFVLITIPNTLVMGTPLLAAMYGAGPGDLTVQAVVLQCIIWYTLLLV    150
                     :||||:|.|||||||:||||||||||:.||.||||||||||||||||||||
PINCTM1          101 VITLFMLTTIPNTLVIGTPLLAAMYGSKPGQLTVQAVVLQCIIWYTLLLV    150

PINATM1          151 MYEYR    155
                     |||||
PINCTM1          151 MYEYR    155
```

PpPINB TM1 and PpPINC TM1

```
Length: 155
Identity:     137/155 (88.4%)
Similarity:   145/155 (93.5%)
Gaps:           0/155 (0.0%)
Score: 732.0

PINBTM1            1 MINGHDIYNVLSAMVPLYVAMMLAYGSVKWWGILTPQQCGGINRFVSIFA     50
                     ||.|||:||||||||||||||||||.||||||||||||||.||||||||||
PINCTM1            1 MITGHDMYNVLSAMVPLYVAMMLAYASVKWWGILTPQQCDGINRFVSIFA     50

PINBTM1           51 VPLLSFQFISGNNPYAMNFRFIAADAVSKVFVLLCLGLWARYSKRGSLEW    100
                     ||||||||:||||||.||||||||||||||||||.||||||.|:||||||||
PINCTM1           51 VPLLSFQFVSGNNPYEMNFRFIAADAVSKVFVLSCLGLWVRFSKRGSLEW    100

PINBTM1          101 MITLFVLITIPNTLVMGTPLLAAMYGPGPGDLTIQAVVLQCIIWYTLLLL    150
                     :||||:|.|||||||:||||||||||..||.||:||||||||||||||||:
PINCTM1          101 VITLFMLTTIPNTLVIGTPLLAAMYGSKPGQLTVQAVVLQCIIWYTLLLV    150

PINBTM1          151 MYEYR    155
                     |||||
PINCTM1          151 MYEYR    155
```

PpPINA TM2 and PpPINB TM2

```
Length: 150
Identity:     143/150 (95.3%)
Similarity:   148/150 (98.7%)
Gaps:           0/150 (0.0%)
Score: 739.0

PINATM2            1 LVWNPNTYSSLLGVIWSLVANRWHLSMPLILYKSVHILSDAGLGMAMFSL     50
                     |||||||||||||||||||||||||.:||||||||||||||||||||||||
PINBTM2            1 LVWNPNTYSSLLGVIWSLVANRWHFTMPLILYKSVHILSDAGLGMAMFSL     50

PINATM2           51 GLFMGLGDRIIVCGTKMAVFGMALRFLAGPAVFAAASYLVGLRGVPLKVS    100
                     ||||||||||:|||.|||:|||:||||||||||||||||||||||||||||
PINBTM2           51 GLFMGLGDRIVVCGRKMAIFGMSLRFLAGPAVFAAASYLVGLRGVPLKVS    100

PINATM2          101 IVQAALPQGIVPFVFAKEYGVHPEILSTAVIFGMLIALPITMVYYILLGL    150
```

bioRxiv preprint doi: https://doi.org/10.1101/2022.07.05.498815; this version posted July 5, 2022. The copyright holder for this preprint (which was not certified by peer review) is the author/funder, who has granted bioRxiv a license to display the preprint in perpetuity. It is made available under aCC-BY-NC-ND 4.0 International license.

```
                        |||||||||||||||||||||||||:||||||||||||||||||||||||||
PINBTM2          101 IVQAALPQGIVPFVFAKEYGVHPEMLSTAVIFGMLIALPITMVYYILLGL    150
```

PpPINA TM2 and PpPINC TM2

```
Length: 150
Identity:     120/150 (80.0%)
Similarity:   132/150 (88.0%)
Gaps:           0/150 (0.0%)
Score: 621.0

PINATM2            1 LVWNPNTYSSLLGVIWSLVANRWHLSMPLILYKSVHILSDAGLGMAMFSL     50
                     |..|||||||||||:|||::.:.||.||||||||.||:||||:|||||||
PINCTM2            1 LTRNPNTYSSLLGVVWSLISFKCHLDMPLILYKSYHIISDAGIGMAMFSL     50

PINATM2           51 GLFMGLGDRIIVCGTKMAVFGMALRFLAGPAVFAAASYLVGLRGVPLKVS    100
                     |||||:|||||.||||.|:|.|.||||.||||||||||||||||.|.||
PINCTM2           51 GLFMGMGDRIIACGTKHALFAMLLRFLVGPAVFAAASYLVGLRGVSLNVS    100

PINATM2          101 IVQAALPQGIVPFVFAKEYGVHPEILSTAVIFGMLIALPITMVYYILLGL    150
                     .||||||||||||||||||.||||||||||||||::.||..::|||||||
PINCTM2          101 TVQAALPQGIVPFVFAKEYNVHPEILSTAVIFGMIVTLPTALLYYILLGL    150
```

PpPINB TM2 and PpPINC TM2

```
Length: 150
Identity:     116/150 (77.3%)
Similarity:   130/150 (86.7%)
Gaps:           0/150 (0.0%)
Score: 606.0

PINBTM2            1 LVWNPNTYSSLLGVIWSLVANRWHFTMPLILYKSVHILSDAGLGMAMFSL     50
                     |..|||||||||||:|||::.:.|..||||||||.||:||||:|||||||
PINCTM2            1 LTRNPNTYSSLLGVVWSLISFKCHLDMPLILYKSYHIISDAGIGMAMFSL     50

PINBTM2           51 GLFMGLGDRIVVCGRKMAIFGMSLRFLAGPAVFAAASYLVGLRGVPLKVS    100
                     |||||:||||:.||.|.|:|.|.||||.||||||||||||||||.|.||
PINCTM2           51 GLFMGMGDRIIACGTKHALFAMLLRFLVGPAVFAAASYLVGLRGVSLNVS    100

PINBTM2          101 IVQAALPQGIVPFVFAKEYGVHPEMLSTAVIFGMLIALPITMVYYILLGL    150
                     .||||||||||||||||||.||||:|||||||||::.||..::|||||||
PINCTM2          101 TVQAALPQGIVPFVFAKEYNVHPEILSTAVIFGMIVTLPTALLYYILLGL    150
```

b)

```
CLUSTAL O(1.2.4) multiple sequence alignment


Pp3c10_24880V3.1.p      MITGHDMYNVLSAMVPLYVAMMLAYASVKWWGILTPQQCDGINRFVSIFAVPLLSFQFVS  60
Pp3c23_10200V3.1.p      MINGHDIYNVLSAMVPLYVAMMLAYGSVKWWGILTPQQCGGINRFVSIFAVPLLSFQFIS  60
Pp3c24_2970V3.1.p       MINGHDIYNVLSAMVPLYVAMMLAYGSVKWWGILTPQQCGGINRFVSIFAVPLLSFQFIS  60
AT5G57090.1             MITGKDMYDVLAAMVPLYVAMILAYGSVRWWGIFTPDQCSGINRFVAVFAVPLLSFHFIS  60
AT1G73590.1             MITAADFYHVMTAMVPLYVAMILAYGSVKWWKIFTPDQCSGINRFVALFAVPLLSFHFIA  60
AT2G01420.2             MITWHDLYTVLTAVVPLYVAMILAYGSVQWWKIFSPDQCSGINRFVAIFAVPLLSFHFIS  60
AT1G70940.1             MISWHDLYTVLTAVIPLYVAMILAYGSVRWWKIFSPDQCSGINRFVAIFAVPLLSFHFIS  60
AT1G23080.1             MITWHDLYTVLTAVIPLYVAMILAYGSVRWWKIFSPDQCSGINRFVAIFAVPLLSFHFIS  60
                        **.  *:* *::*::******:***.**:** *::*:**.******::********:*::

Pp3c10_24880V3.1.p      GNNPYEMNFRFIAADAVSKVFVLSCLGLWVRFSKRGSLEWVITLFMLTTIPNTLVIGTPL  120
Pp3c23_10200V3.1.p      GNNPYAMNFKFIAADAVSKVLVLLCLGLWARYAKRGSLEWMITLFVLITIPNTLVMGTPL  120
Pp3c24_2970V3.1.p       GNNPYAMNFRFIAADAVSKVFVLLCLGLWARYSKRGSLEWMITLFVLITIPNTLVMGTPL  120
AT5G57090.1             SNDPYAMNYHFLAADSLQKVVILAALFLWQAFSRRGSLEWMITLFSLSTLPNTLVMGIPL  120
AT1G73590.1             ANNPYAMNLRFLAADSLQKVIVLSLLFLWCKLSRNGSLDWTITLFSLSTLPNTLVMGIPL  120
AT2G01420.2             TNDPYAMNFRFVAADTLQKIIMLVLLALWANLTKNGSLEWMITIFSLSTLPNTLVMGIPL  120
AT1G70940.1             TNNPYAMNLRFIAADTLQKIIMLSLLVLWANFTRSGSLEWSITIFSLSTLPNTLVMGIPL  120
AT1G23080.1             SNNPYAMNLRFIAADTLQKLIMLTLLIIWANFTRSGSLEWSITIFSLSTLPNTLVMGIPL  120
                         *:** ** :*:***::.*:.:*  * :*   :: ***:* **:* * *:*****:* **

Pp3c10_24880V3.1.p      LAAMYGSKPGQLTVQAVVLQCIIWYTLLLVMYEYRAARILIMHRFPENAASIVSFKVESD  180
Pp3c23_10200V3.1.p      LAAMYGAGPGDLTVQAVVLQCIIWYTLLLVMYEYRAAKILIMQQFPENAASIVSFKVDSD  180
Pp3c24_2970V3.1.p       LAAMYGPGPGDLTIQAVVLQCIIWYTLLLLMYEYRAAKILIMQQFPENAGSIVSFKVDSD  180
```

bioRxiv preprint doi: https://doi.org/10.1101/2022.07.05.498815; this version posted July 5, 2022. The copyright holder for this preprint (which was not certified by peer review) is the author/funder, who has granted bioRxiv a license to display the preprint in perpetuity. It is made available under aCC-BY-NC-ND 4.0 International license.

```
AT5G57090.1             LRAMYGDFSGNLMVQIVVLQSIIWYTLMLFLFEFRGAKLLISEQFPETAGSITSFRVDSD  180
AT1G73590.1             LKGMYGNFSGDLMVQIVVLQCIIWYTLMLFLFEYRGAKLLISEQFPDTAGSIVSIHVDSD  180
AT2G01420.2             LIAMYGTYAGSLMVQVVVLQCIIWYTLLLFLFEYRGAKLLIMEQFPETGASIVSFKVESD  180
AT1G70940.1             LIAMYGEYSGSLMVQIVVLQCIIWYTLLLFLFEFRGAKMLIMEQFPETAASIVSFKVESD  180
AT1G23080.1             LIAMYGEYSGSLMVQIVVLQCIIWYTLLLFLFEYRGAKILIMEQFPETGASIVSFKVESD  180
                        * .***   *.* :* ****.******:*.::*:*.*::** .:**:...**.*::*:**

Pp3c10_24880V3.1.p      VMSLDGPDPVLTEAEFRNDGKLHVRVRRSVSSRSQGV--HSANHSIPSSKALTPRASNLS  238
Pp3c23_10200V3.1.p      VMSLDGREPVLTEAEIGDDGKLHVKVRRSVSSRSQGM--HSAHHSMPSSKALTPRPSNLT  238
Pp3c24_2970V3.1.p       VMSLDGREPVLTEAEIGDDGKLHVKVRRSVSSRSQGM--HSAHHSMPSSKALTPRPSNLT  238
AT5G57090.1             VISLNGREPLQTDAEIGDDGKLHVVVRRSSAASSMISSFNKSHGGGLNSSMITPRASNLT  240
AT1G73590.1             IMSLDGRQPLETEAEIKEDGKLHVTVRRSNASRSDIY------SRRSQGLSATPRPSNLT  234
AT2G01420.2             VVSLDGHDFLETDAEIGNDGKLHVTVRKSNASRRSL--------------MMTPRPSNLT  226
AT1G70940.1             VVSLDGHDFLETDAEIGDDGKLHVTVRKSNASRRSFC------G-----PNMTPRPSNLT  229
AT1G23080.1             VVSLDGHDFLETDAQIGDDGKLHVTVRKSNASRRSFY------GG--GGTNMTPRPSNLT  232
                        ::**:* : : *:*:: :****** **:* ::                    *** ***:

Pp3c10_24880V3.1.p      NAEIYSMNSSVNLTPRGSSFDRGEDCSTMAHRDPNRKSN------------FDTSDIYSL  286
Pp3c23_10200V3.1.p      GAEIYSMHSSVNLTPRDSSFNQGEFHSMMSQRSPHRQSN------------FDTSDVYSL  286
Pp3c24_2970V3.1.p       GAEIYSMHSSVNLTPRDSSFNQGEYFSMMAQRSPHRQSN------------FDISDVYSL  286
AT5G57090.1             GVEIYSVQSSREPTPRASSFNQTDFYAMFNASK-APSPRHGYTNSYGGAGAGPGGDVYSL  299
AT1G73590.1             NAEIYSLQSSRNPTPRGSSFNHTDFYSMMASGG-GRNSN------------FGPGEA--V  279
AT2G01420.2             GAEIYSLS----STPRGSNFNHSDFYSVMGFPG-GRLSN------------FGPADLYSV  269
AT1G70940.1             GAEIYSLS----TTPRGSNFNHSDFYNMMGFPG-GRLSN------------FGPADMYSV  272
AT1G23080.1             GAEIYSLN----TTPRGSNFNHSDFYSMMGFPG-GRLSN------------FGPADMYSV  275
                        ..****:      *** *.*:: :    :         .               .:   :

Pp3c10_24880V3.1.p      QSSRGPTPRNSNFNEENSKEVHNHRGALNVNIPRFAPPLYRNGSGGRLFMARSDLGGVGA  346
Pp3c23_10200V3.1.p      QSSRGPTPRSSNFNEENSKDIHTHHRGLNMNSPRFAPPLYRNGMGARMFTPRPGLGGIGV  346
Pp3c24_2970V3.1.p       QSSRGPTPRTSNFNEENSKDMHTHHRGLNLTSPRFVPPLYRNVAGGRMFMPRTGLGGLPV  346
AT5G57090.1             QSSKGVTPRTSNFDEEVMKTAKKAG-R-GGRS-----------------MSGELYNNN--  338
AT1G73590.1             FGSKGPTPRPSNYEEDGGPAKPTAAGT-AAGAGRF------------HYQSG-GSGGG--  323
AT2G01420.2             QSSRGPTPRPSNFEENNAV--------------KY------------GFYNNTNSSVP--  301
AT1G70940.1             QSSRGPTPRPSNFEENCAMASSP----------RF------------GYYPG-----G--  303
AT1G23080.1             QSSRGPTPRPSNFEESCAMASSP----------RF------------GYYPG-----G--  306
                         .*:* *** **::*.

Pp3c10_24880V3.1.p      LSFEPAA---------HSMGPDGRTIYPGITVVTNSV---------AAVPASGVSTHIIN  388
Pp3c23_10200V3.1.p      PGTDCTGHGTLSTLGAPGMGPDGRTIYPGSQTAINILTLGGAANVNATAPSTAVNTQIVN  406
Pp3c24_2970V3.1.p       HGNDPTGHGSLSTLGTPGMGPDGRTIYPGSQTAISLVTPGGTGNIAT-PLSSSLNTQIVN  405
AT5G57090.1             ----------------------SVPSYPPPNPMFTGSTSGASGVK-KK------------  363
AT1G73590.1             ----------------------GGAHYPAPNPGMFSPNTGGGGGTAAK-----------G  350
AT2G01420.2             ----------------------AAGSYPAPNPEFSTGTGVS------T-----------K  322
AT1G70940.1             ----------------------GAGSYPAPNPEFSSTTTSTANKSVNK-----------N  330
AT1G23080.1             ----------------------APGSYPAPNPEFSTGNKTG-----SK-----------A  328
                                                .   **

Pp3c10_24880V3.1.p      PVFSPLVSQVAKKVNDPRASIPKTDEEAKELHMFVSSANPTSVSEGE-LHVFGGS-DISI  446
Pp3c23_10200V3.1.p      PVYSPQASQIAKKVKDPKAS-PRADEDAKELHMFVWSANASPVSEAG-LHVFGGN-DTSA  463
Pp3c24_2970V3.1.p       PVYSPRASQIAKKVKDTRTS-PKSDEDAKELHMFVWSANASPVSEAG-LHVFGGN-DTSA  462
AT5G57090.1             ------ES-----GGGGSGGGVGVGGQNKEMNMFVWSSSASPVSEANAKNAMTRGSSTD-  411
AT1G73590.1             --------------NAPVVGGKRQDGNGRDLHMFVWSSSASPVSDVFGGG----GGNHHA  392
AT2G01420.2             PNKIPKEN-----QQQLQEKDSKASHDAKELHMFVWSSSASPVSDVFG----GGAGDNVA  373
AT1G70940.1             PKDVNTNQ-----QTTLPTGGKSNSHDAKELHMFVWSSNGSPVSDRAGLNVFGGAPDNDQ  385
AT1G23080.1             PKE------------NHHHVGKSNSNDAKELHMFVWGSNGSPVSDRAGLQVDNGANE-QV  375
                                                . : ::::*** .:. : **:           .

Pp3c10_24880V3.1.p      --NLQQSVNPKELHVHVHPQSEHHLPGA-ANHKTQDEHARQGFSFGNRRDLKVEDVDNNG  503
Pp3c23_10200V3.1.p      --NLQQRFDPKEVRMLVHPQLDRGLAAA--SPRTYDEYTREDFSFGNRNDLKLEDLDKDG  519
Pp3c24_2970V3.1.p       --NLHQSFDPKEVRMLVHPQSDLRHPEA--NPRTYDNYAQEDFSFGNRNDLKLEDLDKDG  518
AT5G57090.1             --------VSTDPKVSIPPHDNLA-TKAMQNLIENMSPG-------RKGHVE----M--D  449
AT1G73590.1             DYSTATNDHQKDVKISVPQG----------NSNDNQYVEREEFSFGNKDDDSKVLAT---  439
AT2G01420.2             --TEQSEQGAKEIRMVVSDQPRKSNARGGGDDI----GGL------DSGEGEREIEK--A  419
AT1G70940.1             --GGRSDQGAKEIRMLVPDQSHNGETKAVAHPASGDFGGEQQFSFAGKEEEAERPKD--A  441
AT1G23080.1             --GKSDQGGAKEIRMLISDHTQNGENKA--GPMNGDYGGE---------EESERVKE--V  420
                                  .: :: :                                   .

Pp3c10_24880V3.1.p      SKLDKKFRSILTAELAPKHPMD----EGKTSMPPSSVMIKLICVMTFRKLTRNPNTYSSL  559
Pp3c23_10200V3.1.p      PRLD-KFGSTSTAELTPKLAED----EAKKSMPPSAVMIKLIAVMTFRKLVWNPNTYSSL  574
Pp3c24_2970V3.1.p       PRLDNKFGSTSTAELTPKVPED----EAKKSMPPSAVMIKLIAVMTFRKLVWNPNTYSSL  574
AT5G57090.1             QDGNNGGK-SPYMGKKGSDVEDGGPGPRKQQMPPASVMTRLILIMVWRKLIRNPNTYSSL  508
AT1G73590.1             -D---------------GGNNISNKTTQAKVMPPTSVMTRLILIMVWRKLIRNPNSYSSL  483
AT2G01420.2             TAGLNKMGSNSTAELEAAGGDGGG--NNGTHMPPTSVMTRLILIMVWRKLIRNPNTYSSL  477
AT1G70940.1             ENGLNKLAPNSTAALQSKTGLGGAEASQRKNMPPASVMTRLILIMVWRKLIRNPNTYSSL  501
AT1G23080.1             PNGLHKLRCNSTAELNPKEAIETGETVPVKHMPPASVMTRLILIMVWRKLIRNPNTYSSL  480
                                                     ***::** :** :*.:***  ***:****

Pp3c10_24880V3.1.p      LGVVWSLISFKCHLDMPLILYKSYHIISDAGIGMAMFSLGLFMGMGDRIIACGTKHALFA  619
```

bioRxiv preprint doi: https://doi.org/10.1101/2022.07.05.498815; this version posted July 5, 2022. The copyright holder for this preprint (which was not certified by peer review) is the author/funder, who has granted bioRxiv a license to display the preprint in perpetuity. It is made available under aCC-BY-NC-ND 4.0 International license.

```
Pp3c23_10200V3.1.p      LGVIWSLVANRWHLSMPLILYKSVHILSDAGLGMAMFSLGLFMGLGDRIIVCGTKMAVFG  634
Pp3c24_2970V3.1.p       LGVIWSLVANRWHFTMPLILYKSVHILSDAGLGMAMFSLGLFMGLGDRIVVCGRKMAIFG  634
AT5G57090.1             FGLAWSLVSFKWNIKMPTIMSGSISILSDAGLGMAMFSLGLFMALQPKIIACGKSVAGFA  568
AT1G73590.1             FGITWSLISFKWNIEMPALIAKSISILSDAGLGMAMFSLGLFMALNPRIIACGNRRAAFA  543
AT2G01420.2             IGLIWALVAYRWHVAMPKILQQSISILSDAGLGMAMFSLGLFMALQPKIIACGNSVATFA  537
AT1G70940.1             IGLIWALVAFRWHVAMPKIIQQSISILSDAGLGMAMFSLGLFMALQPKLIACGNSVATFA  561
AT1G23080.1             IGLIWALVAFRWDVAMPKIIQQSISILSDAGLGMAMFSLGLFMALQPKLIACGNSTATFA  540
                        :*: *:*:: : .. ** ::  *  *:****:***********.:  :::.**   * *.

Pp3c10_24880V3.1.p      MLLRFLVGPAVFAAASYLVGLRGVSLNVSTVQAALPQGIVPFVFAKEYNVHPEILSTAVI  679
Pp3c23_10200V3.1.p      MALRFLAGPAVFAAASYLVGLRGVPLKVSIVQAALPQGIVPFVFAKEYGVHPEILSTAVI  694
Pp3c24_2970V3.1.p       MSLRFLAGPAVFAAASYLVGLRGVPLKVSIVQAALPQGIVPFVFAKEYGVHPEMLSTAVI  694
AT5G57090.1             MAVRFLTGPAVIAATSIAIGIRGDLLHIAIVQAALPQGIVPFVFAKEYNVHPDILSTAVI  628
AT1G73590.1             AAMRFVVGPAVMLVASYAVGLRGVLLHVAIIQAALPQGIVPFVFAKEYNVHPDILSTAVI  603
AT2G01420.2             MAVRFITGPAIMAVAGIAIGLHGDLLRIAIVQAALPQGIVPFVFAKEYNVHPTILSTGVI  597
AT1G70940.1             MAVRFLTGPAVMAVAAIAIGLRGDLLRVAIVQAALPQGIVPFVFAKEYNVHPAILSTGVI  621
AT1G23080.1             MAVRFFTGPAVMAVAAMAIGLRGDLLRVAIVQAALPQGIVPFVFAKEYNVHPAILSTGVI  600
                          :**..***:: .:.  :*::*  *.:: :*****************.*** :***.**

Pp3c10_24880V3.1.p      FGMIVTLPTALLYYILLGL     698
Pp3c23_10200V3.1.p      FGMLIALPITMVYYILLGL     713
Pp3c24_2970V3.1.p       FGMLIALPITMVYYILLGL     713
AT5G57090.1             FGMLVALPVTVLYYVLLGL     647
AT1G73590.1             FGMLIALPITLLYYILLGL     622
AT2G01420.2             FGMLIALPITLVYYILLGL     616
AT1G70940.1             FGMLIALPITLVYYILLGL     640
AT1G23080.1             FGMLIALPITLVYYILLGL     619
```

c)

```
Pp3c10_24880V3.1.p      EENSKEVHNHRGALNVNIPRFAPPLYRNGSGGRLFMARSDLGGVGALSFEPAA-------  353
Pp3c23_10200V3.1.p      EENSKDIHTHHRGLNMNSPRFAPPLYRNGMGARMFTPRPGLGGIGVPGTDCTGHGTLSTL  360
Pp3c24_2970V3.1.p       EENSKDMHTHHRGLNLTSPRFVPPLYRNVAGGRMFMPRTGLGGLPVHGNDPTGHGSLSTL  360
                        *****::*.*: .**:. ***.******  *.*:*  * .***: . . : :.
Pp3c10_24880V3.1.p      --HSMGPDGRTIYPGITVVTNSV---------AAVPASGVSTHIINPVFSPLVSQVAKKV  402
Pp3c23_10200V3.1.p      GAPGMGPDGRTIYPGSQTAINILTLGGAANVNATAPSTAVNTQIVNPVYSPQASQIAKKV  420
Pp3c24_2970V3.1.p       GTPGMGPDGRTIYPGSQTAISLVTPGGTGNIAT-PLSSSLNTQIVNPVYSPRASQIAKKV  419
                           .***********  .. . :         :   ::.:.*:*:***:** .**:****
```

Supplemental Figure S2: Alignments of protein sequences of Physcomitrella and Arabidopsis PIN proteins. a) Needleman-Wunsch (Needleman & Wunsch, 1970) alignments of the hydrophilic loop (HL) as well as N'- and C'-terminal transmembrane regions (TM) of the three canonical Physcomitrella PIN proteins. b) Multiple sequence alignment (Madeira *et al.*, 2019) of the canonical PIN proteins of Physcomitrella and Arabidopsis. c) Differences in the middle of the loop structure of the three canonical PIN proteins in Physcomitrella. Cyan blue = fully conserved, yellow = conserved in two of three; (*) = fully conserved (:) = conservation between amino acid groups of similar properties; (.) = conservation between amino acid groups with weak similar properties.

bioRxiv preprint doi: https://doi.org/10.1101/2022.07.05.498815; this version posted July 5, 2022. The copyright holder for this preprint (which was not certified by peer review) is the author/funder, who has granted bioRxiv a license to display the preprint in perpetuity. It is made available under aCC-BY-NC-ND 4.0 International license.

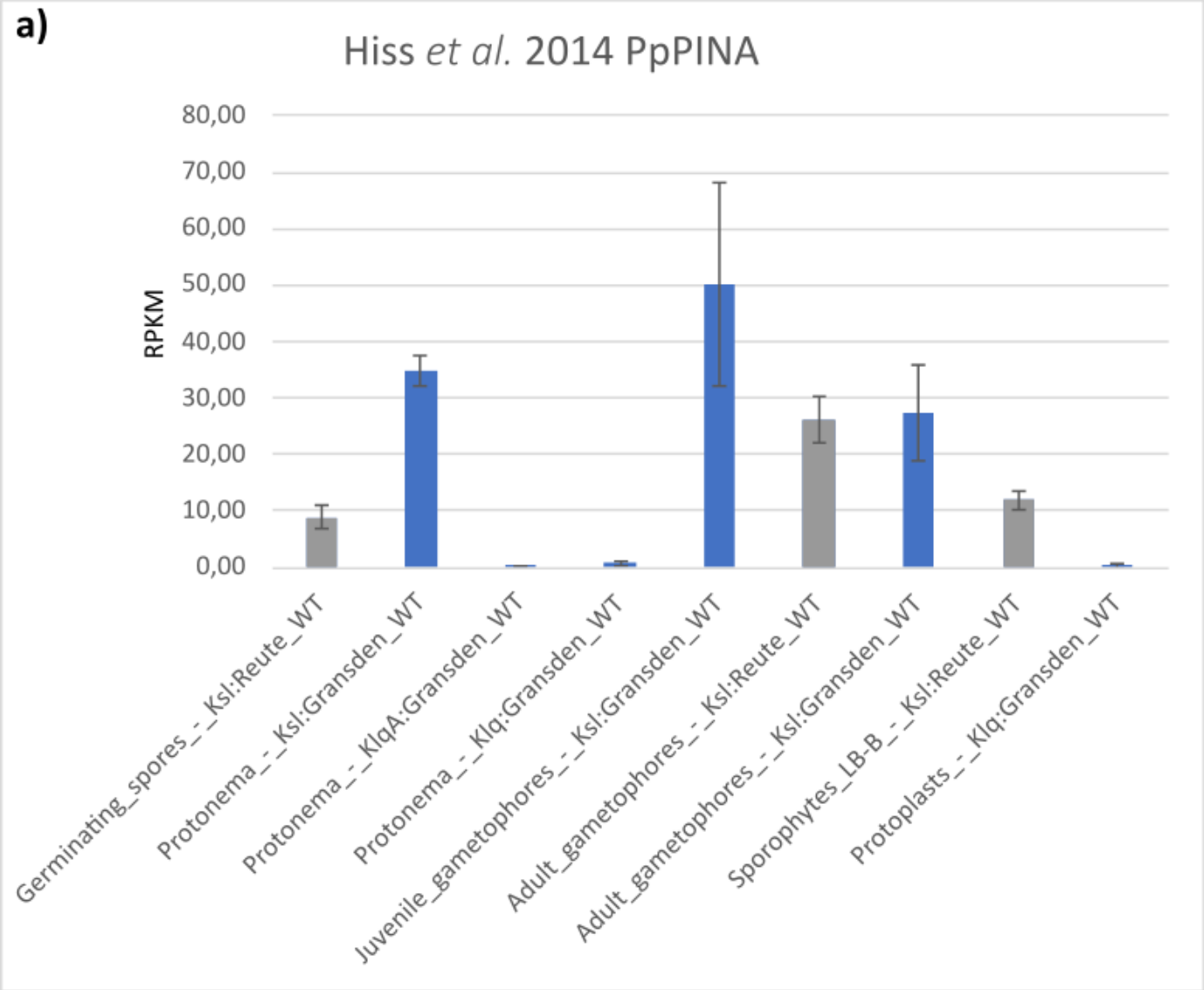

1310

bioRxiv preprint doi: https://doi.org/10.1101/2022.07.05.498815; this version posted July 5, 2022. The copyright holder for this preprint (which was not certified by peer review) is the author/funder, who has granted bioRxiv a license to display the preprint in perpetuity. It is made available under aCC-BY-NC-ND 4.0 International license.

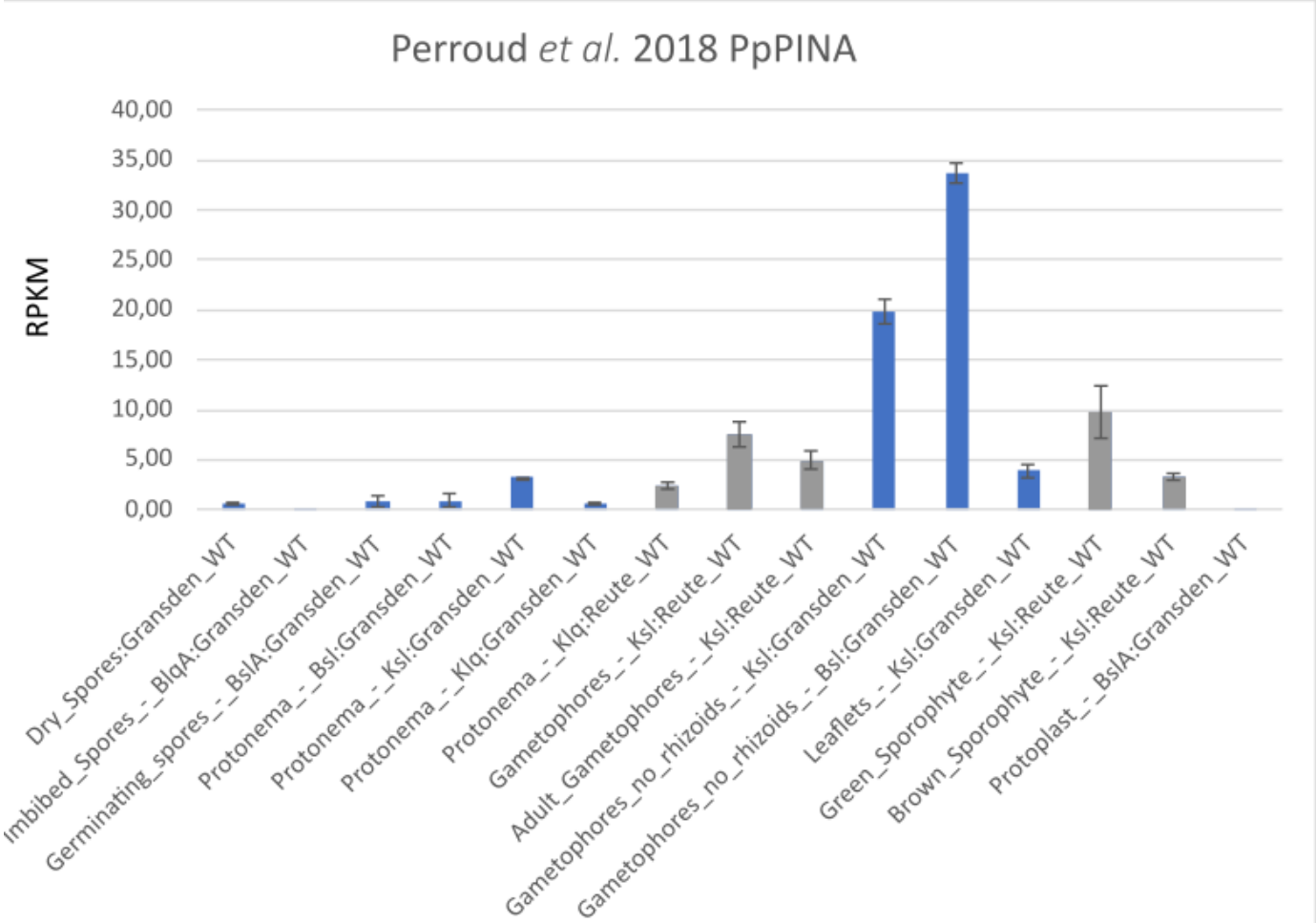

1311

bioRxiv preprint doi: https://doi.org/10.1101/2022.07.05.498815; this version posted July 5, 2022. The copyright holder for this preprint (which was not certified by peer review) is the author/funder, who has granted bioRxiv a license to display the preprint in perpetuity. It is made available under aCC-BY-NC-ND 4.0 International license.

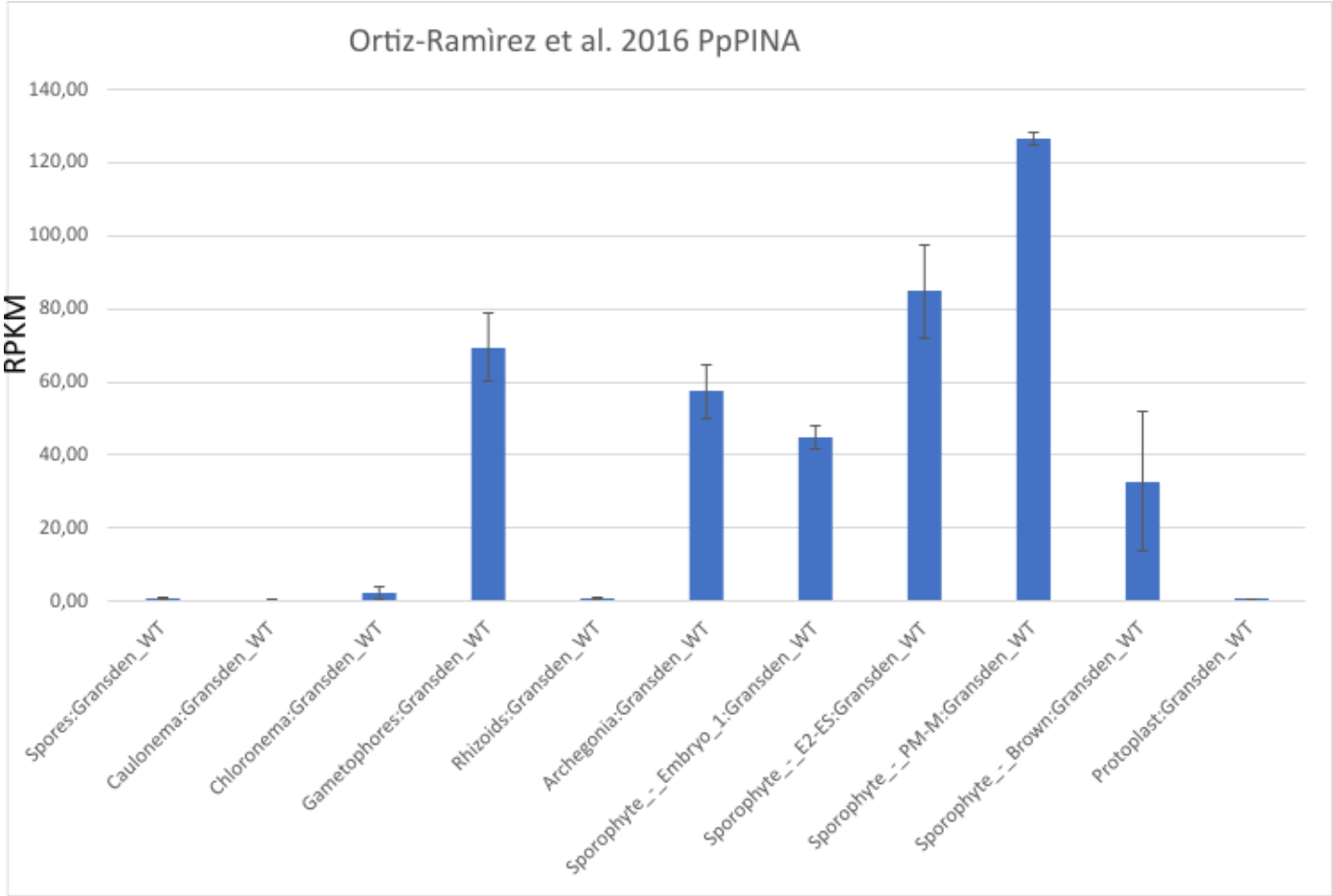

1312

bioRxiv preprint doi: https://doi.org/10.1101/2022.07.05.498815; this version posted July 5, 2022. The copyright holder for this preprint (which was not certified by peer review) is the author/funder, who has granted bioRxiv a license to display the preprint in perpetuity. It is made available under aCC-BY-NC-ND 4.0 International license.

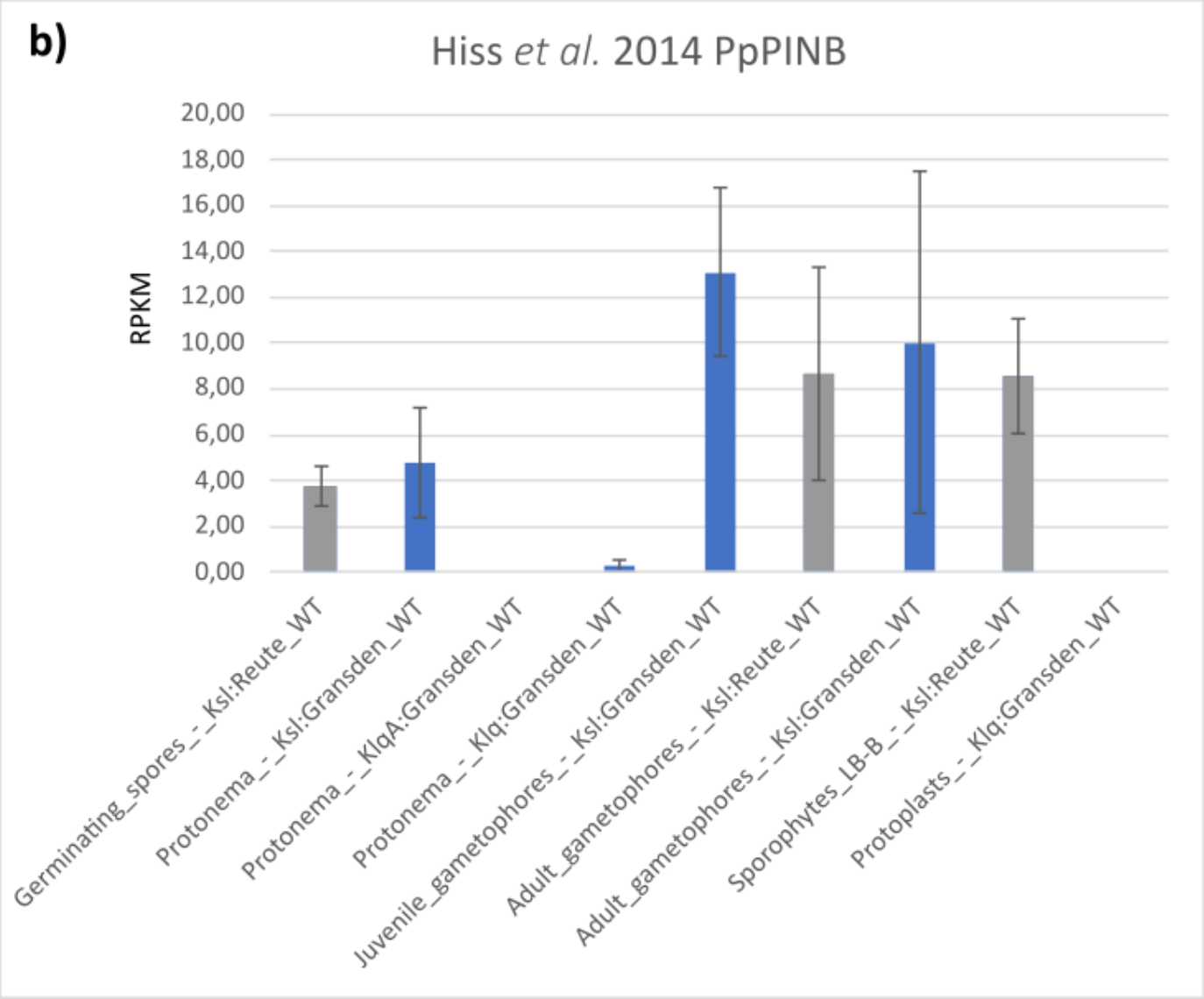

1313

bioRxiv preprint doi: https://doi.org/10.1101/2022.07.05.498815; this version posted July 5, 2022. The copyright holder for this preprint (which was not certified by peer review) is the author/funder, who has granted bioRxiv a license to display the preprint in perpetuity. It is made available under aCC-BY-NC-ND 4.0 International license.

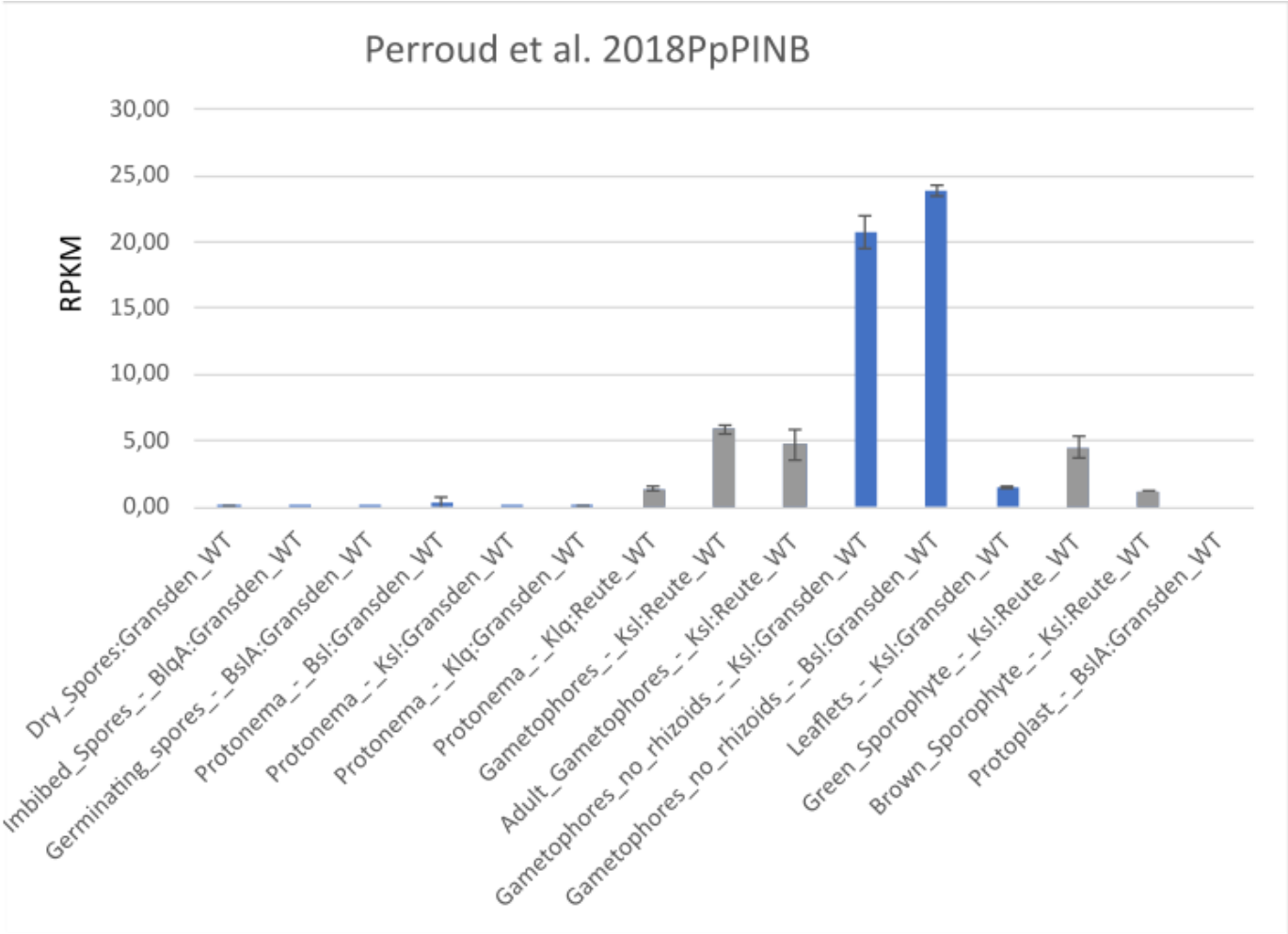

1314

bioRxiv preprint doi: https://doi.org/10.1101/2022.07.05.498815; this version posted July 5, 2022. The copyright holder for this preprint (which was not certified by peer review) is the author/funder, who has granted bioRxiv a license to display the preprint in perpetuity. It is made available under aCC-BY-NC-ND 4.0 International license.

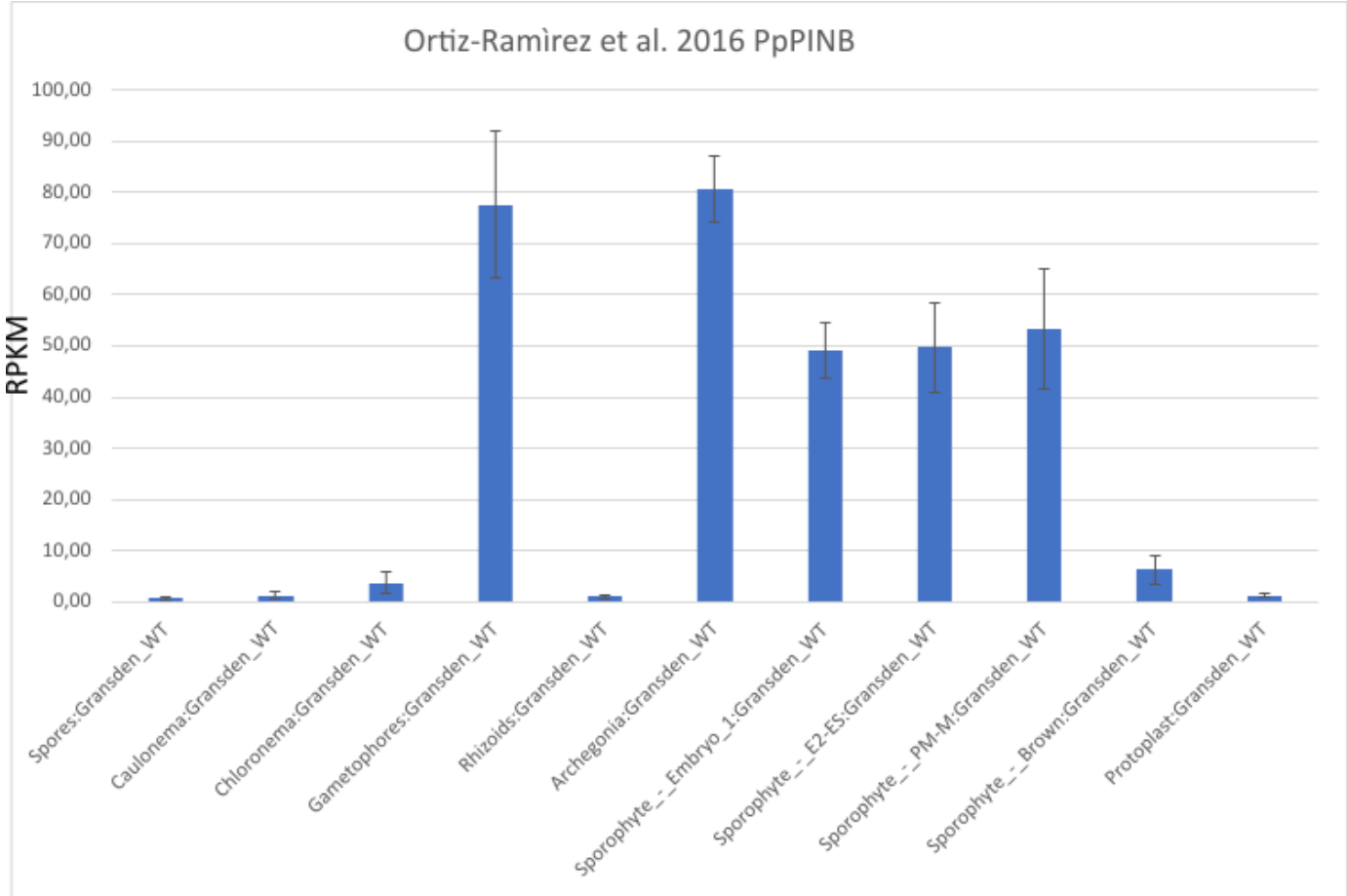

1315

bioRxiv preprint doi: https://doi.org/10.1101/2022.07.05.498815; this version posted July 5, 2022. The copyright holder for this preprint (which was not certified by peer review) is the author/funder, who has granted bioRxiv a license to display the preprint in perpetuity. It is made available under aCC-BY-NC-ND 4.0 International license.

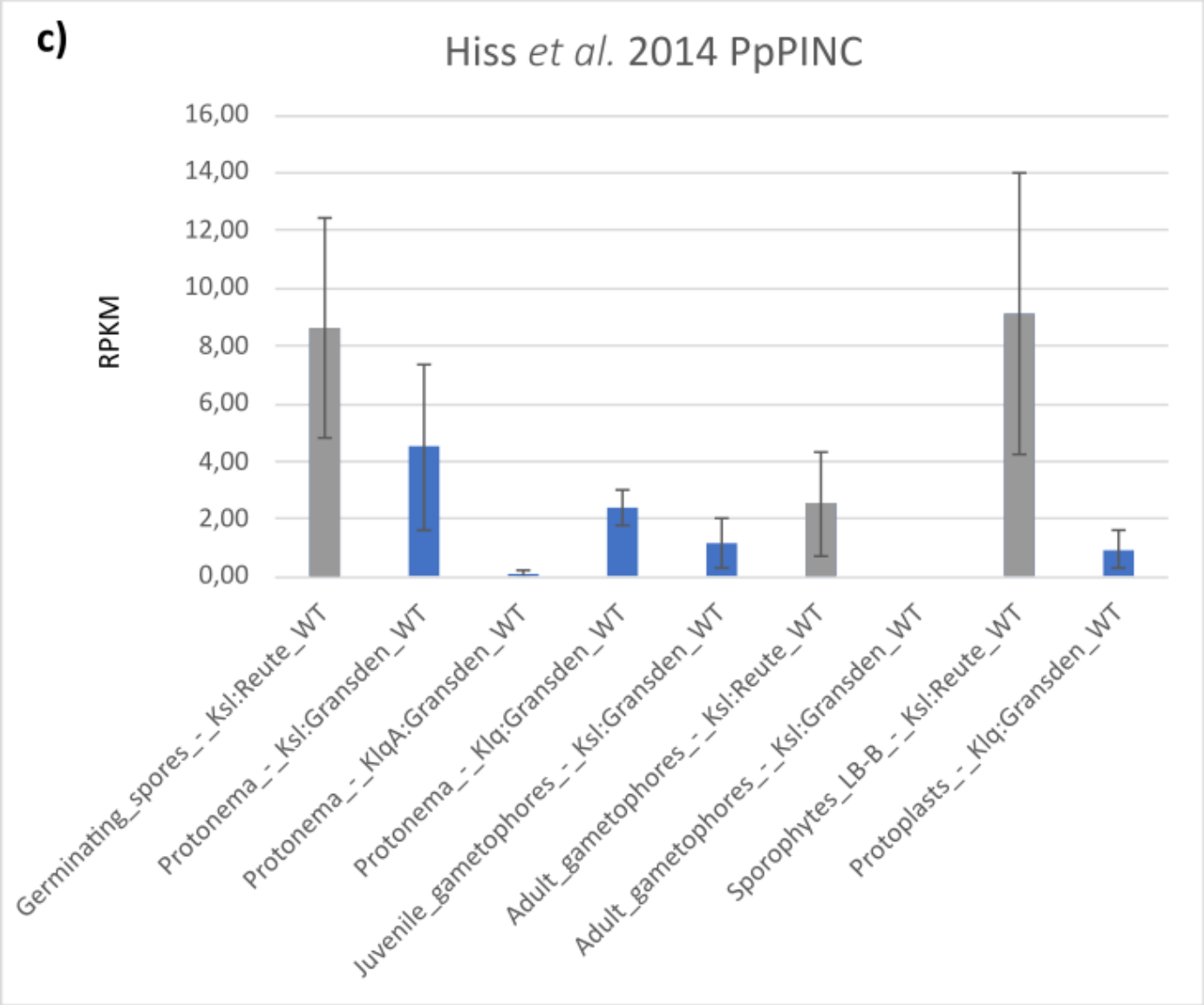

1316

bioRxiv preprint doi: https://doi.org/10.1101/2022.07.05.498815; this version posted July 5, 2022. The copyright holder for this preprint (which was not certified by peer review) is the author/funder, who has granted bioRxiv a license to display the preprint in perpetuity. It is made available under aCC-BY-NC-ND 4.0 International license.

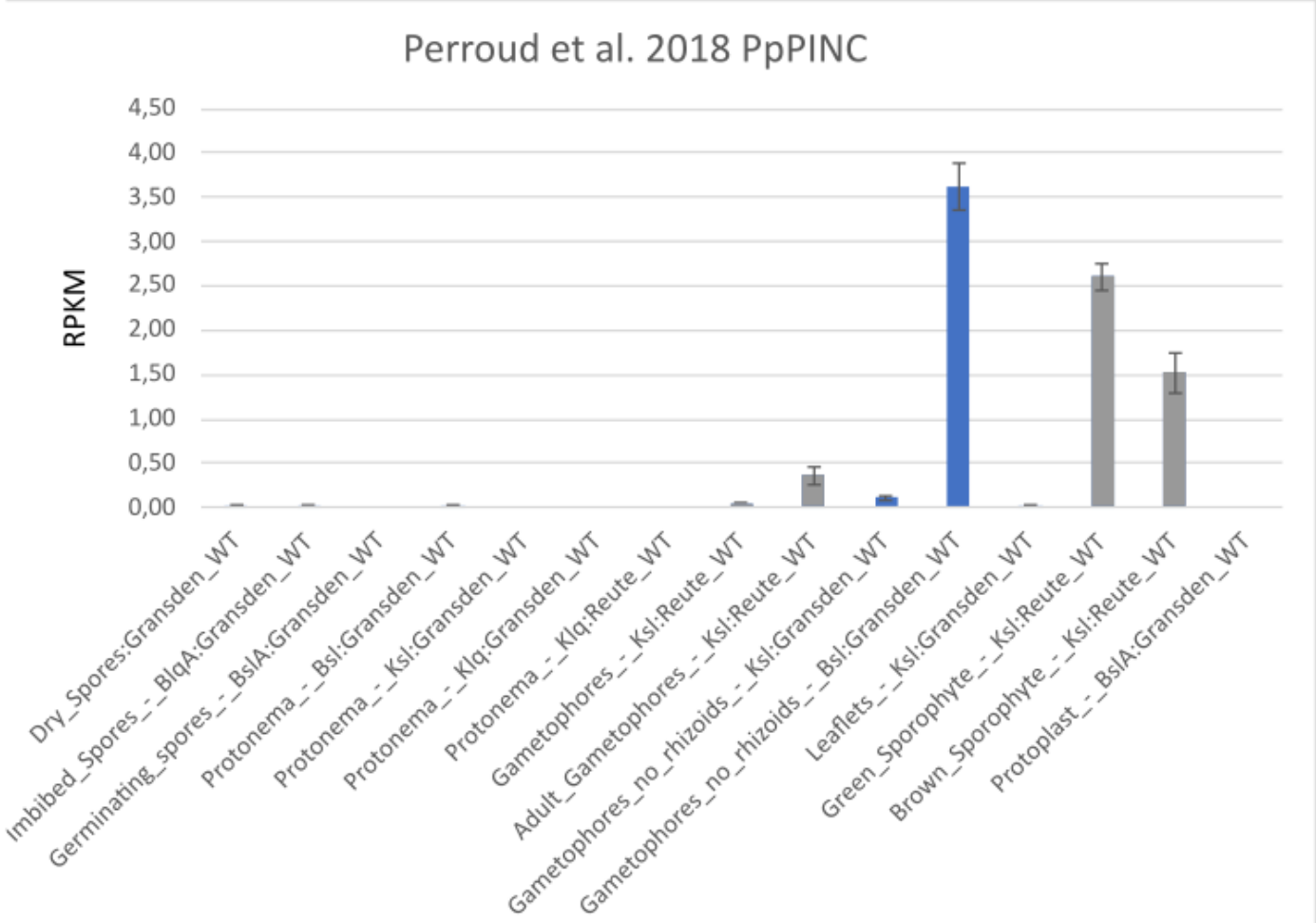

1317

bioRxiv preprint doi: https://doi.org/10.1101/2022.07.05.498815; this version posted July 5, 2022. The copyright holder for this preprint (which was not certified by peer review) is the author/funder, who has granted bioRxiv a license to display the preprint in perpetuity. It is made available under aCC-BY-NC-ND 4.0 International license.

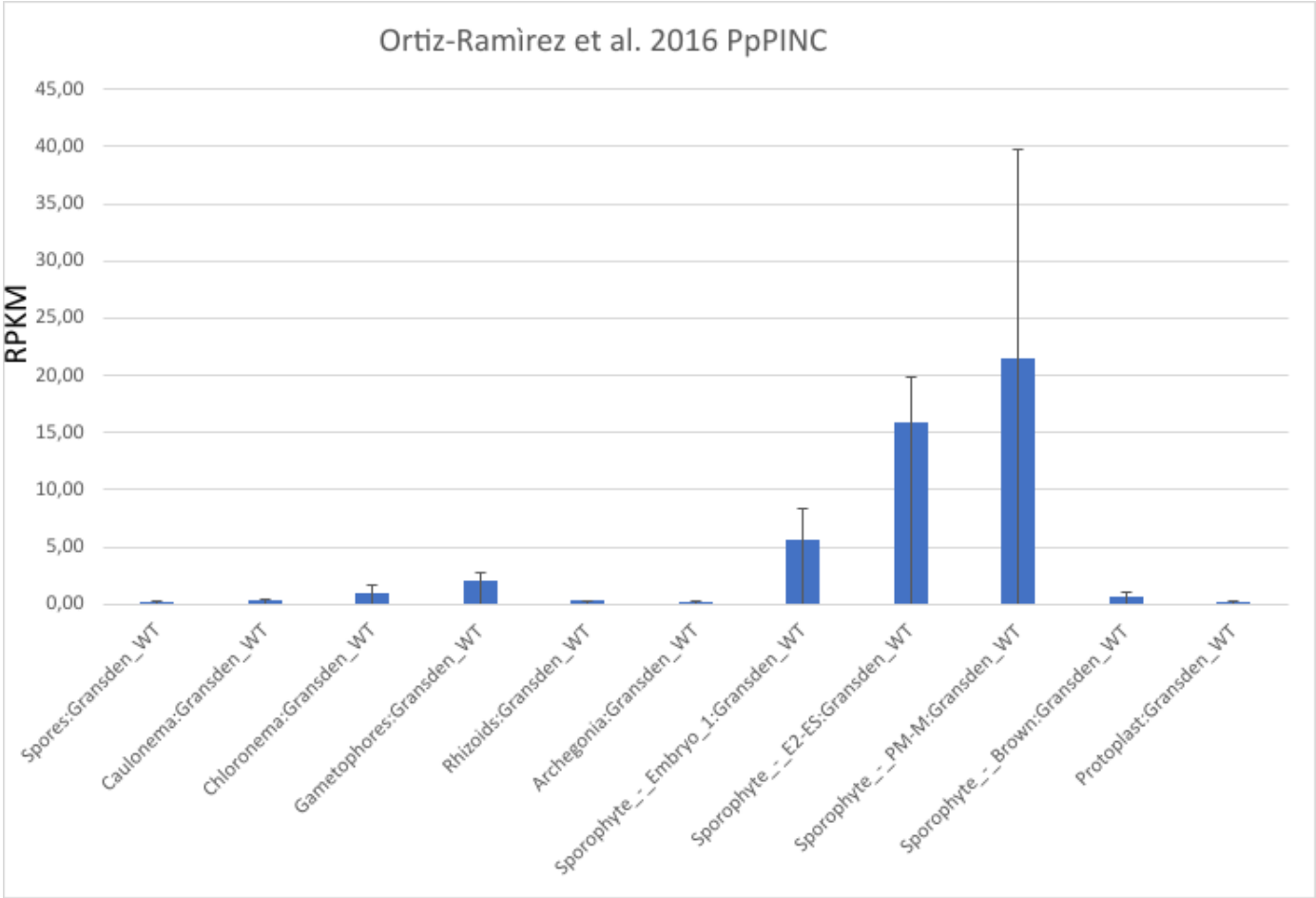

Supplemental Figure S3: Expression data of Physcomitrella PIN genes from PEATmoss database. Expression of *PpPINA*, *B* and *C* in different gene expression sets accessed via the PEATmoss database (Fernandez-Pozo *et al.*, 2020) in the two Physcomitrella ecotypes Gransden (blue bars) and Reute (grey bars), used data sets: Hiss *et al*. (2014), Perroud *et al*. (2018), and Ortiz-Ramirez *et al*. (2016). a) *PpPINA* b) *PpPINB* c) *PpPINC*. Blq = BCD liquid, BlqA = BCD (ammonium) liquid, Bsl = BCD solid, BslA = BCD (ammonium) solid, Klq = Knop liquid, Ksl = Knop solid, Sporophyte LB-B = light brown to brown sporophyte, Sporophyte PM-M = premeiotic to meiotic green sporophyte, sporophyte Embryo 1= first embryo stage, sporophyte E2-ES = early developing sporophyte. n = 3, RPKM = reads per kilobase per million.

bioRxiv preprint doi: https://doi.org/10.1101/2022.07.05.498815; this version posted July 5, 2022. The copyright holder for this preprint (which was not certified by peer review) is the author/funder, who has granted bioRxiv a license to display the preprint in perpetuity. It is made available under aCC-BY-NC-ND 4.0 International license.

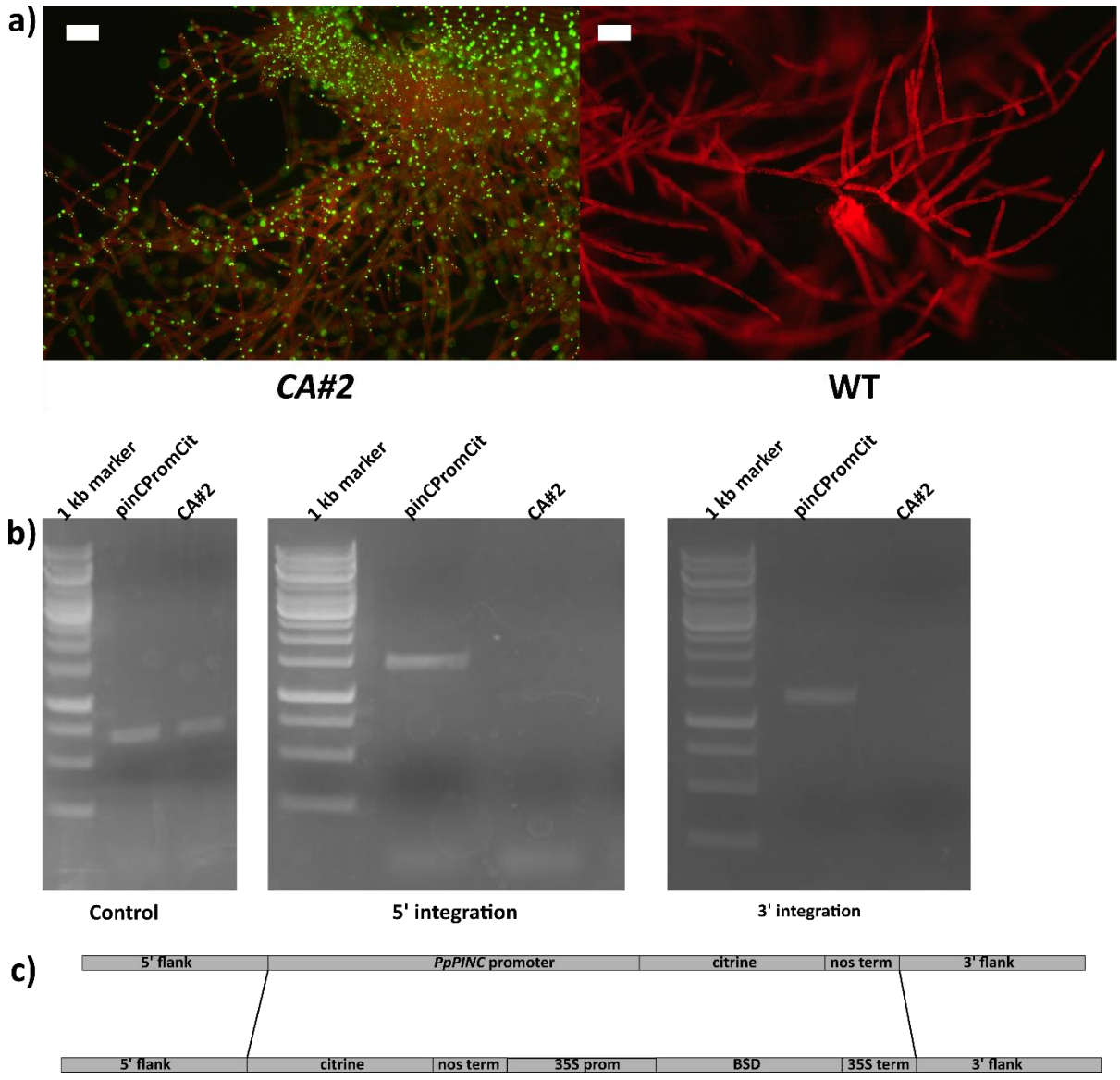

Supplemental Figure S4: Molecular evaluation of *pinCPromCit*. a) Fluorescent microscopy pictures of CA#2, parental line of *pinCPromCit* (left) and Physcomitrella WT (right) protonema and budding gametophore, scale bar = 100 µm. b) Control PCR using constitutive expressed gene Ef1α for *pinCPromCit* and *CA#2*, 3' integration (PCR product = 1.4 kb) and 5' integration (PCR product = 1.5 kb) of *PpPINC* promoter construct, no PCR product for *CA#2* parental line. c) Construct used for creating *pinCPromCit* by targeting the whole construct used in Wiedemann *et al*. (2018). BSD = selection marker, prom = promoter, term = terminator.

bioRxiv preprint doi: https://doi.org/10.1101/2022.07.05.498815; this version posted July 5, 2022. The copyright holder for this preprint (which was not certified by peer review) is the author/funder, who has granted bioRxiv a license to display the preprint in perpetuity. It is made available under aCC-BY-NC-ND 4.0 International license.

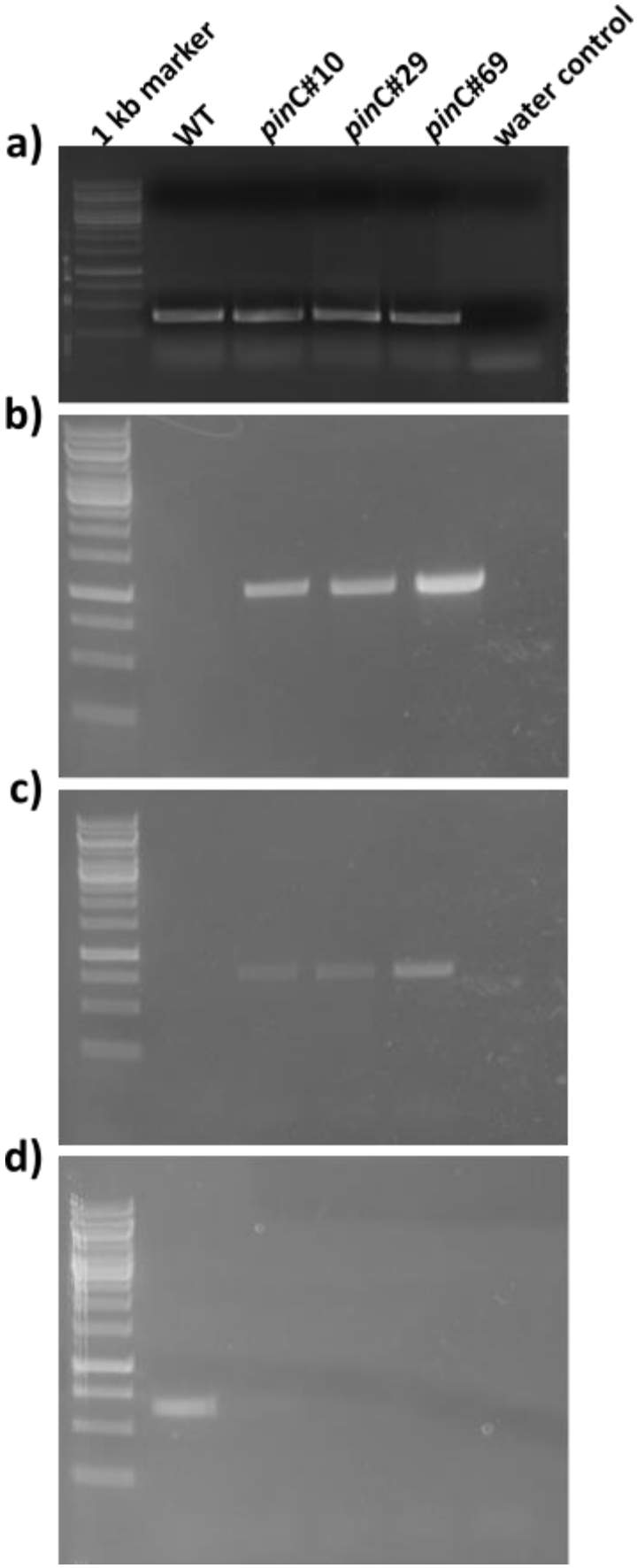

bioRxiv preprint doi: https://doi.org/10.1101/2022.07.05.498815; this version posted July 5, 2022. The copyright holder for this preprint (which was not certified by peer review) is the author/funder, who has granted bioRxiv a license to display the preprint in perpetuity. It is made available under aCC-BY-NC-ND 4.0 International license.

Supplemental Figure 5: Molecular analysis of Physcomitrella *pin*C mutant lines. a) Control PCR using the L21 gene (C45 primers). b) 5' integration of targeting construct (1 kb). c) 3' integration of targeting construct (770 bp). d) RT-PCR amplifying a region from exon 3 to exon 5 (700 bp).

bioRxiv preprint doi: https://doi.org/10.1101/2022.07.05.498815; this version posted July 5, 2022. The copyright holder for this preprint (which was not certified by peer review) is the author/funder, who has granted bioRxiv a license to display the preprint in perpetuity. It is made available under aCC-BY-NC-ND 4.0 International license.

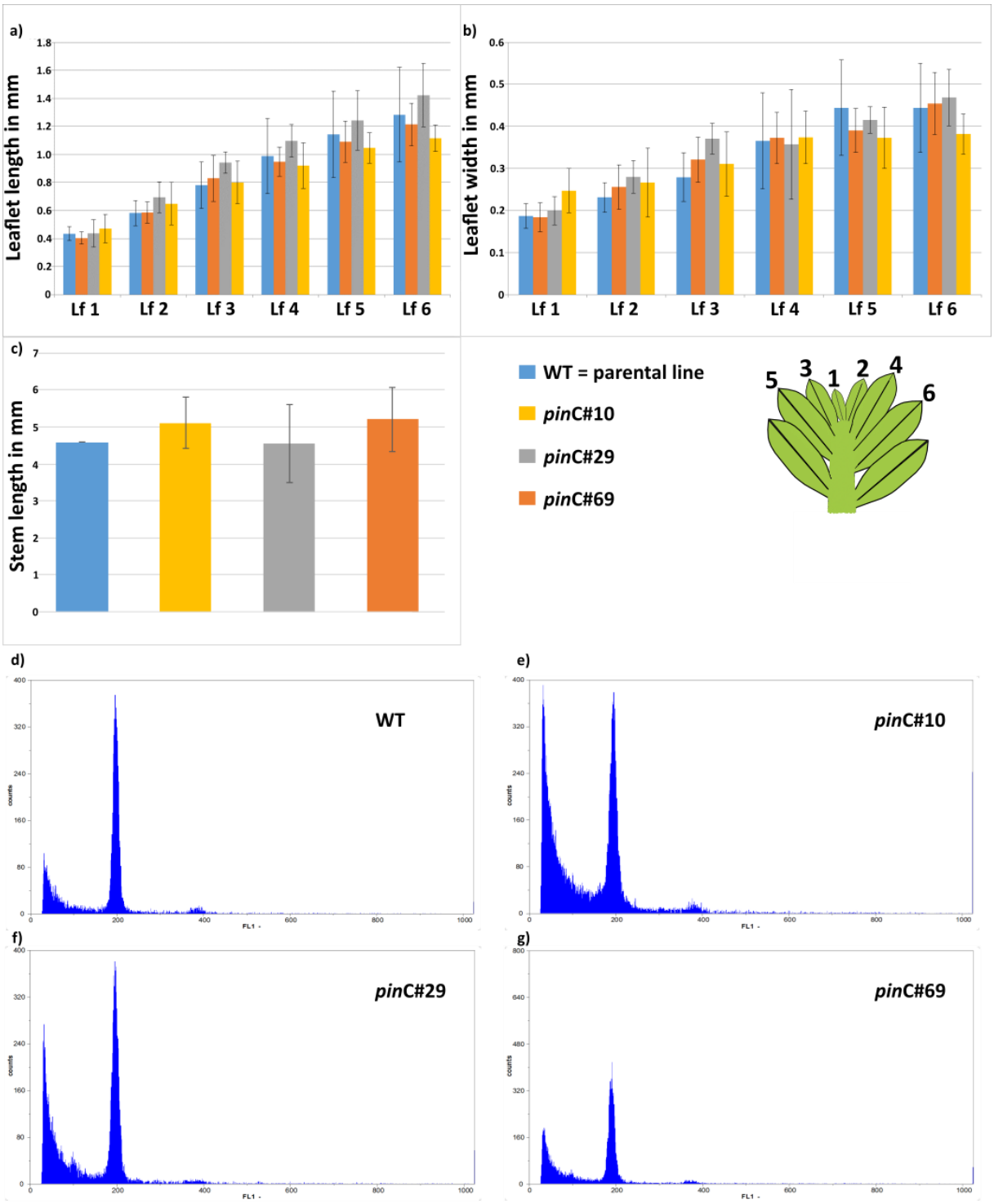

Supplemental Figure 6: Phenotypical characterization of vegetative tissue for Physcomitrella wild type (WT) and *pin*C mutant lines. a) Length and b) width of the first six leaves of a gametophore. c) stem length d)-g) flow cytometric measurements confirmed haploidy of the generated *pin*C knockouts. Number of measured leaves and stems a) + b) n= 7; c) WT: n = 13, *pinC*#10: n = 14, *pinC*#29: n = 16, *pinC*#69: n = 18.

bioRxiv preprint doi: https://doi.org/10.1101/2022.07.05.498815; this version posted July 5, 2022. The copyright holder for this preprint (which was not certified by peer review) is the author/funder, who has granted bioRxiv a license to display the preprint in perpetuity. It is made available under aCC-BY-NC-ND 4.0 International license.

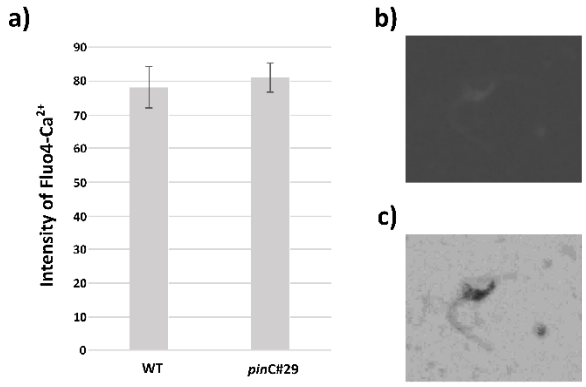

Supplemental Figure S7: Calcium concentration in Physcomitrella spermatozoids. No difference in Ca^{2+} concentration in Physcomitrella WT and mutant sperm cells. a) Intensity of single sperm cells after treatment with Fluo-4. b) grey scale picture of fluorescence image of sperm cell treated with Fluo-4. c) negative image of b) to show sperm cell with flagellum. For a) n = 15 spermatozoids from three different antheridia were examined.

bioRxiv preprint doi: https://doi.org/10.1101/2022.07.05.498815; this version posted July 5, 2022. The copyright holder for this preprint (which was not certified by peer review) is the author/funder, who has granted bioRxiv a license to display the preprint in perpetuity. It is made available under aCC-BY-NC-ND 4.0 International license.

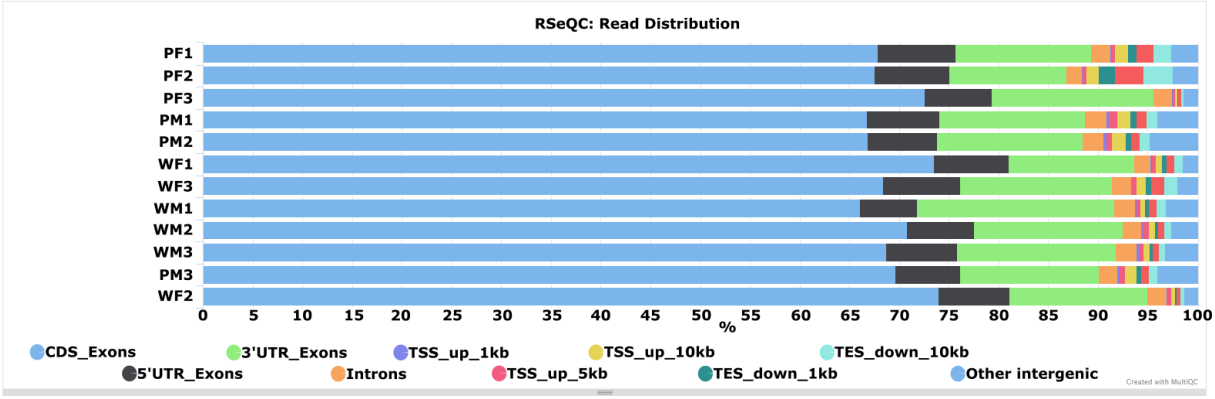

	% Assigned	M Assigned
PF1	47.7%	19.0
PF2	49.5%	25.6
PF3	69.8%	30.9
PM1	54.3%	22.9
PM2	60.1%	25.5
PM3	57.1%	39.8
WF1	61.2%	20.7
WF2	65.7%	30.3
WF3	56.9%	25.0
WM1	57.2%	21.9
WM2	61.5%	25.9
WM3	65.0%	26.3

Supplemental Figure S8: Quality control RNAseq. Read distribution in Physcomitrella WT and *pin*C mutant gametangia, WM = WT antheridia, WF = WT archegonia, PM = *pin*C#29 antheridia, PF = *pin*C#29 archegonia. CDS = coding sequence, UTR = untranslated region, TSS = transcription start sequence, TES = transcription end sequence. Quality control done with MultiQC (Galaxy Version 1.11+galaxy0).

bioRxiv preprint doi: https://doi.org/10.1101/2022.07.05.498815; this version posted July 5, 2022. The copyright holder for this preprint (which was not certified by peer review) is the author/funder, who has granted bioRxiv a license to display the preprint in perpetuity. It is made available under aCC-BY-NC-ND 4.0 International license.

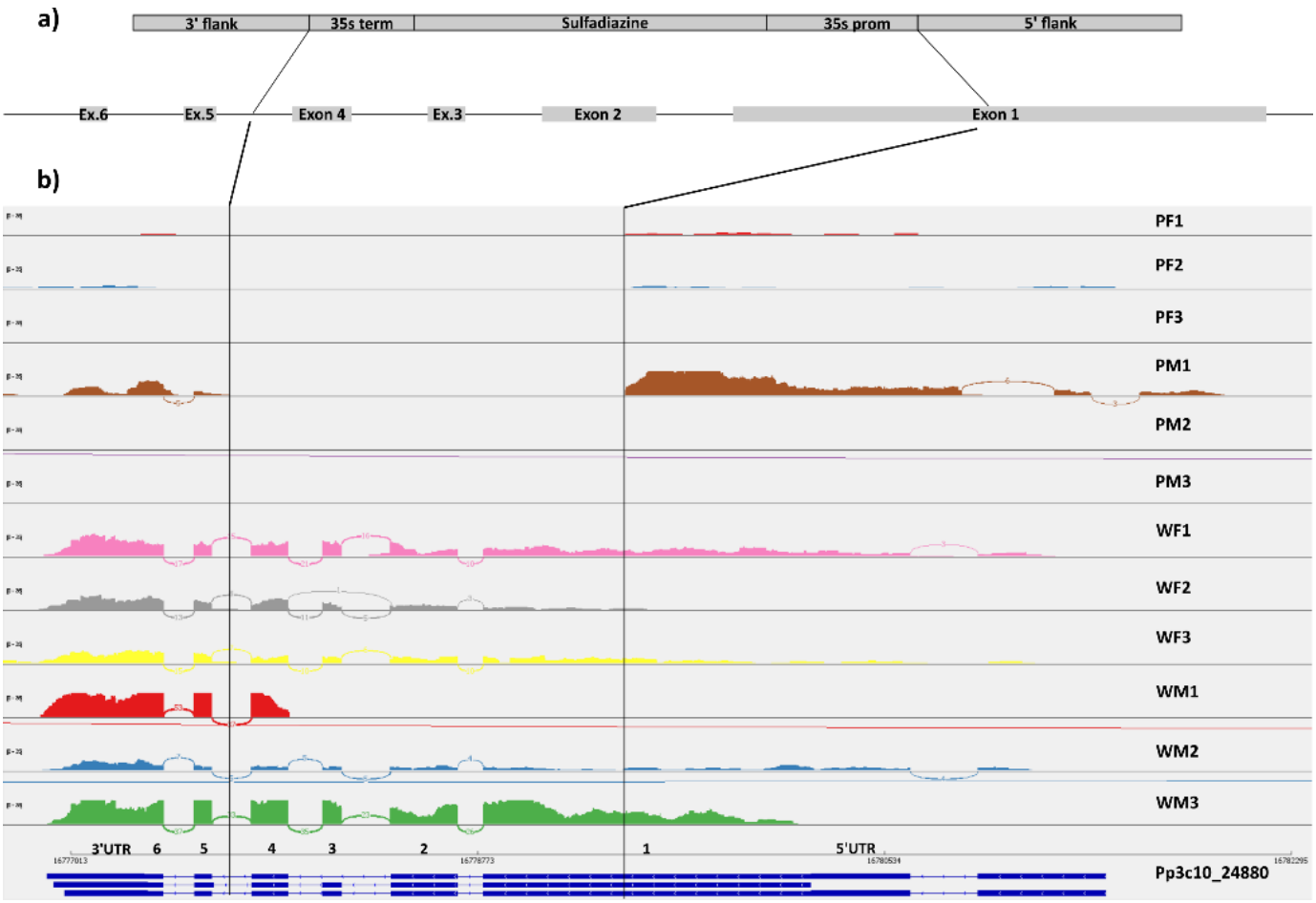

Supplemental Figure S9: Proof of *PpPINC* mutation in *pin*C#29. Sashimi plot showing integration of knockout construct in Physcomitrella WT background. a) Knockout construct for the *PINC* gene. Black lines indicate the integration into the gene starting from the middle of exon 1 to the intron between exon 4 and 5. b) Sashimi plot for the PINC gene in all samples. Continuous read through of mapped fragments only in WT samples, confirming knockout of the gene in the mutant.

bioRxiv preprint doi: https://doi.org/10.1101/2022.07.05.498815; this version posted July 5, 2022. The copyright holder for this preprint (which was not certified by peer review) is the author/funder, who has granted bioRxiv a license to display the preprint in perpetuity. It is made available under aCC-BY-NC-ND 4.0 International license.

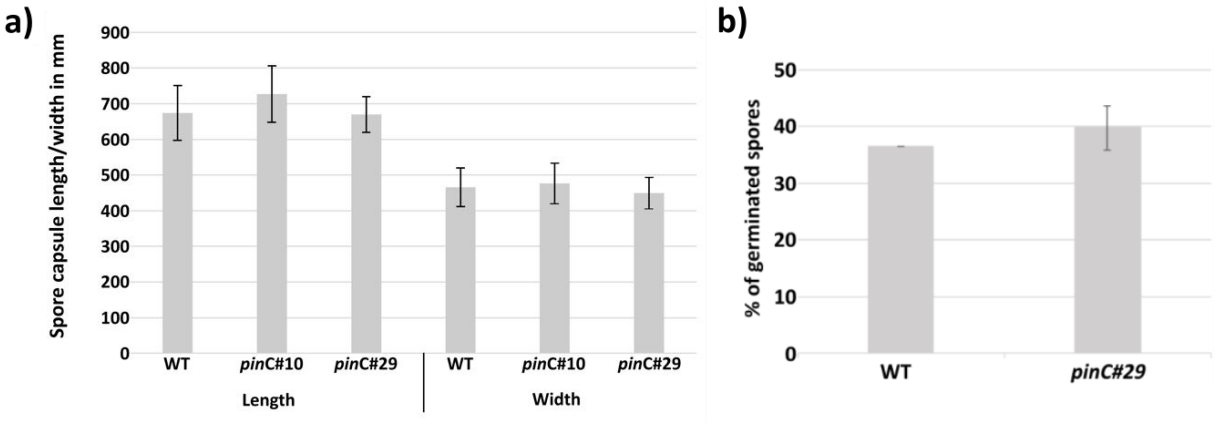

Supplemental Figure S10: **Size of spore capsules and spore germination rate.** a) Length and width of mature spore capsules from Physcomitrella WT n = 15, mutant *pin*C#10 and mutant #29, n = 16. b) Germination rate of spores three days after plating. n = 3 plates.

bioRxiv preprint doi: https://doi.org/10.1101/2022.07.05.498815; this version posted July 5, 2022. The copyright holder for this preprint (which was not certified by peer review) is the author/funder, who has granted bioRxiv a license to display the preprint in perpetuity. It is made available under aCC-BY-NC-ND 4.0 International license.

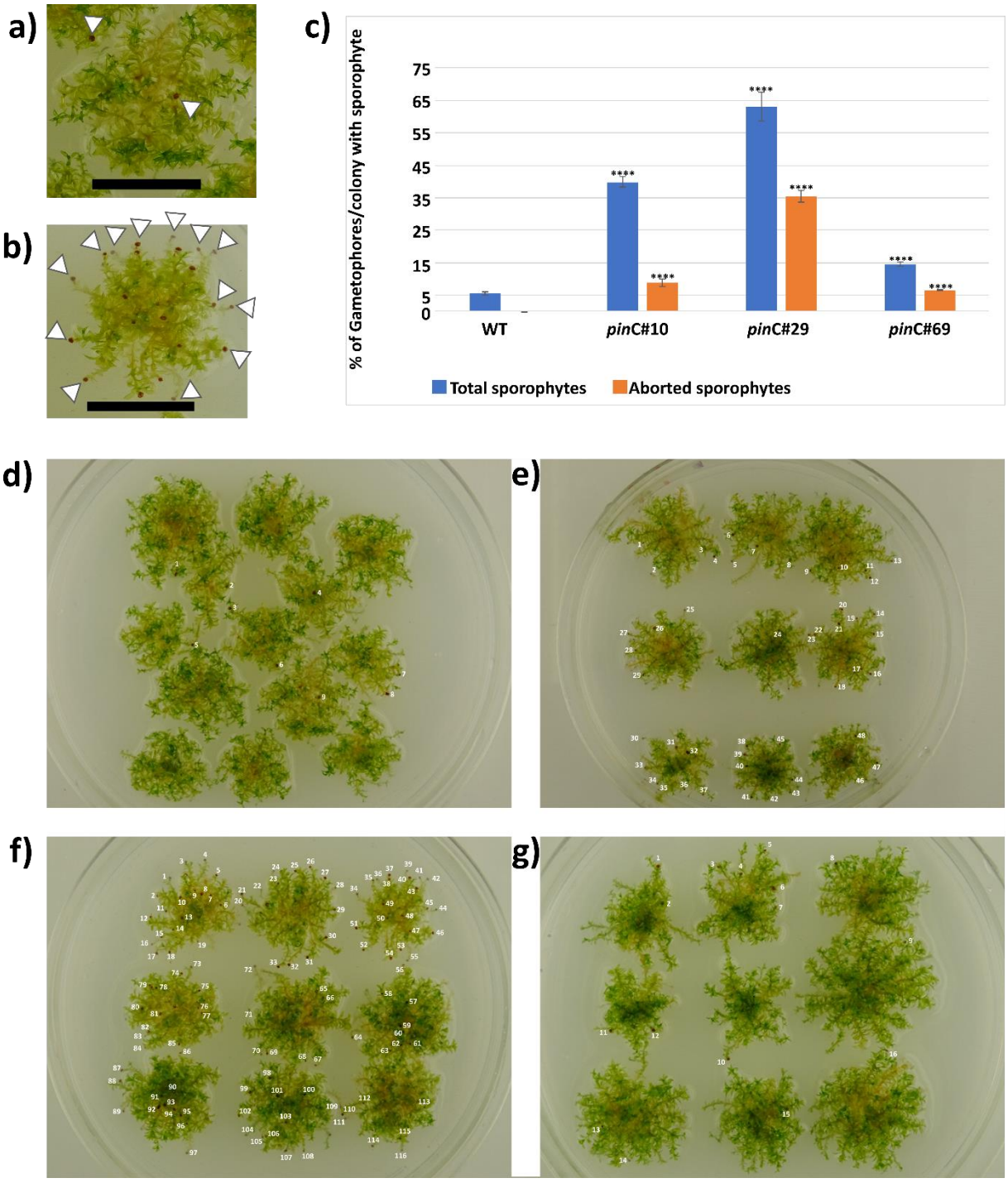

Supplemental Figure S11: Spore capsule numbers. Physcomitrella spore capsules in a) WT and b) *pin*C#29 mutant, white arrows mark sporophytes (for visibility reasons, not all sporophytes in b) are marked while all visible sporophytes are marked in a)). bar = 1cm. c) Percentage of gametophores with a sporophyte per colony, in blue total number of sporophytes (adult + aborted), in orange are only aborted sporophytes. Asterisks = $p<0.00005$ of mutant lines against wild type, n (colonies) = WT (41), *pin*C#10 (30), *pin*C#29 (42), *pin*C#69 (32) d) wild type plate with 9 sporophytes counted. e) *pin*C#10 plate with 48 sporophytes. f) *pin*C#29 plate with 116 sporophytes. g) *pin*C#69 with 16 sporophytes.

bioRxiv preprint doi: https://doi.org/10.1101/2022.07.05.498815; this version posted July 5, 2022. The copyright holder for this preprint (which was not certified by peer review) is the author/funder, who has granted bioRxiv a license to display the preprint in perpetuity. It is made available under aCC-BY-NC-ND 4.0 International license.

1393 **Supplemental Table 1:** Primers used in Physcomitrella WT and mutant lines.

Name	Sequence	Comment
P3-KO Fw	5'-GGGATCCATGTTGGCCTACGCGTCTGT-3'	Amplified region for *pin*C knockout construct
P3-KO Rv	5'-GAAGCTTCTGGGGAGTTCAACACCATT-3'	
5PinCprom_f+CA5	5'- agcttaacgttagccactcTCCTTTGTGTGGAGTAGAG-3'	Gibson primers for amplification of PpPINC promoter region, (capital letters)
3PinCprom_r+Citrin	5'-CACGTCGACAGATCGTCAAGgcagaagttcatgggaggtgga-3'	
Pin3f_ex1-2	*5'*-ACGTGAACATTCCTCGGTTC-*3'*	RT-PCR, middle of exon 1 to exon 2 of PpPINC
Pin3r_ex2	*5'*-GTTCGGATTGCGAGTGAGTT-*3'*	
C45_fwd	*5'*-GGCTGGTCATGGGTTGCG-*3'*	cDNA reference gene
C45_rev	*5'*-GAGGTCAACTGTCTCGCC-*3'*	
35SPqPCR_f	5'-CCATTGCCCAGCTATCTGTC-3'	Determination of transgene *pin*C copy number via qPCR
35SPqPCR_r	5'-CATTGCGATAAAGGAAAGGC-3'	

1394

bioRxiv preprint doi: https://doi.org/10.1101/2022.07.05.498815; this version posted July 5, 2022. The copyright holder for this preprint (which was not certified by peer review) is the author/funder, who has granted bioRxiv a license to display the preprint in perpetuity. It is made available under aCC-BY-NC-ND 4.0 International license.

Supplemental Table 2: Differentially expressed genes in Physcomitrella WT and mutant. Single genes found in comparisons of Physcomitrella a) mutant (PM) vs wildtype (WM) antheridia b) mutant (PF) vs wild type (WF) archegonia; BP = biological process, CC = cellular compartment, MF = molecular function.

a)

Upregulated genes mutant (PM) vs. wildtype (WM) antheridia					
geneID	Foldchange	p-Adjust	GO_annot_BP	GO_annot_MF	GO_annot_CC
Pp3c26_6020	2,61799094	0,00574099	single-multicellular organism process; anatomical structure development; ion transmembrane transport; single-organism developmental process	ion channel activity	cell part; integral component of membrane
Pp3c26_3990	2,60429982	3,58E-08	transmembrane transport	substrate-specific transmembrane transporter activity	chloroplast envelope; integral component of membrane

geneID	PM1	PM2	PM3	WM1	WM2	WM3
Pp3c26_6020	209	282	1259	15	50	32
Pp3c26_3990	676	735	822	79	101	101

Downregulated genes mutant (PM) vs. wildtype (WM) antheridia					
geneID	Foldchange	p-Adjust	GO_annot_BP	GO_annot_MF	GO_annot_CC
Pp3c9_8920	-2,14177862	0,00160142	dolichol biosynthetic process	amino acid binding	chloroplast stroma; chloroplast thylakoid membrane
Pp3c14_8940	-2,3368623	0,01313347	.	.	integral component of membrane
Pp3c20_22670	-2,48823907	0,00673352	positive regulation of transcription, DNA-templated	zinc ion binding; sequence-specific DNA binding; sequence-specific DNA binding transcription factor activity	nucleus
Pp3c1_22810	-2,68377153	0,00973054	cell wall modification:pectin catabolic process	pectinesterase activity:aspartyl esterase activity	cell wall:extracellular region
Pp3c19_15670	-2,68772125	0,00973054	cellular component organization or biogenesis; cellular process	.	cytoplasm

bioRxiv preprint doi: https://doi.org/10.1101/2022.07.05.498815; this version posted July 5, 2022. The copyright holder for this preprint (which was not certified by peer review) is the author/funder, who has granted bioRxiv a license to display the preprint in perpetuity. It is made available under aCC-BY-NC-ND 4.0 International license.

Pp3c3_4950	-2,71566077	0,009008	regulation of biological quality; regulation of transcription, DNA-templated; asymmetric cell division; leaf development; radial pattern formation	sequence-specific DNA binding; sequence-specific DNA binding transcription factor activity	nucleus
Pp3c3_11110	-3,07745056	4,01E-08	proteolysis	aspartic-type endopeptidase activity	.
Pp3c21_8410	-3,24497467	5,52E-05	peptidyl-tyrosine dephosphorylation	protein tyrosine phosphatase activity	.
Pp3c12_11710	-4,86650335	1,63E-14	.	.	.

1403

geneID	PM1	PM2	PM3	WM1	WM2	WM3
Pp3c9_8920	1079	1248	2115	10980	5147	6717
Pp3c14_8940	531	119	190	1918	3043	2972
Pp3c20_22670	36	8	48	286	383	271
Pp3c3_11110	170	141	99	1975	1576	1902
Pp3c21_8410	1	5	7	100	197	253
Pp3c12_11710	232	115	230	71101	8547	41718
Pp3c1_22810	1	0	0	184	76	86
Pp3c19_15670	1	0	2	123	90	54
Pp3c3_4950	2	0	0	231	161	82

1404

1405 **b)**

Upregulated genes mutant (PF) archegonia vs. wildtype (WF) archegonia					
geneID	Foldchange	p-Adjust	GO_annot_BP	GO_annot_MF	GO_annot_CC
Pp3c11_4360	3,28704921	5,88E-11	proteolysis	serine-type endopeptidase activity	cell part

1406

geneID	PF1	PF2	PF3	WF1	WF2	WF3
Pp3c11_4360	154	241	220	0	0	4

1407

Downregulated genes mutant (PF) archegonia vs. wildtype (WF) archegonia					
geneID	Foldchange	p-Adjust	GO_annot_BP	GO_annot_MF	GO_annot_CC
Pp3c7_8820	-2,55854236	6,08E-07	.	.	.
Pp3c6_26100	-6,49563884	9,91E-73	.	metal ion binding	.

1408

geneID	PF1	PF2	PF3	WF1	WF2	WF3
Pp3c7_8820	72	129	58	1134	1082	3960
Pp3c6_26100	0	0	0	989	1581	1305

1409